CHALMERS

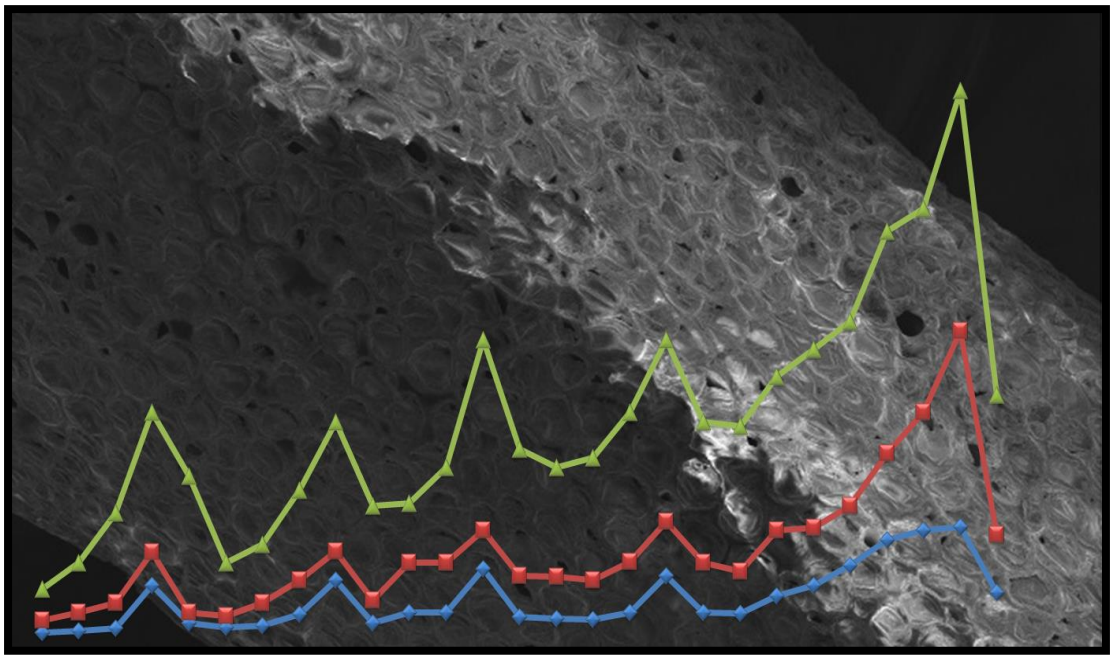

Cleaning and characterization of radioactive wastewater with hollow fiber membrane filters

A study performed at Ringhals AB and Vattenfall R&D

Master of Science Thesis In The Master Degree Programme, Nuclear Engineering

Khaled El Tayara

Chalmers University of Technology

Department of Chemical and Biological Engineering

Gothenburg, Sweden, September 2013

Preface

This report is the result of the master thesis performed during the spring of 2013 at Ringhals Nuclear facility and is sponsored by Vattenfall AB. The master thesis has been the final part of the Nuclear Engineering Master's Program MPNUE provided by the department of Chemical and Biological Engineering at Chalmers University of Technology.

I would like to show my gratitude and appreciation to all who made this possible:

My family (Lebanon):

- For all the love, sacrifices and support they provided me

My wife Sanna and the little Tayaras:

- For her love, support, sacrifices and patience

Gunnar Skarnemark at Chalmers department of Chemical and Biological Engineering:

- For his guidance and patience to answer my shower of questions

Magnus Oskarsson at Vattenfall R&D:

- For giving me the chance to make this happen.

Henrik Widestrand at Vattenfall R&D:

- For supporting and guiding me through the whole project

Patrik Fors at Vattenfall R&D:

- For his guidance when explaining how things work in the real world, and making my report "catchy".

Christina Lillfors-Pinter at Vattenfall R&D:

- For the early and long rides to Ringhals, the tour guide at R2C chemistry department and the help she provided me to execute my experiments.

Bernt Bengtsson at Ringhals AB:

- For the support, advice and expertise that he shared with me during the experimental course of this project

Anders Höglund at Ringhals AB:

- For his help and support during the experimental part of the project.

Carl-Henrik Hansson (Calle) at NORDCAP:

- For help and guidance he provided to run, improve and tackle all the problems that surfaced when running the pilot plant.

Staffan Redén: at Ringhals AB:

- For his help in providing the necessary tools that facilitated my experimental work at Ringhals.

The entire chemistry department (R2C) at Ringhals:

- For giving me the time to use their instruments despite their busy schedule.

Khaled El Tayara

Abstract

Sluiced ion exchanger resin is collected in spent resin storage tanks with a volume of backwash water used for this process. This water is radioactive since it contains colloids of activation products that are deemed difficult to remove using ion exchangers. One effective method of separation is the hollow fiber filter membrane (HFM), which is based upon the cross-flow filtration technology. These filters are easy to clean by backwash process and have low tendency to fouling. A volume of $8m^3$ of radioactive wastewater with an activity concentration of 0.3 Mbq/kg was reduced to 10 liters retentate with an activity concentration of 0.2Gbq/kg, which is 80% of the original radioactivity in the wastewater. The permeate had an average of 2.3 kBq/kg which was then reduced to 45 Bq/kg using a mixed bed ion exchanger. The most important radionuclides in the wastewater were Co-58, Co-60, Ag-110m and Sb.125.

Keywords: Activation products, Cross-flow filtration, Hollow fiber membrane, fouling, Backwash, Dose rate build-up.

Table of Contents

Glossary

AP: Activation Product

BW: Back wash

BWR: Boiling Water Reactor

CC: Chemical Cleaning

CFF: Cross-Flow Filtration

CIP: Cleaning In Place

FT: Fouling Tendency

FWHM: Full Width at Half Maximum

MWCO: Molecular Weight Cutt-Off

HFF: Hollow Fiber Filtration

HFM: Hollow Fiber Membrane

HPE: Hagen-Poiseuilles Equation

HPGe: High Purity Germanium

ICP-MS: Inductive Coupled Plasma Mass Spectroscopy

ICRP: International Committee on Radiation Protection

IXr: Ion Echanger

LWR: Light Water Reactor

MDA: Minimum Detectable Activity

MF: Microfiltrarion

NF: Nanofiltration

NPP: Nuclear Power Plant

ORE: Occupational Radiation Exposure

OTF: Once-Through Filtration

PDI: Pressure Driven Inside-out

PDO: Pressure Driven Outside-in

PES: Polyethyl Sulfone

PWR: Pressurized Water Reactor

RO: Reverse Osmoses

SEM: Scaning Electron Microscope

SRST: Spent Resin Storage Tank

SWM: Spiral Wound Membrane

TMP: Transmembrane Pressure

TT: Tanktainer

UF: Ultrafiltration

1 Introduction

Ion exchangers are periodically sluiced into spent resin storage tanks (SRST) when they have reached their loading capacity limit [1]. The water that is used in this process is termed backwash water. This water contains radioactive particles/colloids which remain waterborne after the sedimentation of the resin. These particles are difficult, if not impossible, to remove with an ion exchanger if not impossible, since the particles have been in contact with the resin beads for a long time (around 12 months) [2].

That constitutes a problem because the water is destined to be released back to nature, a release associated with strict regulations set by the environmental court (Miljödomstolen) in Sweden. These regulations set an activity concentration upper limit of 100 Bq/kg as a condition for release on water that has been a dose carrier. One possible solution to the problem is the usage of filters of suitable molecular weight cut-off (MWCO) that would remove the particles/colloids and reduce the activity concentration below 100 Bq/kg.

The hypothesis is to filter the radioactive wastewater utilizing membrane filtration technology. A cross flow filter (CFF) is used, such as the hollow fiber membrane (HFM) filter. The choice of this filter type was based on past thesis work where a spiral wound membrane (SWM) filter was used in one of those studies yielding good separation efficiency.

However, fouling was a serious matter and the filter was difficult to clean by back flushing which lead to dose rate build-up within the SWM. HFM on the other hand is supposed to be very easy to clean by back flushing decreasing the dose rate build-up and cleaning time.

Moreover, there is the problem of concentrating boric acid which would cause problems when the retentate is to be concentrated further by the use of evaporators, as intended at Ringhals. These problems arise when the final retentate volume is taken for embedment in cement moulds. According to experts at Ringhals, high concentrations of boric acid (it is a range of concentrations) affect the settling time of cement negatively (see appendix E). An optimization of the MWCO is thought to aid in choosing a filter size that that would meet the process demands.

1.1 Aim and goals

The aim of this work has been to decontaminate radioactive waste water bearing particulate contaminants by means of a HFM.

The goals of the experiments, that were executed in both the laboratory- and pilot-scale, were to examine:

- Laboratory-scale experiments:
    - Examine the particle distribution after filtration; That would be important because constituents of the tanktainer water might differ from one fuel-cycle to another (in Sweden one fuel-cycle is 12 months)

    - Monitor the concentration of boric acid; a filter MWCO that causes deviations in the boric acid concentration would be rejected. That was the optimization step and would aid the decision to use certain filters with adequate MWCO.

The results of those points would then help in assessing which filter MWCO to use for an optimal filtration.

- Pilot-scale experiments:
    - To test a predetermined HF module with a MWCO $5 \cdot 10^4$ Da and compare its results to those of the laboratory-scale.
    - To monitor the concentration of boric acid, pH and conductivity to examine the data consistency with data acquired at the laboratory-scale
    - To examine the profiles of dose rate build-up in the filter module. The collected data would then be used to assess the importance of cleaning the filter module with a backwash procedure.
    - To choose a filter module with a MWCO taken from the optimization analysis done at the laboratory-scale and apply the same type of measurements and analysis as done at the first filter module of the pilot-scale experiment.
    - To empty the tanktainer without backwash; that way the extent of fouling and dose rate build-up would be more prominent.

1.2 Delimitations

The center of this master thesis will be on the hollow fiber membrane filter. All waters that was used in the experiments in the filter assessment came from the same tank, roughly $8m^3$. This is to ensure that the operating conditions are kept constant.

The samples were not measured at equal times with the HPGe detector due to limitations in detector availability. The duration of measurements will be displayed in the appendices of each experiment. There was limited time for the experimental parts at Ringhals (12 weeks), which also included planning the experiments according to detectors and means of measurement that were available. Not all the ion echanger samples were analyzed by HPGe due to to the same time limitations mentioned above.

2 Theory

This chapter gives short introductions to the theories that are involved in this study. These are theories that explain ionizing radiation, filters and filtration phenomena, fouling and methods of its mitigation and ion exchangers.

2.1 Membrane technology

2.1.1 Definitions

Membrane technology is based on the semi-permeable properties of certain material that enables for separation of substances based on particle size and/or charge. Membrane material is usually manufactured from synthetic polymer; however, there are varieties that include ceramic and metallic membranes. [3] [4]

Membranes are characterized by their molecular weight cut-off (MWCO) which has the unit Dalton (Da; g/mol); it is the molar weight of the particle that is the limiting factor. Sometimes the radius in Angstroms (Å) or Micrometer (µm) is used instead of Da, see figure 2.2. [3] [4]

The polymeric membranes are significantly less expensive than those constructed of other material. Membrane applications include removal of microorganisms (bacteria, viruses), particulates and organic material (natural and synthetic). They are also used to e.g. concentrate juices, clarify wine, reduce or eliminate contaminants from wastewater as in wastewater treatment, in the food-, leather-, textile-, and electronic industry. [3] [4] [6]

Membrane filtration is a divided into two types depending on the filtration path:

1- Cross-flow filtration (CFF) where the feed travels tangentially along the filter. The filtration occurs perpendicular to the feed producing two streams: a retentate (concentrate) and permeate (filtrate).
2- Once through filtration (OTF) where the feed stream is perpendicular to the filter producing permeate (filtrate) and a cake. [3] [4] [5] [7]

Suspension mode

Cross-flow filtration operates in suspension mode (figure 2.1). Contaminants are sucked onto the membrane due to the pressure drop on the other side (hydraulic forces) of the membrane causing it to foul. A scouring force using water (backwash) or air bubbles to create a turbulent flow at the boundary layer is applied periodically. The objective of this process is to bring the contaminant accumulation down to minimum. In that way cake formation is prevented reducing fouling as a result. [3]

Tangential Flow Filtration Benefits

- Maximized Product Yields
- Extended Filter Life
- Improved Filtration Time
- Minimized Product Loss

- Immediate Detection of Breakthrough
- Reduced Costs by Optimizing Control [7]

Deposition mode

The once through filtration (OTF) process has only one in-flow (feed) and one out-flow (permeate) stream. The cake is produced under the action of hydraulic forces acting perpendicularly to the membrane that accumulates the suspended contaminants in the feed (figure 2.1). [3]

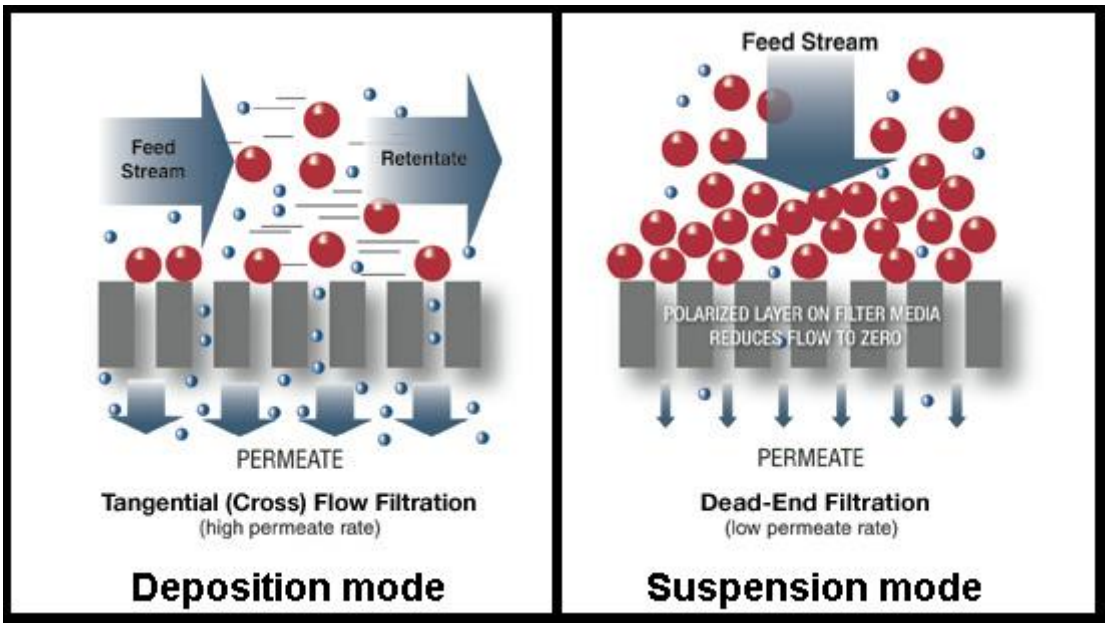

Figure 2.1: Two pictures showing OT filtration to the (left image) and CF filtration (right image) [38]

2.1.2 Structure design

Trans-membrane pressure (TMP) is the pressure difference between the applied pressure (feed side) and the recovered pressure (permeate side). Mechanical strength is a key property of a membrane filter as greater strength allows for larger TMP levels adding operational flexibility and usage of higher pressures to membrane properties. [3] [4] [5]

There are membranes that are bi-directional (can operate in reverse) which may allow cleaning in place (CIP) from either sides (feed or permeate) of the membrane. Membranes with a certain surface charge are able to remove particulate or microbial contaminants of opposite charge because of electrostatic attraction. There are also hydrophilic and hydrophobic membranes; all these design properties increase the ability of different membranes to resist fouling and enhance their performance under the filtration process. [3] [4] [5]

Types of membrane filtrations and construction material

The different structural designs mentioned in the preceding section have led to the production of different types of filtration that span the entire filtration spectrum depending on the properties of the target particles to be filtered out (figure 2.2). [3] [4] [5]

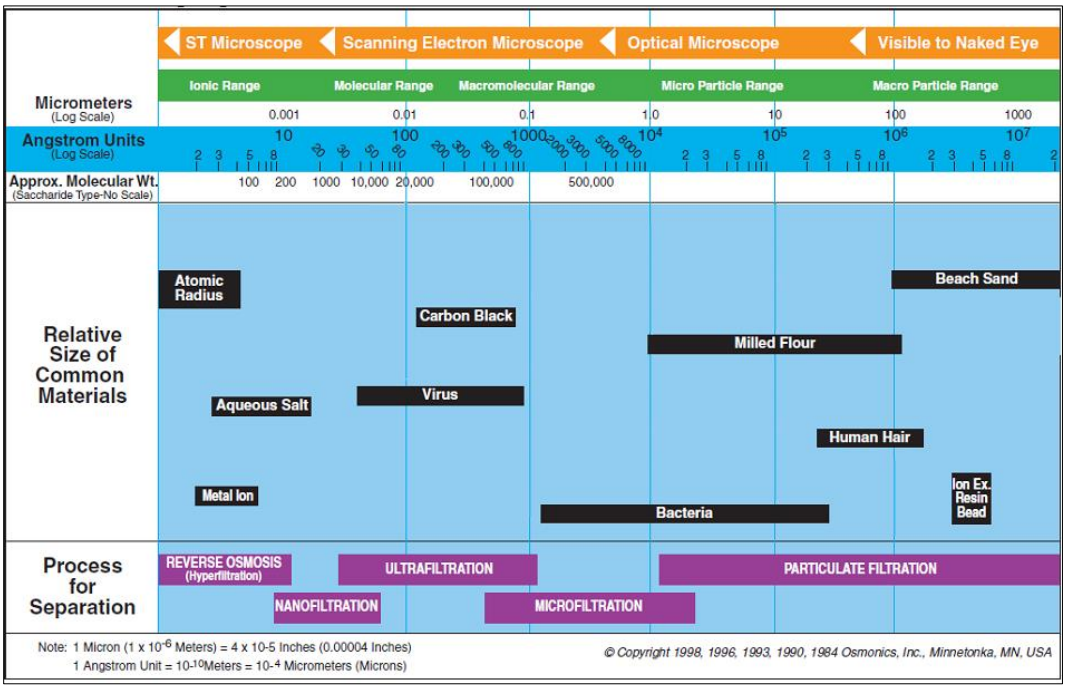

Figure 2.2: The total filtration spectrum with the types of membrane filtration regions highlighted in purple. [39]

Microfiltration (MF)

This type of filtration uses membranes with a pore size of 0,03-10 µm, a molecular weight cut-off (MWCO) that is greater than 1,00106 Daltons and a feed water operating under a pressure of 10-40 bars. MF is used to remove materials such as sand, clays, and silt among other macro particulates. [3] [4] [5]

Ultrafiltration (UF)

This type of filtration uses membranes with a pore size around 0,002-0,1 µm, a MWCO of $1{,}0010^4$ to $1{,}0010^5$ Daltons and operates under the pressure of 20-70 bars; some UF operate at much lower pressure levels and that has its advantages (mentioned below). UF is used to remove all microbiological organisms, some viruses and colloidal substances of suitable sizes. [3] [4] [5]

The main advantages of UF compared with other chemical clarification and disinfection are:

- No need for pre-chemical treatment of the feed (coagulation, flocculation, disinfectants, pH adjustments)
- Constant quality of the treated water with respect to particle removal.
- Process and plant compactness
- Simple automation

The only drawback is that fouling can arise would diminish the productivity of the membrane, thus cleaning in the form of reverse flow (back wash) or chemical treatment of the membrane might have to be employed. [4][5][8]

Nanofiltration (NF)

Nanofiltration (NF) uses membranes that have a nominal pore size of 0.001 µm and a MWCO of 10^3 to 10^5 Da. NF requires a higher operation pressure, much higher than MF or UF. The operational pressure is usually between 60-100 bars. They remove practically all microorganisms, viruses, natural organic material (NOM) and humus material. NF could render the filtrate water corrosive due to alkalinity removal; this require post-treatment to reduce corrosivity. [3] [4] [5] [9]

Reverse Osmosis (RO)

Reverse osmosis (RO) has pore size less than 0.001 µm and a very low MWCO. They are usually used for particles that have comparable sizes with the pores such as aqueous salts and metallic ions. RO requires very high operational pressure due to the high hydrodynamic resistance created by such a compact design. [3]

Some of the advantages of RO are:

- Removes nearly all contaminant ions and most dissolved non-ions
- Low permeate (filtrate) concentration possible
- Bacteria and particles are also removed
- Operational simplicity and automation

Some disadvantages of RO are:

- High capital and operating costs,
- High level of pretreatment is required in some cases,
- Membranes are prone to fouling [3] [4] [5]

2.1.3 Construction material

MF and UF membranes are constructed from a variety of materials such as cellulose acetate, polypropylene, polyethylsulfone (PES) or other polymers. UF and RO membranes are manufactured from cellulose acetate or polyamides materials in general. Cellulose-membrane is susceptible to biodegradation and must operate within a limited pH range usually between 4-8. [3] [4] [5] [10]

Membrane modules

Membrane filters are produced as flat sheet stock (spiral-wound membranes) or as hollow fibers which are then formed into different types of membrane modules. The membrane construction involves sealing the membrane material into an assembly (potting), such as the hollow fiber module. These modules are designed for durability and long term use. [3] [4] [5]

Spiral-wound Modules

In this module flat sheet stocks are wrapped around a central tube (permeate tube). The membrane is glued at the sides (figure 2.3). The porous spaces are sandwiched within the wrapping allowing the permeate to flow radially through the pores and preventing the membrane from collapsing under pressure. The feed flows in the membrane parallel to the permeate tube through feed spacers and out at the end of the module. Feed spacers are formed like a net with the role of keeping the membranes apart and determining the pressure drop of the module. [3] [4] [5]

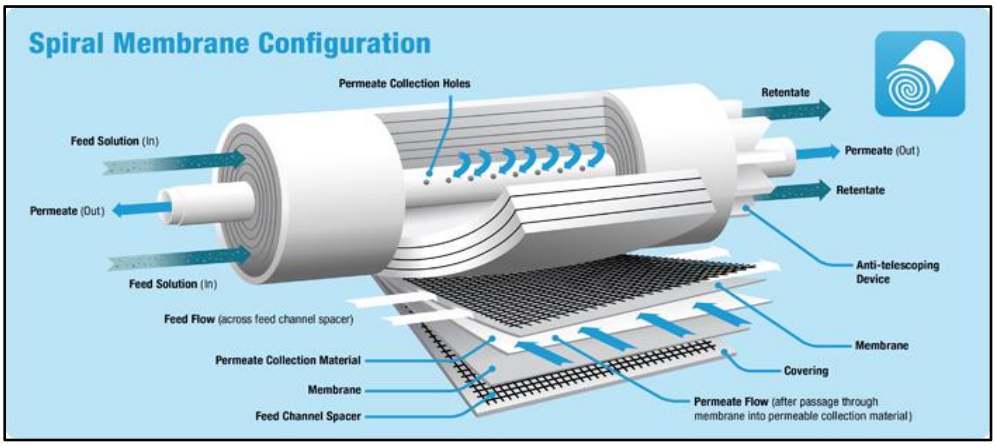

Figure2.3: Spiral wound filter showing the different layers that make up the filter module. [10]

Hollow-Fiber Modules

Hollow fiber modules (figure 2.4) are comprised of bundles of hollow fiber membranes (HFM), which are long and narrow (sometimes very narrow) tubes. These fibers are bundled in several arrangements. The fibers can be bundled together longitudinally, sealed (potted) in a resin on both ends and encased in a pressure vessel. These modules could be mounted horizontally, although vertical mounting is more usual (as in this study). [3] [4] [5] [10]

The number of fibers in a hollow fiber module ranges from several hundred to several thousand fibers. Some of the usual approximate ranges for hollow fiber construction are:

- Outside diameter 0.5 – 2.0 mm
- Inside diameter 0.3-1.0 mm

- Fiber wall thickness 0.1-0.6 mm
- Fiber length 1-2 meters [3]

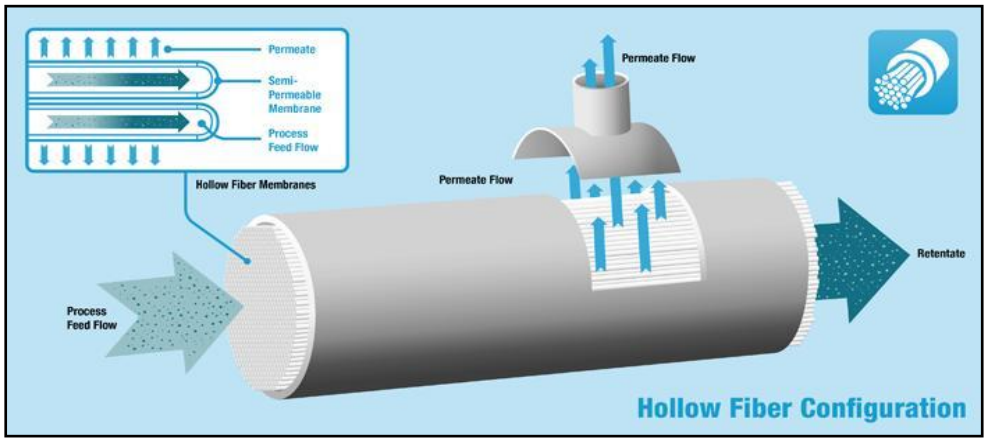

Figure 2.4: HFM filter module with the main in/out streams [10]

Operational modes

There are two types of modes that the HFFs operate in: an **inside-out** or **outside-in** mode (figure 2.5). In the inside-out mode the feed water enters the center of the fiber and is filtered radially through the fiber wall (fiber membrane) producing a permeate that is then collected from outside the fiber (in the mantel side).

The feed continues outside the module with a higher concentration than the fresh feed entering the module. In the outside-in process the feed water passes from outside the fiber (mantel side) where the permeate is collected in the center of the fiber. [3]

Most hollow fiber systems operate in direct filtration mode and are backwashed periodically to remove accumulated solids and reduce fouling in order to maintain their performance [3]. This is the case in both pressure driven inside-out (PDI) and pressure driven outside-in (PDO) formats.

The hydrodynamics in backwashing a membrane working in PDI mode are much more effective than in PDO formats caused by the fact that retentate is flushed out through a well-defined (circular) flow channel in PDI, whereas stagnant zones or, dead-zones, with very low flow velocity exist outside of the hollow fiber membranes at the bottom of PDO modules at backwash [11].

The back wash procedure is a very easy, practical and important step in maintaining the operational quality and extending the longevity of the HFF module [3].

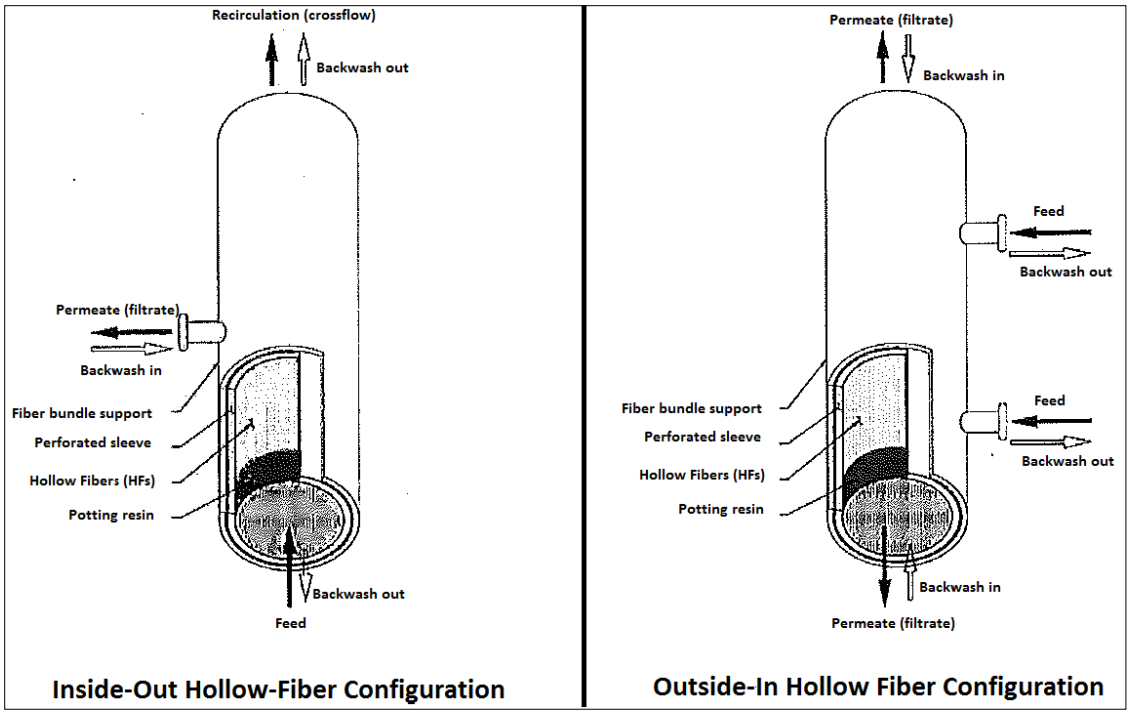

Figure 2.5: The two filtration configuration of a HFM module. [3]

2.1.4 Mass transport and membrane characteristics

Material separation through a filter membrane occurs due to the properties of the filter that enables some components to pass, while others remain in the feed and are up-concentrated. There are different types of filter material based on physical and/or chemical properties of the filter membrane. As a result there are different driving forces acting on the components in the feed that would eventually carry them through or onto the surface of the membrane [12] [13].

In UF it is the pressure gradient that is the driving force. The permeate flux can be best described by the Hagen-Poiseuille equation (HPE) if the pores are considered parallel:

$$J = \frac{\varepsilon r^2 \cdot \Delta P}{8 \eta \tau \cdot \Delta x} \qquad (eq\ 1)$$

Where $\mathbf{J}$ is the permeate flux through the membrane (l/m^2*s), $\boldsymbol{\varepsilon}$ is the surface porosity, $\boldsymbol{r}$ is the radius of the pores (all pores have the same radius) (m), $\Delta \boldsymbol{P}$ is the pressure difference (bars), $\boldsymbol{\eta}$ is the dynamic viscosity (Pa*s), $\boldsymbol{\tau}$ is the pore tortuosity (curvy channels) and $\boldsymbol{\Delta x}$ is the thickness of the membrane (m). [4] [5] [12]

The permeate flux through the fiber membrane is directly proportional to the pressure difference. It is also clear that the physical properties of the membrane such as pore radius and tortuosity affects the flux. The driving force has to overcome the concentration gradient (potential gradient) over both sides of the membrane; this is shown by Fick's first law of diffusion:

$$\mathbf{J} = -D \cdot \frac{\partial \theta}{\partial x} \qquad (eq\ 2)$$

Where $\boldsymbol{D}$ is the diffusion coefficient (m^2/s), $\boldsymbol{\theta}$ is the concentration for ideal mixture ($mole/m^3$) and $\boldsymbol{x}$ is the thickness.

The retention (also known as recovery) coefficient $\boldsymbol{R}$ is a dimensionless figure that gives information about the performance of the membrane usually expressed in percent. [12]

$$R = 1 - \frac{C_P}{C_F} \qquad (eq\ 3)$$

$\boldsymbol{C_P}$ is the concentration of the permeate and $\boldsymbol{C_F}$ is the concentration of the feed (mole/unit volume)

In addition to retention a mass balance across the membrane gives information about how much mass is being accumulated on the surface of the membrane due to fouling and how much mass is leaving out of the system [4] [5]:

$$M_B = \frac{Q_P \cdot C_P + Q_C \cdot C_C}{Q_F \cdot C_F} \qquad (eq\ 4)$$

Where $\boldsymbol{Q_P}$ is the flux of permeate, $\boldsymbol{Q_F}$ is the flux of the feed and $\boldsymbol{Q_C}$ is the flux of the concentrate (m^3/s or l/h); $\boldsymbol{C_P}$ is the concentration of the permeate, $\boldsymbol{C_C}$ is the concentration of the concentrate, and $\boldsymbol{C_F}$ is the concentration of the feed (mole/unit volume). [4][5]

2.1.5 Fouling

The accumulation of suspended material at the surface of the semi-permeable membrane creates concentration polarization and cake build-up, which affects the efficiency of MF and UF negatively. The major blocking mechanisms of MF/UF membrane process at initial and final stage are standard blocking of pore (caused by colloid materials) and cake blocking of pore (caused by suspended particles), respectively. [8] [13] [14]

The resulting hydraulic resistance of the cake layer affects the permeate velocity and the corresponding flux leading to a substantial loss of capacity or higher pumping energy cost. Frequent cleaning as well as replacement of membrane modules also significantly increases operation and maintenance cost. [4][5] [9] [13]

The layer of retained particulates then poses a resistance called concentration polarization resistance ($\mathbf{R_C}$). Some particles are absorbed onto the membrane or within the pores, creating the absorption resistance ($\mathbf{R_A}$); another type is the gel layer resistance which is when the concentration of the solute is high enough to build up a gel layer in the boundary layer. This resistance is denoted ($\mathbf{R_G}$). Pore blocking is another type of resistance which happens when a particle is lodged within the pore of the membrane; this resistance is denoted ($\mathbf{R_P}$) The membrane itself has a constant resistance ($\mathbf{R_M}$). The total resistance is denoted as $\mathbf{R_T}$; it is the sum of all the resistances mentioned (eq 5). [4] [5] [6] [13] [14]

$$R_T = R_C + R_A + R_G + R_P + R_M \qquad (eq\ 5)$$

Fouling tendency (FT)

Fouling can be calculated and detected using the ratio between the TMP and the flux of the permeate. The following equations (6 and 7) could both be used to calculate the fouling tendency (FT). The permeate velocity is governed by Darcy's law [13] [15]:

$$V_p = \frac{\Delta P}{\mu \cdot (R_m + r_c \Gamma)} \; ; here \; FT = \mu \cdot (R_m + r_c \Gamma) \qquad (eq\ 6)$$

where $\boldsymbol{V_p}$ is the permeate flow velocity (l/s); $\Delta \boldsymbol{P}$ pressure difference (or TMP); $\boldsymbol{\mu}$ the dynamic viscosity; $R_m = \frac{\Delta P}{\mu V_0}$ is the clean membrane resistance; $\boldsymbol{r_c}$ is the specific cake resistance and Γ the specific cake deposit (cake mass per square meter filter shell surface area);

Alternatively, FT can be calculated using the flux of the permeate as in the equation:

$$J = \frac{\Delta P}{\mu \cdot R_T} = \frac{TMP}{FT} ; here \; FT = \mu \cdot R_T \qquad (eq\ 7)$$

This value gives information about the filter system during operation. A constant FT means absence of fouling. An increasing FT with time means that fouling exists in the system. [4] [6] [13] [14]

Pore size could also contribute to increase in fouling; one type of fouling due to pore blockage is irreversible fouling, reducing the life time of the filter module. A feed that has particulates of comparable sizes to the pores in the membrane could foul worse than with a membrane with very small pores (relative to the particulates). A reversible fouling could occur which is easily washed away by reverse flushing (backwash). [12] [16]

HFM

The advantage of HFM over other membranes is the low tendency to foul and the ease to perform backwashes regularly. The hollow fibers themselves represent better and more efficient flow mixing devices. The module free from stagnant zones caused the turbulence promoters that touch the membrane surface or zones with low mixing intensity on the membrane surface situated in the center of the promoter grid [3] [5] [13]

Mitigation of fouling and membrane maintenance

The methods that would reduce fouling and prolong the lifespan of a membrane module are backwashing (BW) and chemical cleaning (CC). [3][4]

Backwashing

The BW process is utilized to remove contaminants accumulated on the surface of the membrane. The process requires that the flow direction is reversed for a suitable amount of time, 20 seconds up to 2-3 minutes. The slag is dislodged from the surface of the membrane (feed side) by the force and direction of the flow. The contaminants are washed away from the system through discharge lines. [3][5][17]

The BW procedure is recommended when the performance of the system exceeds certain operating limits, such as increase in TMP, operating time, volume and/or flux decline. Theoretically, the BW process should restore the TMP to its clean level, but that is not the case. Membranes usually exhibit a gradual increase in TMP after each BW indicating that some of the lodged foulants cannot be removed by BW only; they are then treated chemically through CC. [3] [4] [5]

Backwashing is almost exclusively associated with hollow fiber MF and UF processes. Because spiral-wound membranes generally do not permit reverse flow, NF and RO membrane systems are not backwashed. For these systems, membrane fouling is controlled with CC, flux control, and cross-flow velocity. [3] [4]

Chemical Cleaning

CC is used when befouling is not adequately removed by BW. It controls inorganic and organic scaling. Like the BW process, the goal of CC is to restore the TMP of the system to its clean level. There is a wide variety of different chemicals that may be employed for membrane cleaning, each removing a specific form of fouling. Acids are used to dissolve inorganic scaling. Strong bases are used to dissolve organic material. Detergents and tensides are sometimes used to remove organic and particulate foulants which were difficult to dissolve with a normal CC. [3] [4] [5]

The cleaning process starts off by recirculating a cleaning solution (i.e. strong base or H_2O_2) through high velocities in order to generate high turbulence (scouring action). A soak cycle (i.e. with an acid) follows the first recirculation phase. After the soak cycle the membrane is washed with clean water to remove residual traces of the cleaning solutions. The process might be repeated with the use of other chemicals to remove other types of foulants until the membrane is cleaned (table 2.1). [4] [6] [13] [14] [17]

BW, CC and filter modules

Backwashing may be conducted more regularly, while CC is done when necessary. Chemical cleaning is conducted on MF, UF, NF and RO systems; MF/UF undergoes CC only if backwashing fails to restore the module to its clean operational state. For NF/RO filters CC is the primary means of foulants removal; these modules do not allow reverse flow, which leads to a gradual accumulation of foulants that only a CC could remove. [3] [4] [14]

Only reversible fouling is mitigated using BW and/or CC. Membrane processes also experience some degree of irreversible fouling that is difficult to remove with BW or CC. All types of

membranes experience irreversible fouling which requires membrane replacement. [3] [6] [8] [14]

Operating membranes sub-critically gives membranes long lifespan, which reduces replacement and maintenance costs (by minimizing physical cleaning costs, i.e. membrane scouring or back-flush). [8] [17]

Table 2.1: The different chemicals that are usually used in industrial processes to clean filter modules. [3] [17]

Category	Chemicals used	Target Contaminants
Acid	Hydrochloric Acid (HCl) Citric Acid Phosphoric Acid (H_3PO_4)	Inorganic Scale
Base	Sodium Hydroxide (NaOH)	Organic material
Disinfectants and/or Oxidants	Sodium Hypochlorite (NaOCl) Chlorine Gas (Cl_2) Hydrogen Peroxide (H_2O_2)	Organics and Biological build-up
Surfactants	A variety of tensides	Organic and inert particles

2.2 Radiation in the backwash wastewater

2.2.1 Neutron activation

A neutron can have many types of interactions with a nucleus (figure 2.6). The types of interactions depend on the energy of the neutrons (fast, moderate, thermal) and the cross section (probability of an interaction to take place) of the interaction. Each category of interaction in the figure consists of all those linked below it. The total cross section expresses the probability of any interaction taking place. [18] [19] [20] [21]

The interaction is usually represented by a simple notation that gives a concise indication of an interaction of interest. If a neutron **n** impacts a target nucleus **T**, forming a resultant nucleus **R** and the release of an outgoing particle **g**, this interaction is represented as **T(n,g)R** (figure 2.6). The heavy nuclei are written outside the parentheses. [18] [19] [21]

Interactions are of two major types: **scattering** or **absorption**. When a neutron is scattered by a nucleus, its speed and direction change but the nucleus is left with the same number of protons and neutrons it had before the interaction. The nucleus will have some recoil velocity and it may be left in an excited state that will lead to the eventual release of radiation. When a neutron is absorbed by a nucleus, a wide range of radiations (see appendix A) can be emitted or fission can be induced. [18] [19] [21]

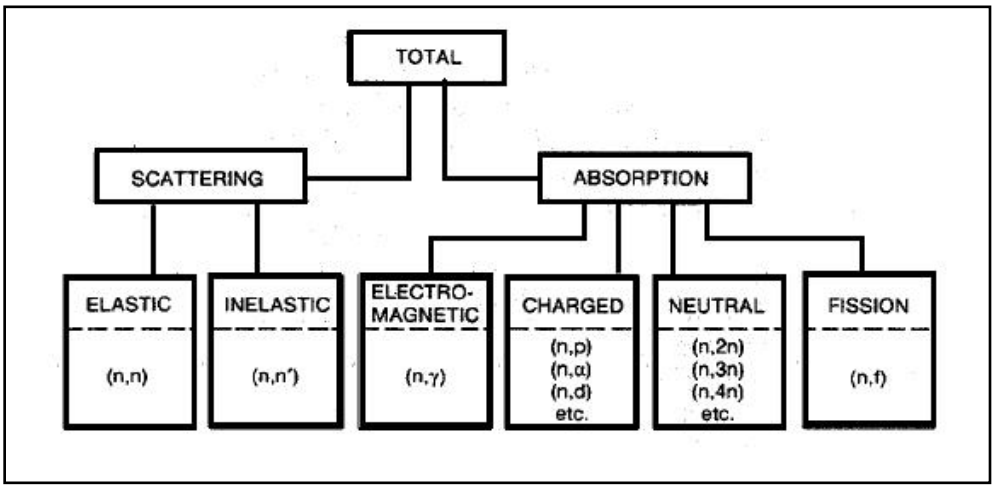

Figure 2.6: The different categories of neutron interaction with matter. The letters separated by commas in the parentheses show the incoming and outgoing particles (in, out). [21]

2.2.2 Activity in process water

There are three main sources of radioactive contamination in LWRs [18] [22]:

- fission products and actinides leaking out of fuel pins,
- coolant activation due to irradiation and
- activated corrosion products

The activity of the last one dominates in post-shutdown activity [22] [23]. Operating parameters of the reactor also strongly affect the types of radionuclides formed, the levels of saturation activity reached and the rates at which the saturation is reached [23]. These include the composition of the materials in contact with the coolant, amount and the types of the impurities present in the coolant, reactor power, residence time of coolant in core, temperatures and pressure, coolant flow rates, corrosion rates, filter efficiency and deposition rates of radioactive elements [23] [24].

The two primary radioactive isotopes generated in the core are Co-60 and Co-58:

- Co-60 forms as a result of neutron capture by naturally occurring Co-59 originating as an impurity in iron-nickel alloys used in reactor power plants or from stellites used as hard-facing materials in valves. The high neutron cross section of Co-59 and the high energy of the radioactive decay emissions from Co-60 cause it to predominate over radioisotopes formed from other elements that are present in higher concentrations. [25]
- Co-58 is formed as a result of a neutron replacing a proton in the nucleus of Ni-58, a naturally occurring isotope of nickel. [25]

There are future plans to prolong the fuel cycle from one year to 18-24 months [23] [24]. This means the concentrations of APs would increase in the water system putting more strain on the chemical and volume control system (CVCS) which might lead to an increase in occupational radiation exposure (ORE) with it [23] [24]. The ICRP-60 has suggested for that reason a more strict reduction of radiation in NPPs. This means that better ways in reducing the APs, such as membrane filtration, are needed as the fuel cycle is prolonged. [18] [22] [26]

2.2.3 Fission Products

The fission products from the defective fuel are partly released into the primary coolant. The magnitude and composition of the released fission products depend on the size of the defect and the number of defective fuel rods in the core. Some fission products are also released as a result of fission recoil from tramp uranium or natural uranium contaminate in the Zircaloy fuel cladding. [22] [23]

2.2.4 Activation Products

Activated corrosion products are produced by neutron activation of corrosion deposits on the surface of the fuel rods or in-core structure material. The now activated products are released from the fuel surface mostly under erosive and hydraulic shear forces. There is another factor contributing to a further increase their concentration and that is dissolution. [22] [25] [26]

Hydraulic shear forces in a nuclear reactor cause APs to be released from fuel surface deposits by abrasion in some cases and by dissolution in others. This means that there are two types of APs: soluble and insoluble; these are transported to various places in the circuits of the coolant of LWRs, some are deposited and re-released by turbulent flow of the coolant. The coolant activity is due to corrosion products is totally dependent on corrosion rates, flow rates, deposition and release rates of APs. [22] [25] [26]

The activity contribution from APs is dominated by the short-lived Mn-56 and Na-24. Most of the activity in the coolant is due to iron, molybdenum and cobalt. Some of those APs are Co-60, Co-58, Zn-65, Mn-65, Fe-59 and Sb-125 see also table 2.2 for some of the nuclear reactions involving neutrons and a corrosion product as a target. [22] [25] [26]

Table 2.2: neutron interaction with metals found in NPP metal alloys, only the most probable reactions are presented in the table. [27]

Radio-nuclide	Half-life	Parent	Possible production mode	Major Decay mode(s)	Daughter (s)	Mass activity (Bq/g)
Co-60	5,3 a	Co-59	(n,γ); σ:18,7barns	(β^-)	Ni-60	4.182E+13
Co-58	71 d	Co-59, Ni-58	(n,2n), (n, p)	(β^+, EC)	Fe-58	1.176E+15
Ag-110m	250 d	Ag-109	(n,γ); σ:4.7barns	(IT, β^-)	Ag-110, Cd-110	1.758E+14
Sb-125	2.76 a	Sn-124	(n,γ)Sn-125m σ:0.13barns Sn-125m(β^-,9.7 min)	(β^-)	Te-125	3.836E+13

2.2.5 Radioactive waste classification

NPPs produce radioactive waste during operation and decommissioning, which should be handled in such a way that the effects on the environment are minimized. The waste should therefore be stored as quickly as possible. [18] [28]

The nuclear waste produced in Sweden is categorized into:

- low-level waste,
- intermediate-level waste
- high-level waste.

The high-level waste consists mainly of spent nuclear fuel, whereas low- and intermediate level waste is created during operation and laboratory work.

The waste is categorized into short and long-lived waste depending on the amount of short- or long-lived nuclides that exist. Nuclides with a half-life under 31 years (i.e. t½ <31a) are categorized as short-lived waste. [18] [28]

2.3 Ion exchanger IXr

Ion exchange is a reversible process where a solid (IXr material) and a liquid interchange ions with no permanent change in the structure of the solid. [29] [30]

Conventional ion exchange resins (IXr) are made up of a cross-linked polymer matrix with a relatively homogeneous distribution of ion-active sites throughout the structure. IX materials are sold as spheres and sometimes as granules with a specific size and homogeneity to meet the need of a specific application. [30]

The following are some of IXs chemical properties [29]:

- **Total Capacity:** is the total number of sites available for IX. It is expressed on a dry weight, wet weight or wet volume.
- **Operating capacity:** is a measure of the useful performance obtained with the ion exchange material when it is operating in a column under a fixed set of conditions.
- **Kinetics:** is the rate of ion exchange that takes place. The exchange process involves diffusion through the film layer of the solution that is in contact with the resin. It also involves diffusion within the resin particle.

Two of the important resin types used in conventional IX are [29] [30]:

- **Anion Exchange Resins:** These are weak base resins that do not contain exchangeable ionic sites; they function as acid adsorbers. They are capable of sorbing strong acids with a high capacity and are readily regenerated with caustic.
- **Cation Exchange Resins:** These are weak acid cation exchange resins, primarily an acrylic or methacrylic acid, that has been crosslinked with a di-functional monomer.

2.3.1 Applications

Ion exchange is usually used in water treatment; it also provides a method of separation in many non-water processes. It has special usability in chemical synthesis, medical research, food processing, mining, agriculture and a variety of other areas. [29] [30]

Some of the applications of IXr in industry [29]:

- **Water Softening:** Hard waters, which contain principally calcium and magnesium ions, cause scale in power plant boilers, water pipes and domestic cooking utensils. Water is usually softened using IXr.
- **Dealkalization**: Is a process where hardness and alkalinity are removed from raw water before the water is used in the process.
- **Demineralization:** the raw water is passed through an intimately mixed bed of cation and anion so that metal ions and anionic ligands are removed from water.

- **Condensate Polishing:** Single or mixed bed IXr are used in deep bed filter demineralizers for reduction of particulate matter and dissolved contaminants in utility power plant condensates.
- **Waste Treatment:** Radioactive. Radiation waste systems in nuclear power plants include ion exchange systems for the removal of trace quantities of radioactive nuclides from water that will be released to the environment. The primary resin system used is the mixed bed.

2.4 Methods

2.4.1 Gamma activity measurements using a HPGe spectrometer.

The radiation sensitive part of a semiconductor detector is the semiconducting crystal. The material in these can be germanium or silicone. High Purity Germanium (HPGe) is a suitable material to use for gamma detection. [18]

The material has a valence band and a conducting band. The electrons in the material are almost all valence electrons, which are bound to a specific germanium or silicone atom with a specific energy. If this energy is given to the electrons, through for example radiation, the electrons are transferred up to the conducting band. [18]

The current that is created by the now mobile electrons is first amplified in amplifiers and the signal is then converted from analog to digital by an analog-to-digital converter (ADC). In the last step, the height (energy) of the pulse is measured and an energy spectrum is created by the multichannel analyzer (MCA). [18]

Different nuclides have different energies and through this it is possible to identify the nuclides that are present. The ability for the detector to resolve two peaks with similar energy is decided by the "Full width at half maximum (FWHM)" value. FWHM is defined as the width of the peak at the half height above the background and values lower than 1.8 keV are common at 1332 keV. [18]

2.4.2 Boric acid concentration

Boric acid is a very weak acid (pK_a=9.2) that behaves as a Lewis acid with water forming the tetrahedral anion $B(HO)_4^-$

$$B(OH)_3 + H_2O \leftrightarrow B(OH)_4^- + H^+ \qquad (eq\ 9)$$

It is analytically not feasible to titrate a weak acid with a strong base using conventional equivalence point detection directly. The addition of an auxiliary reagent to the solution that would cause the release of protons in a stoichiometric manner would make the titration feasible. [31] [32]

The transformation of boric acid to a strong acid is achieved by the addition of an organic compound with at least two hydroxyl groups (polyalcohol known as diols or polyols) such as mannitol (figure 2.7), sorbitol and others. This results in anionic boron complexes and the release of protons (equation 10, 11) [31]:

$$B(OH)_3 + H_2L \leftrightarrow B(OH)_2L^- + H_2O + H^+ \qquad (eq\ 10)$$

$$B(OH)_3 + 2H_2L \leftrightarrow BL_2^- + 3H_2O + H^+ \qquad (eq\ 11)$$

Where H_2L is a diol or a polyol

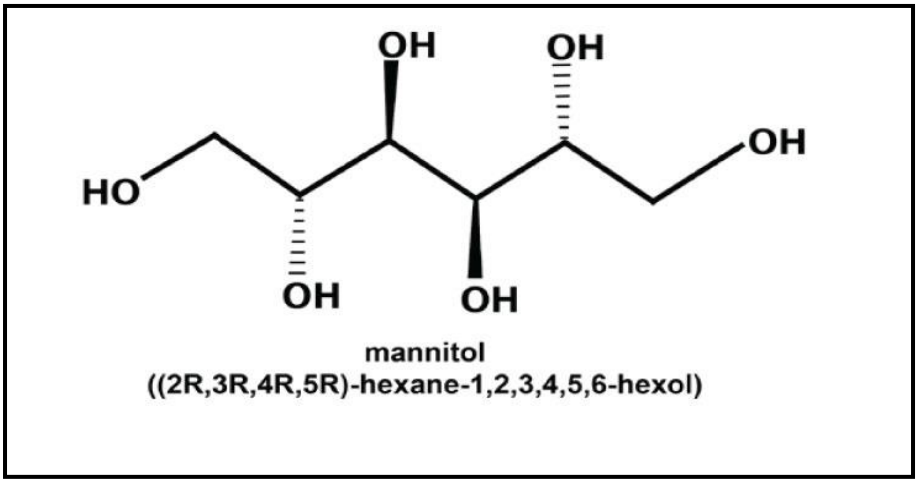

Figure 2.7: The chemical structure of mannitol a polyol used in determining the concentration of boric acid in samples.

2.4.3 pH

pH describes the hydronium ion, H_3O^+, molarity in a sample where pH is the tenth-logarithm of the hydronium ion molarity with changed sign. The solubility of metals increases steadily with decreased pH. This means that at a low pH the radioactive metal nuclides will generally exist as small unhydrolyzed ions and at a high pH in the form of hydrolysis complexes that may form larger particles. Extreme pH variations would certainly have an effect on membrane retention. [32] [33]

2.4.4 Conductivity

Conductivity is a measure of how well a solution conducts electricity. To carry a current a solution must contain charged particles, or ions. Most conductivity measurements are made in aqueous solutions, and the ions responsible for the conductivity come from electrolytes dissolved in the water. Salts (like sodium chloride and magnesium sulfate), acids (like hydrochloric acid

and acetic acid), and bases (like sodium hydroxide and ammonia) are all electrolytes (figure 2.8). [32] [34]

Although water itself is not an electrolyte, it does have a very small conductivity, implying that at least some ions are present. The ions are hydrogen and hydroxide, and they originate from the dissociation of molecular water. Conductivity measurements are widely used in industry. Some important applications are described below [32] [34]:

- Water treatment: The water contains contaminants, largely ionic, that if not removed will cause scaling and corrosion in plant equipment, particularly in heat exchangers, cooling towers, and boilers. It is also used to monitor the build-up of dissolved ionic solids in evaporative cooling water systems and in boilers.

The units of conductivity are Siemens per cm (S/cm). Derived units are µS/cm (one millionth of a S/cm) and mS/cm (one thousandth of a S/cm). S/cm is the same as the older unit (mho/cm). Certain high purity water industries, primarily semiconductor and pharmaceutical, use resistivity instead of conductivity. Resistivity is the reciprocal of conductivity. The units are MΩ cm. [34] [35]

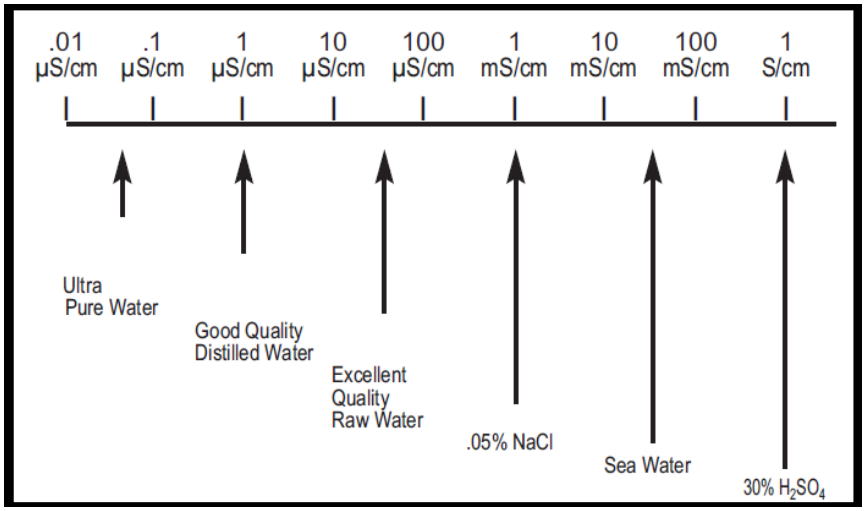

Figure 2.8: Conductivity spectrum with examples at each value. [35]

2.4.5 Scanning electron microscope (SEM)

SEM is a method of analysis where a sample is bombarded with an accelerated thin beam of electrons. Electrons scattering from the surface of the sample are measures by different detectors at different positions in the irradiation chamber. X-rays could radiate from the sample due to the electron bombardment due to excitation and de-excitation of electrons between quantized energy levels of some atoms in the sample. The photon has a distinct wavelength dependent on the atom it was released from. This distinction leads to the determination of the composition of the sample at cite of X-ray generation. [36]

A software assembles the information delivered by these electrons and an image of the sample is obtained. Images with high resolutions could be acquired with SEM which enables to get clear pictures of very small objects. [36]

2.4.6 ICP-MS

The ICP-MS instrument is designed to measure most of the elements in the periodic table (figure 2.9). Samples are introduced into argon plasma as aerosol droplets through a nebulizer. The plasma dries the aerosol, dissociates the molecules, and then removes an electron from the components forming singly-charged ions, which are directed into a mass filtering device known as the mass spectrometer ICP-MS systems employ a quadrupole mass spectrometer which scans the mass range; only one mass-to-charge ratio will be allowed to pass through the mass spectrometer; i.e. if the quadrupole was set to allow ions with a mass to charge ratio of 24/1 to pass through, it would be found that magnesium (Mg) ions, or even NaH^{+}, would be detected , while all other singly charged ions would not. [37]

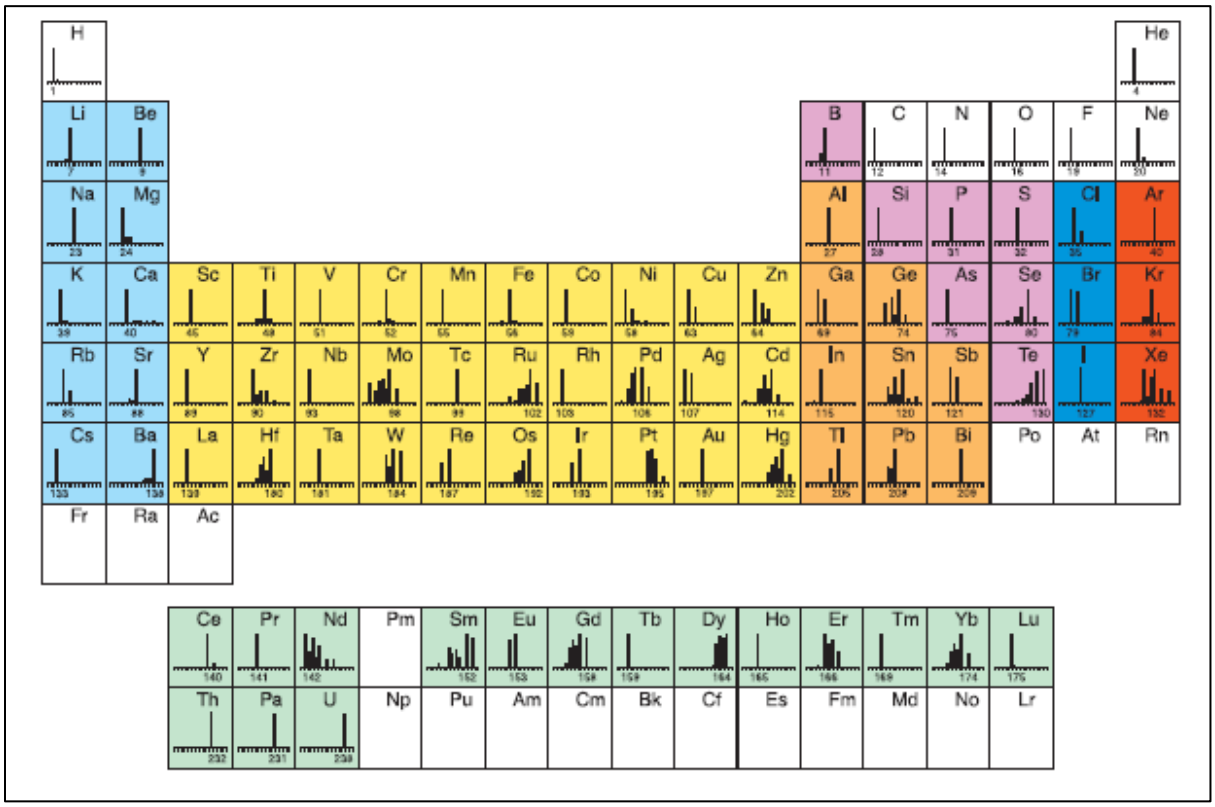

Figure 2.9: ICP-MS can detect most of the elements in the periodic table; the white blocks with no peaks are elements that the instrument cannot detect or they do not have natural occurring isotopes [37].

3 Experiments

This chapter describes the types and methods of analyses that were used in the experiments in the laboratory- and pilot-scale filtration tests.

3.1 Methods of analysis

All analyses were performed twice except those for the activity measurements due to detector availability.

3.1.1 Gamma activity measurements using a HPGe spectrometer.

The HPGe detector used is made by ORTEC of the type GEM-20190 P with a relative efficiency of 26.5 %; it uses Gammavision v.6.08 software, distributed by ORTEC, for energy peaks evaluation. The detectors are usually calibrated using a standard of mixed nuclides. Quality control or (QA) is performed on weekly bases at Ringhals laboratories.

Detectors are shielded from the surrounding by a layer of 10 cm copper-lined lead (R2C) and 5cm iron shield (electric cooled HPGe detector).

Samples were transported into 50 ml Cerbo containers, after rigorously shaking the sample bottles, which suited the geometry of the detector; it is also a geometry which minimizes the effect of sedimentation during measurements. Detection time depended on the radioactivity of the sample. Samples with low activities such as permeate and ion exchangers IXrs had 50 min and 9 hours respectively. Moderate and high activities of the feed and retentate samples had 20 and 10 min respectively. All samples had the same reference time (2013-04-23).

Sample dilution was applied to feed and retentate samples when the dead time limit of 50% was exceeded. A dilution of 50 to 1 was adapted. The activities were then recalculated back by multiplying with 50.

The activity concentrations were in the excess of $1.5 \cdot 10^3$ Bq/kg except for those after the IX. Statistical assessments tests were conducted where a sample would be measured for 2 hours that was done to see if there were large deviation in the acquired activities or if missing radionuclides in a given sample would reappear due to the increased counting statistics.

The software is programmed to calculate the uncertainties and the detection limit also known as the minimum detectible activity (MDA) for each measurement. It takes into consideration the statistical uncertainty in counts, uncertainties in the method of calibration and errors in calibrating instruments.

Uncertainties were already calculated by Gammavision, however some data were processed by addition or subtraction. To calculate the error propagation of independent errors the following equation was used:

$$\Delta Z = \sqrt{(\Delta x)^2 + (\Delta y)^2} \qquad (eq\ 8)$$

3.1.2 Boric acid concentration

The analyses were conducted using Mettler Toledo T70. 40 ml were taken from sample bottles of the feed, permeate and retentate. It was then divided into two equal volumes of 20 ml each. Titration was done twice using a standard titration method at Ringhals termed as BOR2. This method titrated in the concentration interval of 500 to 2000 ppm of boric acid.

The method has an uncertainty of 2% at room temperature of 20 ºC. The uncertainties were dropped since it was the same error in all the results and no remarkable deviations in concentrations were noticed. The machine undergoes calibration on weekly bases that is performed by the laboratory technicians at Ringhals.

3.1.3 pH

pH measurements were conducted at RC2 laboratories at 25ºC using WTW inoLab pH 730.

3.1.4 Conductivity

The instrument used to measure the conductivity of all the samples is WTW inoLab Cond 730, where the electrode LR 325/01 with serial number s/n 10240040. It has a cell constant (ε) of 0,100 and an uncertainty of 2% at 25ºC.

Uncertainties in the obtained values were also dropped since it had no effect on the total value. The conductivities are usually rounded into a whole number which makes ± 2% obsolete.

3.2 Laboratory scale

The filtration experiments with the HFM started off by using laboratory scale filter modules of different MWCOs. The aim of these experiments was to characterize the filtrate for its content of radionuclides and to build a benchmark when choosing a filter with a suitable molecular cut-off to serve the planned purpose. In this study the main goal was to filter out as much active particles as possible without any significant build-up of the concentration of boric acid.

The TT water sample used in the laboratory experiments was not pre-filtered as the pilot TT water was. This sample is taken directly from the TT.

Five different MWCOs were used and each had its own filter module of the model **Vivacell 70** (Appendix B: figure B1.7). All were used with the same volume of 100 ml of TT water that was not subject to the pre-filter procedure. The filtration procedure operated under a pressure of 4 bars as recommended by the manufacturer. The filtrate was then collected and analyzed using an HPGe spectrometer, a conductivity meter, pH and boric acid titration apparatus.

Gamma measurements were executed using a spectrometer belonging to the detector room of Ringhals Chemistry Department at Unit 1 and 2 (R2C) which was more sensitive than that which was used for the pilot scale samples. As a result, the benchmark was suitable to decide which filters were to be used had the filter modules not been pre-decided.

The MWCO of the laboratory filter modules were $3 \cdot 10^5$, 10^5, $3 \cdot 10^4$, 10^4 and $5 \cdot 10^3$ Da denoted as filter module 1, 2, 3, 4 and 5. Each produced a filtrate which was analyzed as mentioned before in this section. The membrane, however, was not analyzed in a gamma spectrometer because of incompatible filter module geometry with those available at Vattenfall's laboratories.

3.3 Pilot scale

Two filter modules were investigated: HFPM50 (filter A) and HFPM5 (filter B), having a MWCO of $5 \cdot 10^4$ Da and $5 \cdot 10^3$ Da respectively. The nomenclature of the filter modules is a shorthand method which is used by the manufacturer as follows:

- HF: Hollow fiber
- PM#: MWCO divided by 1000 in Da (see appendix F2)

The TT water used in the pilot experiment was pre-filtered using a 25 µm filter as seen in appendix C: figure C1.1.

3.3.1 Ultra filtration using filter A

A total volume of 2.7 m^3 were processed through this HFM; six batches were used; the first batch (Batch 0) used up 300 L as a test drive for the filter and the plant components; for this batch no feed, permeate or retentate samples were taken. The final retentate of batch 0 was drained into a special retentate tank.

The following batches (1-4) a total of 12 L of samples were taken out of the system using 1 L sampling bottles and a total of 15 L of samples were taken out of batch 5. These samples were taken at different time intervals. The drainage of batches (0-4) was collected in the retentate tank; the cumulative volume of that tank was named batch 5.

The flow rates of the feed, permeate and retentate were monitored and kept constant at 130, 80 and 50 l/h respectively. The changes in pressure drop, TMP temperature and RPM were noted and are displayed in (appendix C1). The TMP was then used to determine any fouling tendency using equation (7) see also appendix C1.1: equation C3.

The filter was subject to a BW at the end of each batch; the BW volume was collected in a 10 L container. The filter was subject to another BW just before the second batch a day later. Both BW volumes were added to the feed tank of the next batch. BW was used to remove any fouling accumulated at the surface of the HFM.

The HFPM50 was subject to a final cleaning in order to demonstrate if a chemical wash would bring the dose rate down to a level lower than that attained utilizing backwash. The chemical cleaning (CC) was divided into two stages:

> **1-** An alkaline part: where a 37% sodium hydroxide (NaOH) solution was used to create a pH 12.5 which would circulate in the system from a washing tank. A strong base was used to remove and break down any organic material on all the different surfaces of the

system. The time of circulation was around 1.5 hours. The dose rate build-up in the filter and other parts was measured (Appendix C1: figure C1.2.2)

2- A BW was applied, using water from the demineralized water system source known at Ringhals as 733, to wash off the basic solution and to wash out any mobile activity from the system. The dose build-up measurements are displayed in appendix C1 (table C1.2.21)

3- An acidic solution of (phosphoric acid, pH 2) was created to wash the system from any metal oxides that might have adhered to the different surfaces of the pilot plant. This time the system was soaked for 14 hours after which the dose rate was measured (Appendix C1: table C1.2.21).

Scanning electron microscope (SEM)

90 ml of the retentate sample that was obtained from batch 5 of Filter A was filtered with a 45µm Millipore filter paper. The cake collected on the filter was dried in an oven for 2 hours at 60ºC then left to cool down in a vacuum chamber. The dried cake was then analyzed with SEM of the type ZEISS Supar 40VP to determine the shape and size of particles in the sample. Images are found in appendix D2

Fibers from HFPM50 filter were also analyzed by SEM (Appendix D1); the aim was to have an image of the pores and particle sizes. These images would help investigate the fouling phenomenon.

ICP-MS

The ICP-MS used was of the Agilent 7500 CE model. The cake was weighed after drying in the vacuum chamber. The average weight of the Millipore filter paper was obtained by weighing four different Millipore filters. These steps are done to obtain the mass of the cake.

The the cake and its corresponding Millipore filter were then transported to a beaker containing 200 ml of Milli-Q water. Then an 8 % acid matrix (3 ml HCl and 5 ml HNO_3 per 100 ml) was created. The same procedure was followed to create the blank sample, using only a Millipore filter paper.

The samples were introduced into a microwave oven (300 ºC) and left inside for 2 hours. After that the samples were left to cool down and then transported into 25 ml plastic test tubes. The test tubes were used in the ICP-MS analysis, each sample was measured four times. No dilution was performed before the measurements were taken.

3.3.2 Ultra filtration using filter B

This HFM has pores that are ten times smaller in size than those of filter A. The idea is to attain a less active permeate, if possible, while keeping the concentration of boric acid constant. The results however differed from those done at the laboratory scale.

2.2 m^3 of TT water was used. This was divided into five batches that run through the module with the fifth batch as the concentration batch of the retentate volumes collected in the retentate tank from previous batches of the filter B.

There were suspicions that the activity concentration of the TT water was decreasing not due to elapsed time of decay, as the HPGe results are decay corrected to common reference date (2013-04-23), but rather due to the precipitations that co-precipitated the radionuclides to the bottom of the TT. Such a behavior was also observed in the collected samples were the dose rate was much higher at the bottom of the sample bottles than the top section. Samples of TT water were taken prior to mixing in the feed tank (there was no mixing in the TT) and were a part of the sampling procedure described before.

10 samples were taken out of each batch using 0.25 L bottles. The same procedure of analysis was followed with this filter module as the one before. One difference was that only one BW was applied at the end of each batch.

Fouling tendencies were obtained in the same manner as in the previous HFM. All data are found in tables of appendix C1.3.

Emptying the TT

No CC was applied; the next step was to empty the remaining of the TT water (around 3.2 m^3) and 200 L of samples from both of the pilot HFM modules. There was no intermittent BW after batch 5; that was to examine the extent of fouling and dose build-up the HFPM5 filter module could sustain before a BW at the end would theoretically bring down the dose rate build-up and retain the filter module close to its pre-operational efficiency.

The system was to run as a semi-batch tank where more TT water would be added as soon as the feed tank reaches 50 liters.

Dose build-up

Dose build-up in the filter was noted at each sampling using a dose rate meter to measure photon radiation (gamma and X-radiation) of the type 6150AD. The dose rate was also measured after each BW to examine its efficiency in decreasing the dose build up in the filter module.

The dose build-up in the filter module was measured and monitored at each sampling occasion; three positions were used to acquire dose rate readings: the top, middle and bottom sections of the two filter modules.

3.3.3 Process description

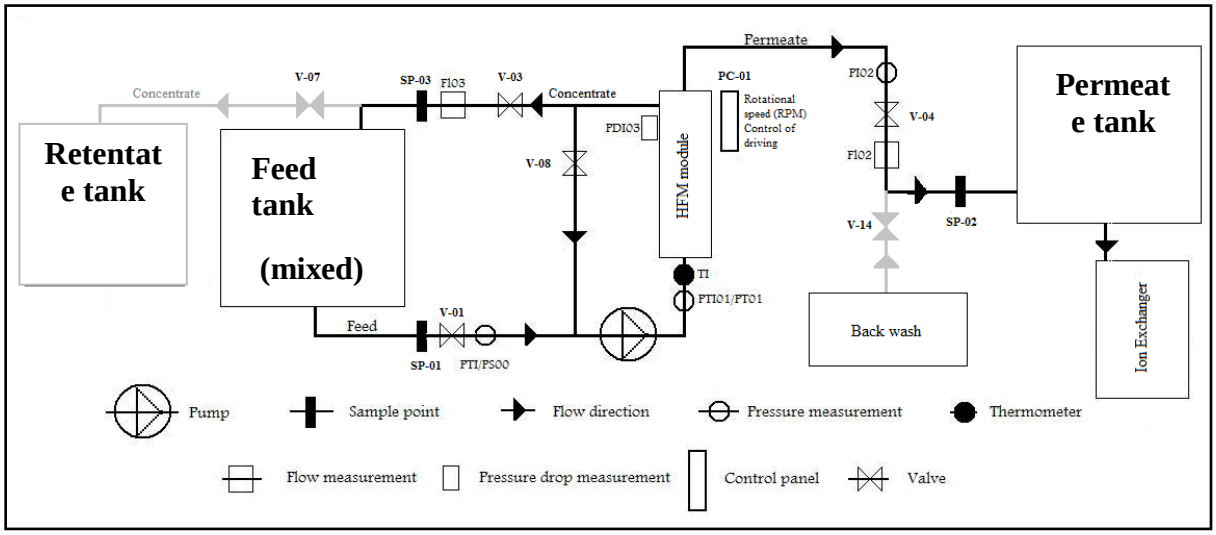

Figure 3.1: a schematic drawing of the pilot process; see even appendix F: figure F1.1.

The main feed flow rate through V-01 130 l/h, was divided between permeate 80 l/h and the retentate 50 l/h. The division was monitored by reading the flow meters FI02 and FI03 respectively. The volume of water in the feed tank was obtained from PTI/PS00 which measures the static pressure of the system as well (figure 3.1).

PIT01/PT01 shows the driving pressure of water entering the module. PDI03 shows the pressure drop along the filter module. PI02 is the pressure at the permeate side. PC-01 is a programmable control regulator with the function of maintaining a designated rotational speed of the pump as well as setting the driving pressure into the filter with a feedback from PTI/PS00. SP-01, SP-02 and SP-03 are the sampling points of the feed, permeate and retentate respectively.

V-07 is the valve through which the final retentate of each batch is drained into the retentate tank. TI is a thermometer measuring the temperature online. The TMP is the difference in the values of PTI/PS00 and PI02.

An air bubble mixer was manually made in order to mix the water in the feed tank to ensure a certain degree of homogeneity in the solution. It was equipped with an air filter to trap dust particles. The filter became a part of the pilot plant at batch 3 of filter A. The volume of the permeate water collected in the permeate tank was determined using a digital balance. The weight of 1 kg in the permeate tank corresponded to 1 liter of permeate. There are no name notations regarding this filter or the balance in the process schematic.

All notations are adapted from the process schematics in appendix F1.

4 Results and Discussions

This chapter displays some of the results that were obtained from the various experiments that were performed when analyzing water samples from both scales (laboratory and pilot). The task is to try to understand how the filter membrane affects the constituents of the TT water and with what efficiency.

4.1 Laboratory scale

4.1.1 Analyses and characterization of wastewater

The filtrates of each OT filter module were sent for analysis and their respective results are found in table 4.1 below. A more detailed description is found in appendix B1, where data obtained from each filter is displayed along with table of radionuclides in TT water and filtrate. A batch specific bar chart with activity contribution of the most probable gamma emitting radionuclides is presented in figure 4.2.

Table 4.1: Analysis results for measurements performed on the sampls acuired at the laboratory scale process.

Sample	Filter size (Da)	Volume used (ml)	Total activity concentration (Bq/kg)	Total activity concentration uncertainty (Bq/kg)	Boric acid concentration (ppm)	Conductivity (µS/cm)	pH	Recovery %
0	N/A	100	$3 \cdot 10^5$	10^3	568,4	3	6	N/A
1	$3 \cdot 10^5$	100	10^4	$2 \cdot 10^2$	566	4	6	96
2	10^5	100	$2 \cdot 10^3$	$6 \cdot 10^1$	565,3	3	6	99
3	$3 \cdot 10^4$	100	$2 \cdot 10^3$	$6 \cdot 10^1$	565,2	3	6	99
4	10^4	100	10^3	$4 \cdot 10^1$	566,7	5	6	99
5	$5 \cdot 10^3$	100	10^3	$4 \cdot 10^1$	564,8	26	6	99

There was a direct relationship between filtrate activity and filter size. There were no changes in the concentration of the boric acid which remained constant. There were no changes in the pH.

The conductivity remained relatively constant except after filter 5; that could be due to the decrease in the concentration of neutral particles that might have obstructed the mobility of ions between the electrodes since ionic species could easily pass unobstructed through the membrane MWCO, hence the increased ion mobility i.e. the conductivity increased as purification of TT water sample (sample 0) increased. The high recovery values coincide with those set by the manufacturer (Appendix F2).

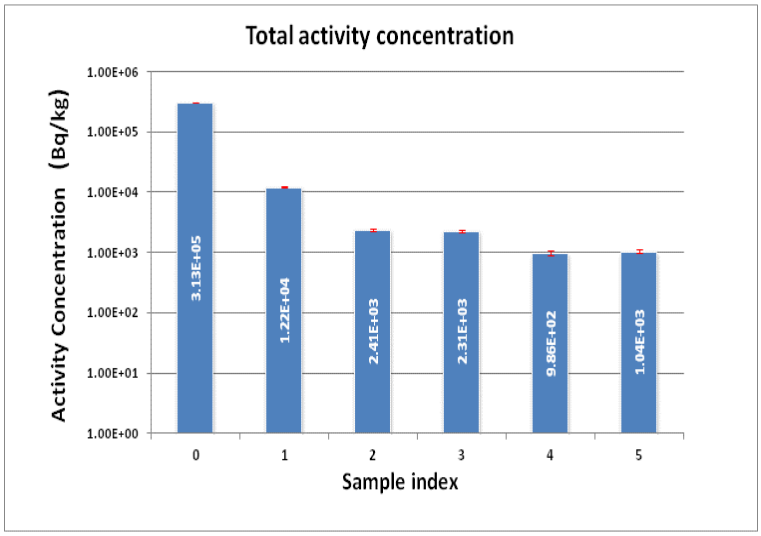

Figure 4.1: The total activity concentration in each sample including TT water; all detected at 95% confidence interval. The coordinate axis is plotted in logarithmic scale as it was difficult to compare sample (0) with the rest of the samples.

The differences in filtration efficiency are more evident in figure 4.1 which represents the total activity in the filtrates of each filter module. Total uncertainties were calculated by using equation 8 and are represented as red error bars wherever radioactivities are plotted.

Figure 4.1 shows that there are at least four discrete particle size populations of different MWCO.

1. The first size population (P1) is in the excess of $3*10^5$ Da; some of the activity is retained in the filter membrane of module 1.
2. The second size population (P2) is within the size boundary of [$3*10^5$, 10^5] Da. Module 3 produced a negligible decrease in the activity in its corresponding filtrate which means the same size populations (P1 and P2) where retained on the filter membrane of module 3.
3. The third size population is (P3) within the size boundary of [10^5, 10^4] Da. This follows the same explanation as P2 while the activity retained on the membrane of modules 4 and 5 is for size populations (P2 and P3).
4. The fourth size population (P4) is for particles that have passed through modules 4 and 5. The radioactivity found in the filtrate samples of these modules originates from particles that have at most a size population that is less than $5*10^3$ Da. A filter module with a MWCO of $2*10^3$-$1.5*10^3$ Da would be suitable to use for this inquiry.

Information about the radionuclides in the TT water and filtrate samples of each filter module were also acquired (figure 4.1). It is easy to associate a particle size to each radionuclide, knowing that those radionuclides are in particulate form.

Radionuclides that were below the MDA detection limits are not present. Therefore, the following result analyses are based on the remaining detected radionuclides: Co-58, Co-60, Ag-110m, Mn-54, Sb-124 and Sb-125.

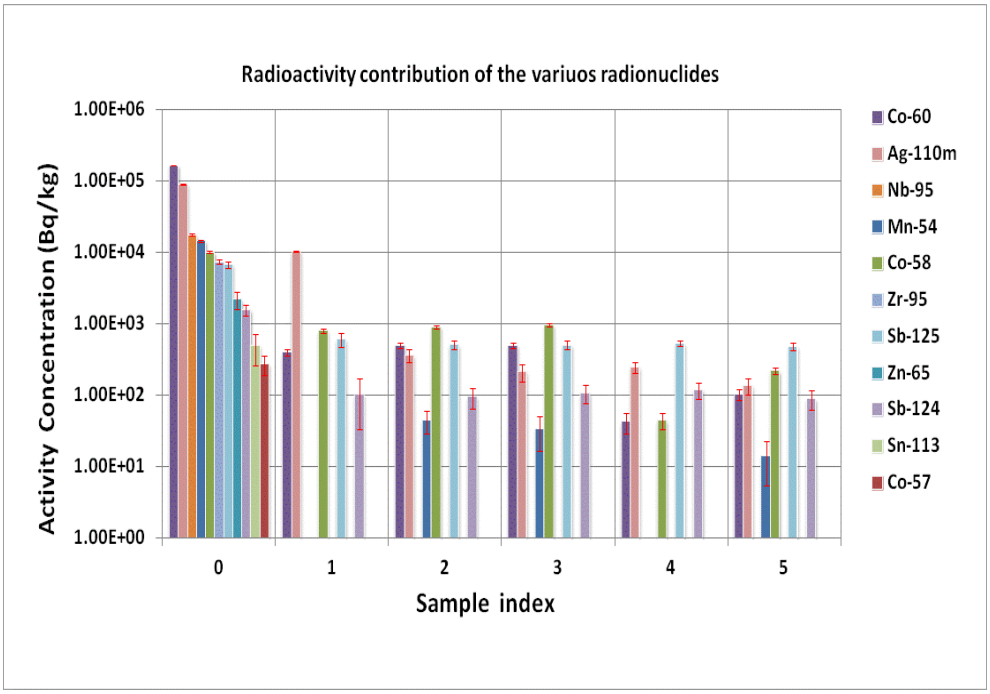

Figure 4.2: The various radionuclides detected in the permeate of each filter using a HPGe detector; sample index 0 is the TT water. Missing nuclides where found to be below their MDA.

The specific activity concentrations of radionuclides that were detected under an HPGe are displayed in figure 4.2; the activity concentrations are arranged in descending order starting with Co-60 and finishing with Co-57.

The filtrates of each OT filter module had only six radionuclides that were detected above their respective MDAs. Using the obtained information from the results that constitute figures 4.1 and 4.2 it was possible to put each radionuclide, which is in particle form, in different particle size population groups as seen in table 4.2.

Table 4.2: The probable particle size population groups that each of the radionuclides is thought to be involved in; these groups were deduced from the analyses of the results in figures 4.1 and 4.2.

Particulate Radionuclide	Particle Size group
Co-58	P1, P3, P4
Co-60	P1, P3, P4
Mn-54	P1, P4
Ag-110m	P1, P2, P4
Sb-124	P1, P4
Sb-125	P1, P4

4.1.2 Decontamination

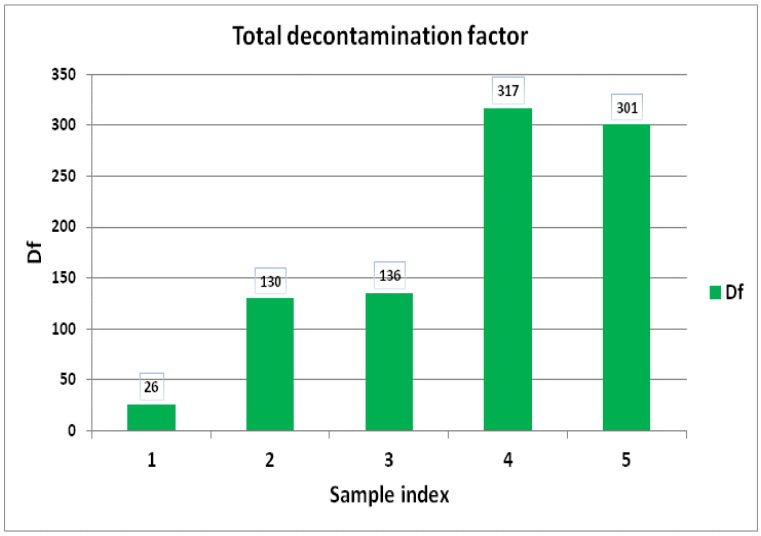

Figure 4.3: The total Df of each module; Df increases as MWCO increases.

The total Df is presented in figure 4.3 and explained in appendix C1.1; it shows that the last two modules (index 4 and 5) are best suited for the TT water type used in this study. The same particle size differentiation that was tabulated in table 4.2 is observed here as well.

Figures 4.1 and 4.3 also show that there are no major differences in decontamination when using a 10^4 Da or $5*10^3$ Da. The only difference was the time it took to filter 100 ml of TT water through filter module 4 and 5 which was 12 min and 40 min respectively under an operational pressure of 4 bars.

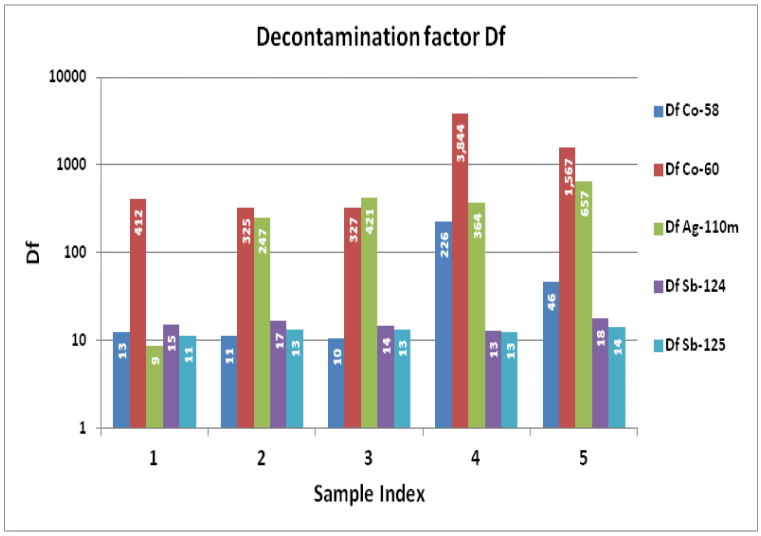

Figure 4.4: the decontamination factor of the laboratory scale filters for each radionuclide.

Figure 4.2 and 4.4 are very similar. The bar chart might seem odd as the Df in not following a stable manner which would be either constant or increasing. The solution in the TT water however cannot be considered a true solution as it contained different particle sizes at different positions of the solution matrix despite rigorous shaking. All samples were taken from the same position within the TT water sample after each shaking.

4.2 Pilot scale

All analyses were performed twice except those for the activity measurements due to detector availability. The values did not deviate significantly from each other maintaining a 2% uncertainty according to manufacturer's calibration methods adapted at the department of Chemistry at Ringhals. There was no increase in the concentration of boric acid in all of the samples (remained around 565 ppm). There was an increase in conductivity as the concentration of the samples of the pilot scale process increased, but that was not because of boric acid.

4.2.1 Filter module A

The total activity concentrations are presented in table 4.3 below. These are the last sampling points before the BW treatment. Detailed tables with individual radionuclides and process parameters are found in appendix C1.2.

Table 4.3:Activity concentrations of the third sample point of each batch along with the corresponding uncertainties.

	Batch 1 (Bq/kg)	Batch 2 (Bq/kg)	Batch 3 (Bq/kg)	Batch 4 (Bq/kg)	Batch5 (Bq/kg)
Feed 0	$1.5 \cdot 10^5 \pm 5.8 \cdot 10^3$	$1.4 \cdot 10^5 \pm 5.5 \cdot 10^3$	$1.4 \cdot 10^5 \pm 5.5 \cdot 10^3$	$9.7 \cdot 10^4 \pm 4.3 \cdot 10^3$	$4.1 \cdot 10^5 \pm 2.7 \cdot 10^4$
Feed	$1.2 \cdot 10^6 \pm 4.3510^4$	$10^6 \pm 4.0 \cdot 10^4$	$1.4 \cdot 10^6 \pm 5.4 \cdot 10^4$	$1.1 \cdot 10^6 \pm 4.09104$	$7.2 \cdot 10^5 \pm 4.2 \cdot 10^4$
Permeate	$2.4 \cdot 10^3 \pm 2 \cdot 10^2$	$2.4 \cdot 10^3 \pm 2.0 \cdot 10^2$	$2.4 \cdot 10^3 \pm 1.8 \cdot 10^2$	$2.5 \cdot 10^3 \pm 2.3 \cdot 10^2$	$2.1 \cdot 10^3 \pm 1.9 \cdot 10^2$
Retentate	$2.6 \cdot 10^6 \pm 9.4 \cdot 10^4$	$2.0 \cdot 10^6 \pm 7.6 \cdot 10^4$	$2.9 \cdot 10^6 \pm 1.1 \cdot 10^5$	$2.1 \cdot 10^6 \pm 8.1 \cdot 10^4$	$1.5 \cdot 10^6 \pm 7.8 \cdot 10^4$

In table 4.3 the total radioactivity of feed 0 along with samples from the third sample point are presented along with their total uncertainty calculated at a 95 % confidence interval.

Batch 5, as explained in the experiment section, is the collection of the retentates of batches (1-4). Further data and detailed batchwise process description of filter A is found in appendix C1.2.

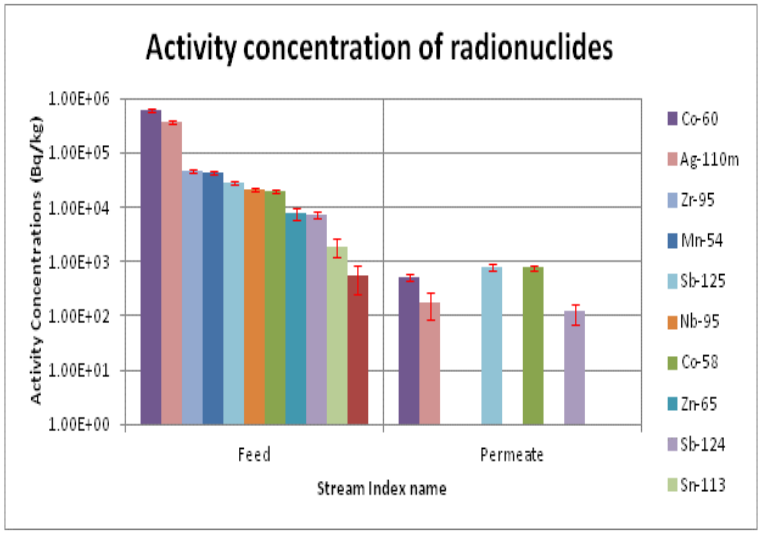

Figure 4.5: The activity concentration of each detected nuclide in the feed and permeate; a general profile found in all the analyzed samples.

Figure 4.5 represents the third sampling point of batch 1. The radionuclides are sorted out in the same manner as in the laboratory scale experiment. The permeate activity concentration was about 450 times less than that of the feed. The values used to construct this bar chart are found in appendix C1.2. The figure shows a difference in the activity concentration of the various radionuclides in a batch. Radionuclides left out of the figure were found to have a permeate concentration below the MDA for the detector system.

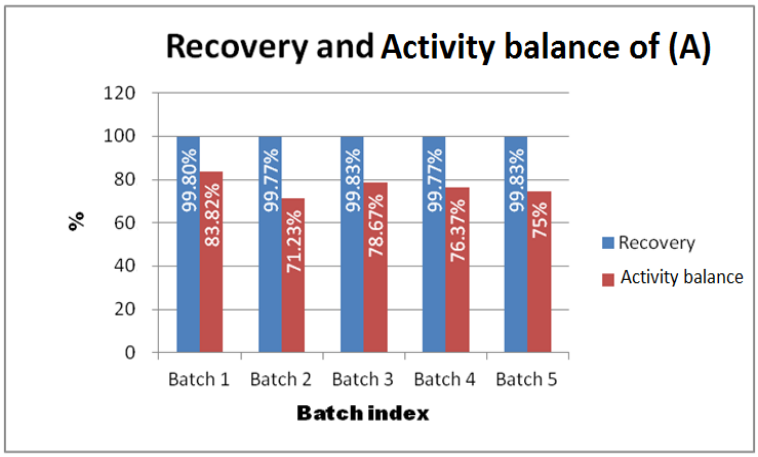

Figure 4.6: Recovery and Activity balance of the various batches in filter A.

A bar chart representing the recovery (the retention of activity in the retentate) and mass balance of each batch is created using equations 3 and 4 (appendix C1.1) respectively (figure 4.6). The recovery results are the same as those of a $5 \cdot 10^4$ Da in the laboratory scale experiment (table 4.1), if interpolated between 10^5 and $3 \cdot 10^4$ Da. The mass balance of batch 2 is a result to the error made when losses of the feed tank were drained into the retentate tank; this lead to a lower

activity in the final retentate of the same batch. Otherwise, mass balance with respect to activity was expected to decrease due to fouling and sludge formation in the plant.

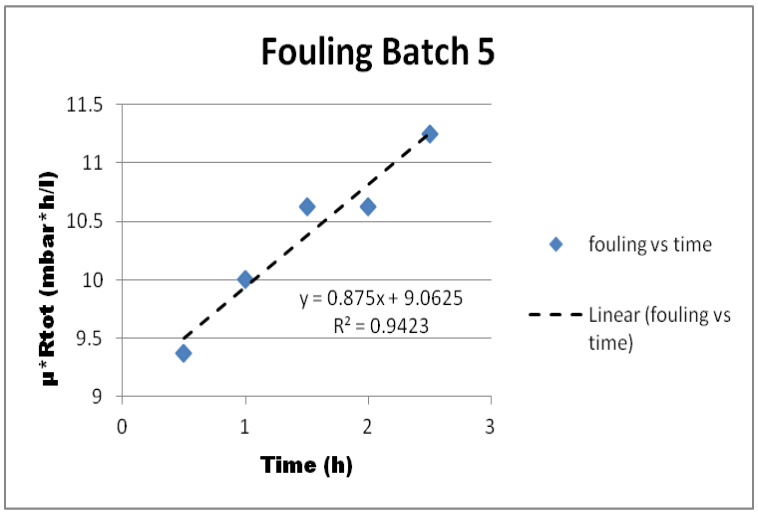

Figure 4.7: Fouling tendency at batch 5 of Filter A.

There was no fouling in batches (1-4) and a clear case of fouling in batch 5 (figure 4.7). As explained in the theory section under fouling, there was another reason for that phenomenon to occur as there was a considerable amount of sedimentation in the retentate tank caused by the agglomeration of particulates in a higher concentration than the original TT water.

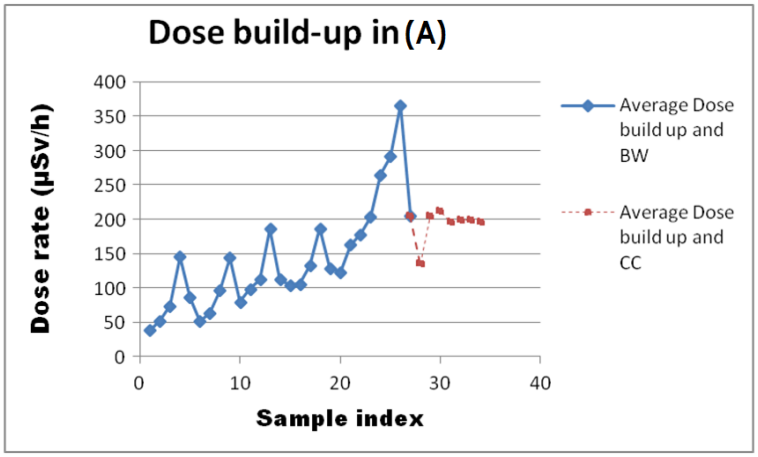

Figure 4.8: Averaged dose rate build-up in filter A; tops represent the maximal dose rate build-up in every batch, while troughs represent dose rates after a BW. The blue line represents the process with BW while the red line represents the CC process after the end of batch 5.

Figure 4.8 represents the dose rate build-up in filter A with respect to sample index. Maxima represent the final dose rate build-up before the BW, while minima are dose rate build-up measurements after a BW. There was a decreased in the Dose rate after each BW. A CC was

applied after batch 5 in order to further decease the dose rate build-up. However, this was not efficient to clean the filter back to original state.

The results were unexpected as the dose rate deceased at first then it seemed to increase instead of decreasing before reaching a stable dose rate build-up in the filter module. That meant that somewhere in the system there was slag build up that became mobile due to the first stage of the chemical wash using NaOH. The pump was measured before the wash up and after, the values before were 1mSv/h and after it decreased to 710µSv/h. The drain samples of the CC were not analyzed due to loss of samples into a waste collection tank leading to loss of vital data that might have been used to evaluate the CC process.

4.2.1.1 SEM

Fibers of filter module A were taken from the bottom section (Appendix D1), where BW was considered to have the least effect, and scanned with SEM revealing the source of dose build-up in the filter module even after BW and CC (figure 4.9). The majority of the pores appear to be partially or fully blocked except for some few that are intact. However, due to the stable permeate flow of 80 l/h throughout the process suggest that the blocked pores are permeable to water or what appears to be a pore-blockage is just a thin film of sludge formed at the end of the CC.

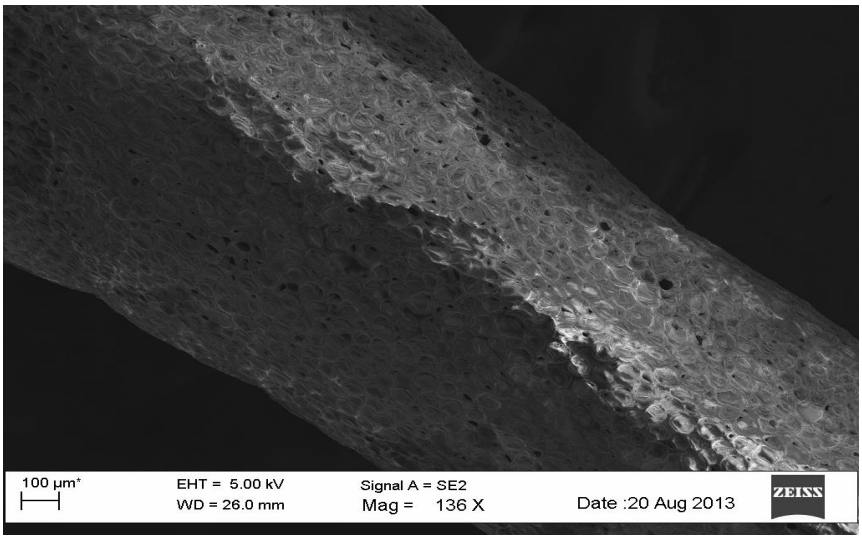

Figure 4.9: SEM image of a fiber belonging to HFPM50 module; the blockage of pores is visible; this fiber underwent both BW and CC, so this constitutes an irreversible fouling.

The obtained samples started to sediment after sometime which means that there are very fine particles that seem to coalesce under the influence of increased particle concentration and time (Appendix D2). Another probable reason, but not yet tested, is the air used to mix the feed tank

was oxygenated and could have caused the formation of oxides or introduced iron oxides into the solution causing flocking or co-precipitation.

The conclusion was already established that all water samples are not true homogeneous solutions, even though shaking was applied before measuring their activities. Further investigation (SEM and ICP-MS) of the final retentate of batch 5 of filter A, where a 0.45micron Millipore OT filtration was used, showed that around 92% of the activity was retained in the cake formed and only 8% in the filtrate (see appendix C1.2: figure C1.2.18).

Measurements with the HPGe detector were made using a 50 ml cerbo container. So sedimentation would have very little effect on detection efficiency. The purpose of investigating the sediments was to examine if most of the activity was found in the sediments and not the bulk of the solution.

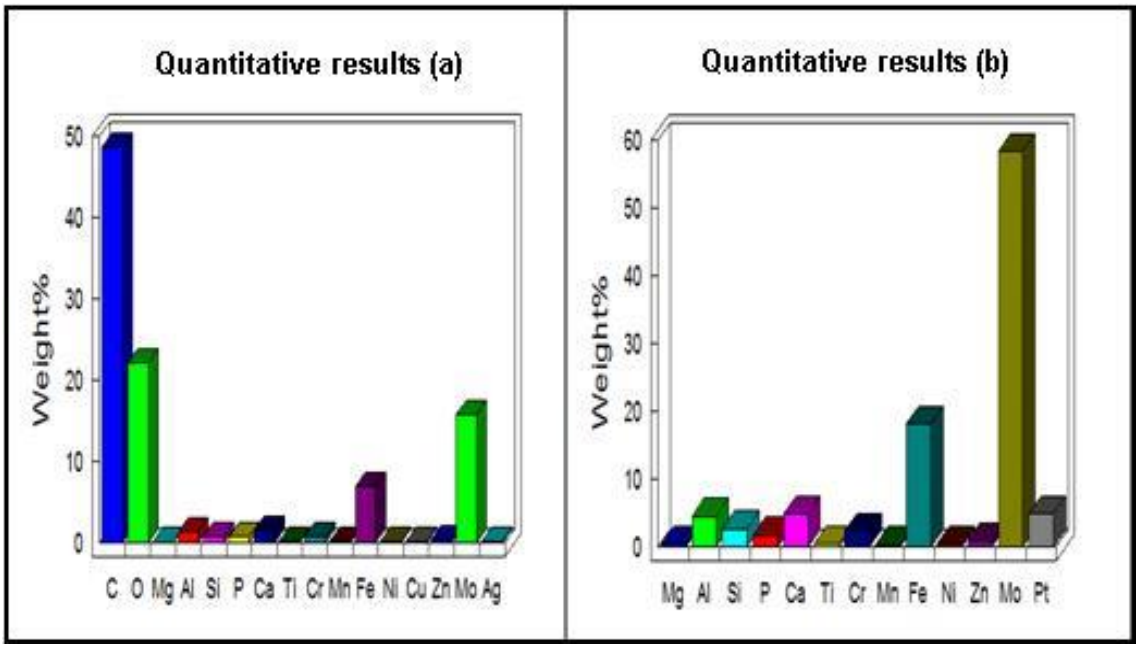

Figure 4.10: SEM quantitative results revealing the probable constituents in the scanned sample: (a) with organic material and (b) after filtering out the effect of organic material.

The figure above (figure 4.10a) shows the composition of the cake formed due to OT filtration. The total percentage by weight of carbon and oxygen in the sample has two origins: traces of the filter paper and the sample at hand. The interesting results for this study were the inorganic minerals and metals in the sample, so a second analysis was carried out by filtering any emissions from carbon and oxygen.

Figure (4.10b) gives a better understanding to the mineral content of the cake and as a result the contents of the sediments in the TT and sample bottles. In that figure Molybdenum formed 58% the weight of the cake (0.018 g) in the filtered volume (0.09 L). Compensating for concentration effect compared to the TT water (which was a factor of 13), the concentration of Mo was found to be 9 ppm and 3 ppm for Fe in the TT water.

A probable reason to why Mo exceeds the concentration of Fe is that sodium molybdate (Na_2MoO_4) is added as a corrosion inhibitor in the component cooling system also known as system 711 at Ringhals 3 and 4.

4.2.1.2 ICP-MS

Table 4.4 displays the results of the ICP-MS analysis. As seen below iron (Fe) was the dominating element in the solution of the cake sample. There was no calibration for molebidium (Mo) in the ICP-MS as a result, no data about the content of Mo in the sample. The results of table 4.4 confirm the findings of the quantitative results acquired from the SEM analysis.

Table 4.4: ICP-MS results after analyzing a solution of the cake with millipore filter and only millipore filter (blank).

Element	Mass (g/mole)	Detection limit (ppb)	Conc. blank (ppb)	SD (ppb)	Conc. Sample (ppb)	SD (ppb)
Mg	24	2.26E-01	1.33E+01	0.2	2.34E+02	0.38
Al	27	2.27E-01	5.95E+00	0.2	2.21E+03	10.5
Ca	44	6.36E-01	8.80E+01	2.7	2.92E+03	21.4
Cr	52	9.35E-02	3.72E+00	0.05	1.69E+03	15.3
Mn	55	8.81E-04	6.60E-01	0.007	1.09E+02	1.15
Fe	56	1.14E-01	1.90E+01	0.15	1.61E+04	197
Co	59	2.44E-03	5.30E-01	0.007	1.92E+01	0.23
Ni	60	5.61E-02	8.00E-01	0.036	5.04E+02	8.9
Cu	63	2.67E-02	9.90E-01	0.017	1.69E+02	1.23
Zn	66	2.36E-01	4.67E+00	0.053	1.02E+03	7.61
Zr	90	9.73E-03	7.00E-02	0.015	4.82E+01	0.47
Nb	93	2.22E-02	1.60E-01	0.066	2.90E+01	0.16
Ag	107	5.78E-03	2.00E-02	0.005	1.47E+02	1.78
Sn	118	3.48E-02	6.00E-01	0.043	5.35E+01	0.4
Sb	121	2.86E-02	2.59E+00	0.05	6.00E+00	0.04
Sb	206	1.16E-02	3.00E-01	0.012	1.24E+02	0.9
Sb	207	5.37E-03	3.20E-01	0.017	1.26E+02	1
Pb	208	3.96E-03	3.10E-01	0.006	1.26E+02	1.13

4.2.2 Filter module B

The second experiment with filter module B had to consider the activity of TT water as an extra parameter. Having noticed the heavy sedimentation under the influence of increasing concentration and time, the activity of TT water was measured to examine the significance of such decrease.

TT activity was decreasing with time due to sedimentation; a conclusion grounded by the OT batch 5 retentate experiment and by visual inspection of the TT when it was empty (table 4.5). The walls of the tank had the characteristic brown sludge that was found at the bottom of the

sample bottles. Radiation protection staff also noticed the increase in activity at the bottom of the TT compared with its bulk.

The procedure was the similar to that of the previous filter module but this time the activity of TT water was monitored and analyzed. More detailed data concerning the samples is found in appendix C1.3.

Table 4.5: Activity concentrations of the third sample point of each batch along with the corresponding uncertainties

	Batch 1 (Bq/kg)	Batch 2 (Bq/kg)	Batch 3 (Bq/kg)	Batch 4 (Bq/kg)	Batch 5 (Bq/kg)
TT	**5.83104 ± 2.53103**	**5.61104 ± 2.45103**	**4.73104 ± 2.14103**	***4.54104 ± 2.03103***	***4.89105 ± 2.01104***
Feed 0	**5.70104 ± 2.52103**	**5.87104 ± 2.57103**	**5.11104 ± 2.27103**	***4.57104 ± 2.10103***	***5.12105 ± 2.11104***
Feed	**3.21105 ± 1.29104**	**3.97105 ± 1.57104**	**7.06105 ± 2.83104**	***1.33106 ± 5.29104***	***1.32106 ± 5.42104***
Permeate	**2.04103 ± 1.40102**	**2.08103 ± 1.34102**	**1.98103 ± 1.48102**	***2.00103 ± 1.37102***	***2.35103 ± 1.48102***
Retentate	**6.32105 ± 2.56104**	**8.09105 ± 3.24104**	**9.25105 ± 3.78104**	***1.61106 ± 6.44104***	***2.49106 ± 1.06105***

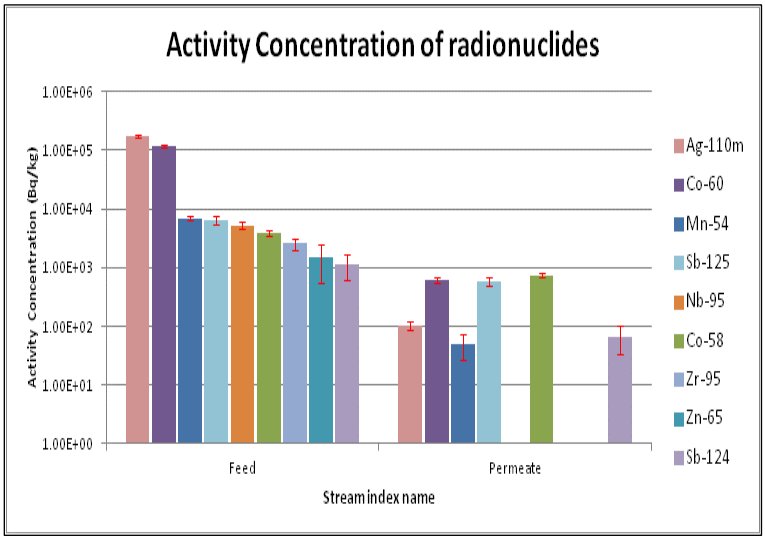

Figure 4.11: The activity concentration of each detected nuclide in the feed and permeate; a general profile found in all the analyzed samples.

Figure 4.11 above shows the same radionuclide distribution between the incoming feed and permeate. The permeate of this filter module contained the same radionuclides as in the previous filter module (figure 4.5). Radionuclides left out of the figure were found to have a permeate concentration below the MDA for the detector system.

The activity balance and recovery were calculated using the data in the appendix C1.3 and equations 3 and 4. Roughly the same results were obtained as with the previous module, except for the last mass balance. The severe decrease in the mass balance was noticed especially after that fouling started at batch 2 of this experiment; a hypothesis was that the BW was not efficient enough with only 1 bar so an increase in BW pressure to 4 bars was applied, which resulted in a better cleaning thus augmenting the mass balance in batch 5 as shown in figure 4.12

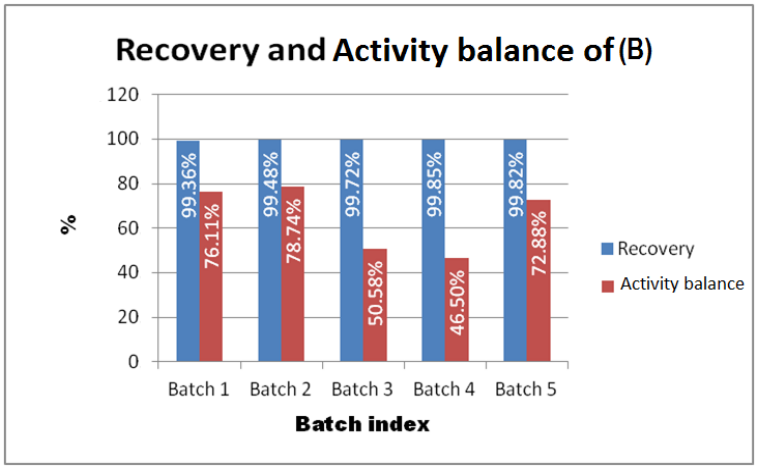

Figure 4.12: Recovery and Mass balance of the varios batched in filter B

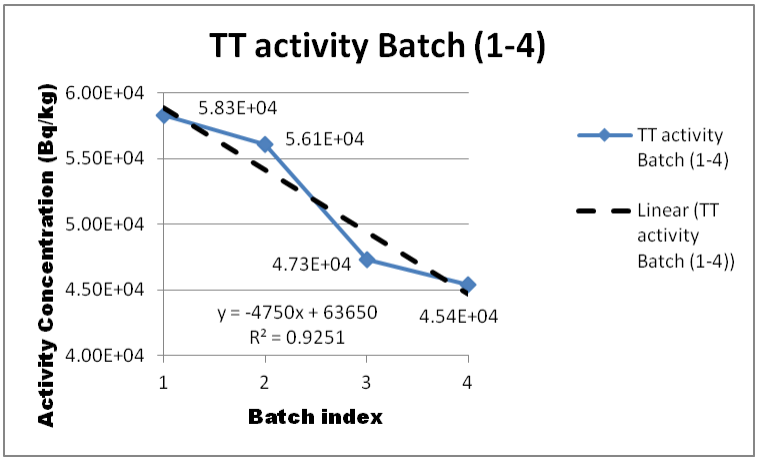

Figure 4.13: Activity concentration profile of TT water with respect to batch index. It shows a decrease in the water activity to the flocking and sedimentation of active particulates.

TT activity was plotted with respect to batch index (figure 4.13) as a qualitative overview to prove that the increased sedimentation in the TT removed part of its activity. A clear evidence of decrease activity is presented by the above figure.

Fouling was observed in batch 5 (Appendix C1.3), but was mitigated with the use of BW. Earlier fouling with filter B was expected, as experiments with that filter size (done at the laboratory scale) took long time to perform (appendix B1: table B1.3) and produced fewer particles in the filtrate of filter module 5 as the majority of them are thought to belong to particle size population larger than P3.

Filter B showed the same tendency to foul as its predecessor and that the effect of the BW procedure was effective as it washed away a great portion of the foulants, thus keeping the dose rate build-up fairly under 200 µSv/h until batch 5 (figure 4.14).

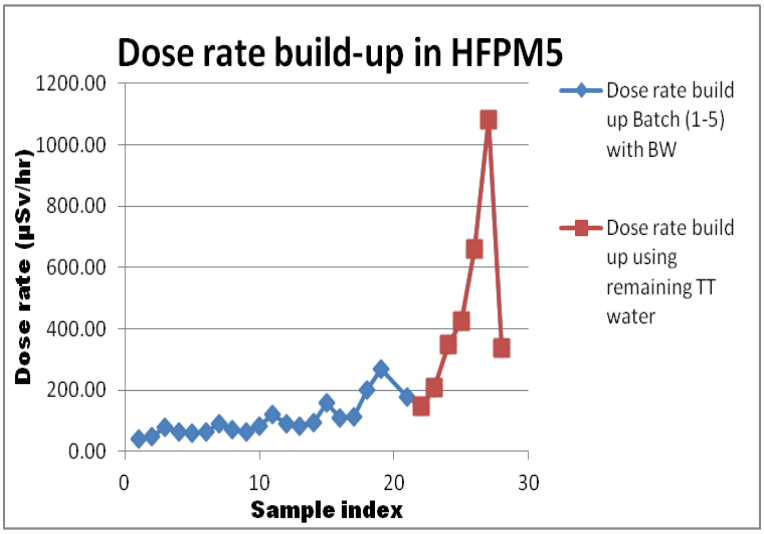

Figure 4.14: Averaged dose rate build-up in filter B; tops represent the maximal dose rate build-up in every batch, while troughs represent dose rates after a BW. The red line represents the processing of the remaining TT volume (3.2 m^3) without intermittent BW.

Dose rate build-up was monitored in the same fashion as before, even when emptying the remaining TT water. The absence of the BW procedure in figure 4.14 (represented by the red part of the curve) led to a sharp increase in the dose rate build-up in the filter module to around 1.1mSv/h; however reapplying the BW procedure at the end decreased the dose rate value to 370 µSv/h which is roughly around 66% decrease of he accumulated dose in the module (see appendix C1.3: figures C1.3.3-5).

4.2.3 Comparison between A and B

The two HFMs produced a significant decrease in the radioactivity of the permeate water as all samples had a total average of $2.5*10^3$ Bq/kg compared to the first TT sample of $3.1 \cdot 10^5$ Bq/kg. this represents a 99% decrease in total activity. The permeate samples exceeded the activity

release 100 Bq/kg, as a result the use of an ion exchanger was inevitable. The final activity downstream to the IXr was around 54 Bq/kg a further 98% decrease in the final activity. Activity measurements had the same reference time (2013-04-23, 12:00).

There was no increase of the boric acid concentration in any of the measured samples for both pilot scale filter modules.

Each filter was run at constant feed, permeate and retentate flows. The only major change in flow was in the retentate flow which was manually adjusted to its original capacity of 50 l/h. BW seemed to retain the original operational efficiency of the filters after each batch. Such response to BW was expected as the HFMs are characterized by the ease to clean on contraire to RO.

The first filter did not develop fouling until the last batch, knowing that there where heavy sedimentation with particles (flock) around 3mm i diameter. The pump played a role in breaking down those clumps into much smaller particle. The PI-02 indicator started decreasing after 30 min, with it the retentate flow. A much more sensitive pressure detector would have been needed because it was suspected for the fouling to appear at the end of each batch.

SEM investigation of the filter fibers was carried out at Ringhals chemistry laboratories. Roughly all the pores were blocked with minor sporadic pores representing the irreversible fouling that did not wash away with either BW or CC.

The second filter displayed a fouling tendency at the fifth batch and when emptying the TT. Sludge build-up was noticed at the top corner pipe leading to the hypothesis that such sludge could contribute to cake build up at the inner walls of the filter tubules. It was not possible to include the investigation of filter B fibers into the experimental program.

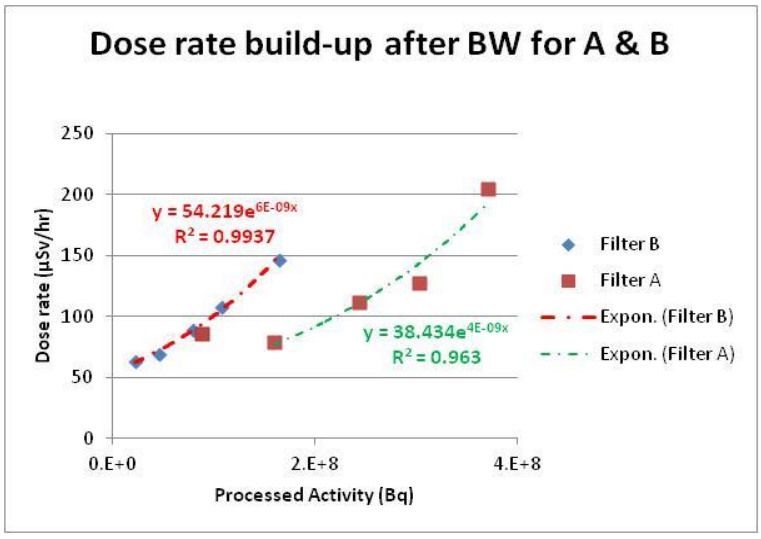

Figure 4.15: a comparison of both filters A and B where the dose rate build-up is plotted against processed activity. Notice the exponential trendlines of both filters.

The filters started off with null activity. Filter A reached a dose rate of 370 µSv/h, while filter B reached 270 µSv/h after the fifth batch and 1.1 mSv/h with the remaining TT water. A trend line was created for the dose rate build-up in each filter (dose rate versus processed activity) which showed that the activity in A and B increases exponentially (figure 4.15).

However, in reality trendlines of figure 4.15 should follow the curve depicting the cake build-up behavior in CF filtration as shown in figure 4.16 below. The region included within the red square is thought to be the domain of the trendlines in figure 4.15. However, the BW procedure prevented cake build-up and thus the dose rate would builds up to a lower stable value due to irreversible fouling.

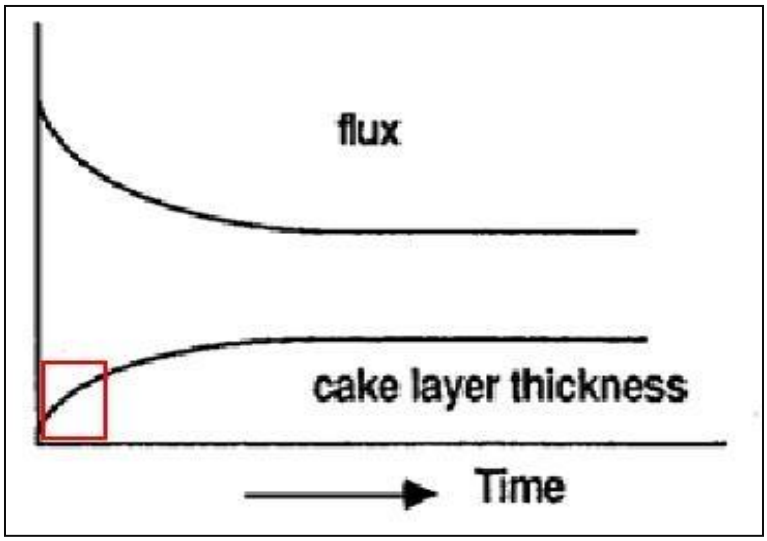

Figure 4.16: the region where the filter dose rate build-up is thought to be; left without intermittent BW the dose rate accumulation due to fouling is supposed to reach a stable value. This is mainly due to the shear forces cause by the turbulent flow limiting cake build-up and dose rate build-up too. [Courtesy of Vattenfall]

BW was very effective in cleaning the filter modules from foulants, especially for the second filter module. The BW water entered both filter modules from the top at a pressure of 1 bar which decreased as it flowed downwards to the bottom section of the filter module. This produced a much lower cleaning efficiency at the bottom (Appendix C1.2: figure C1.2.2). A BW procedure with two entry points, at the top and the bottom, should produce a more efficient process.

The last BW of batch 4 of filter B was run at 4 bars to test if that would clean the module better. The reason behind that was the decreasing activity-balance as the experiment moved from batch (1-3) suggesting that the initial BW parameter was inadequate with the current filter module. The result was a better activity-balance in batch 5 because of the increased driven pressure of 3.5 bars(figure 4.12).

BW water was analyzed in the HPGe detector and showed that the majority of activity was retained in the cake-build up. Visual inspection of BW samples showed flat particulates or flakes. The size and number of the flakes increased as the experiment moved from batch 1 to batch 5 in each filter. All BW were done using System 733 water at 1 bar and for 30 sec producing roughly 5 L. This makes a BW flow rate of 600 l/h. The BW was not batch specific, i.e. the BW could have washed out flakes and sludge from previous batches. As a result, it was not included in the batch activity-balance due to unreasonable values. The sole role of measurements was to test if the activity retained in the filter modules could be mitigated by BW.

Only the filter A was subject to CC procedure as recommended by the manufacturer (Appendix F2). That was also an important step to further decrease the activity and the remaining dose build up in the filter module.

An operational facility using water with an activity concentration around $3 \cdot 10^5$ Bq/kg should have an adequately dimensioned IXr because HFF of the tested MCOs cannot bring down the activity below the allowed limit. Working with two types of IXr (cation IXr and mixed bed IXr) the latter worked much better and needed no recirculation. There were suspicions of channel building and/or little residence time as experts at Ringhals explained that it is possible that these two phenomenons occur. This meant that the final radioactivity would have been even lower than what was achieved. No further investigation was done on IXrs as it was not the focus of the subject matter.

The dose was taken at three different fixed positions on the filter. Each measurement was given sufficient time until the value stabilized. There were noticeable differences in activities when moving from top to bottom with the later having the highest values. The second filter module displayed a trend of asymmetry with the side facing the pump and the TT having remarkably higher values.

The surrounding pipes, pump and proximal space were tested for dose rate levels, but that was not significant enough to cause such an asymmetry. To make sure that only the filter was measured for dose rate build-up the pump (600-1000 μSv/h) was wrapped in lead blankets for isolation and shielding as an average of 30mirocn were attained per operational pass.

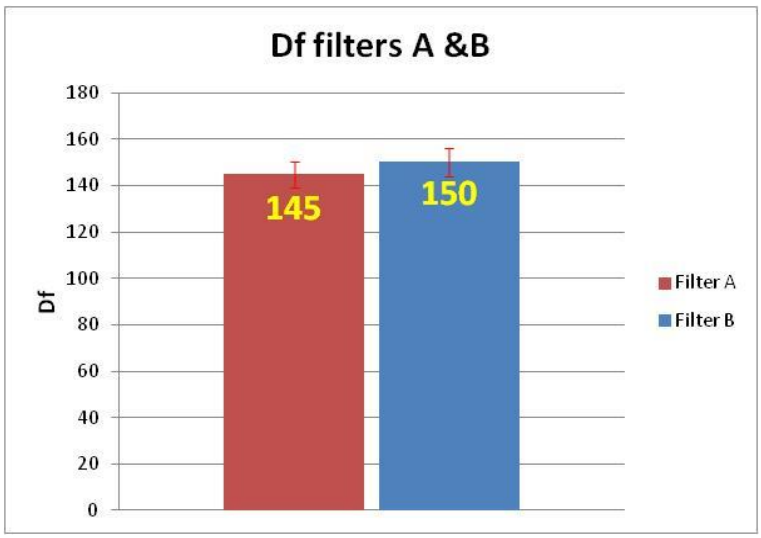

Figure 4.17: the decontamination factor of both filter A and B shows similar decontamination efficiencies.

The total decontamination factors of both filter modules are compared in figure 4.17. Both filters operated similarly and produced the same activity concentration in the permeate ($2.4*10^3$Bq/kg), while filter B was more prone to fouling with the current BW parameters.

4.3 Laboratory-scale versus pilot-scale

The results of the laboratory- and pilot-scale were very similar; the average activity concentration obtained in the permeate of filter A was identical to that of filter modules 2 and 3 of $2.5 *10^3$ Bq/kg (Appendix B1). The permeate of filter B had a larger activity concentration ($2.5 *10^3$ Bq/kg) than that of filter module 5 (10^3 Bq/kg).

This could be due to the fact that the OT filtration was done using module 5 at laboratory scale had a much lower permeate flow rate (0.2 l/h) compared to that of filter B (80 l/h). The TT water sample was not pre-filtered using 25µm filter as it was at the pilot-scale experiment so larger particles in that water sample could have promoted agglomeration during the 32 min it took for 100 ml to pass through filter 5.

The same large particles could have formed a thin film on top of the membrane of filter module 5 thus enhancing the filtration and retaining most of the particles on the membrane as figures 2.1 and 4.18 shows, which would also explain the similar behavior of filter module 4.

Parameters like recovery, pH, conductivity and boric acid concentration were similar in both scales.

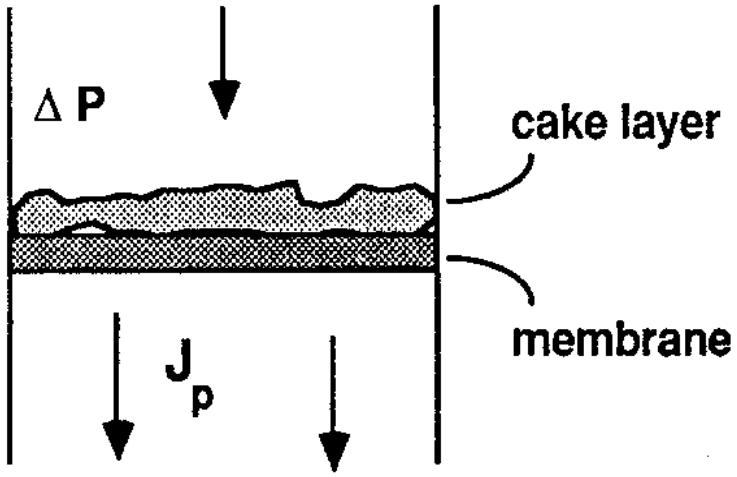

Figure 4.18: OT filtration showing the cake layer build-up on top of the filter membrane [used with permission]

5 Conclusions

HFM produced very good results when operated according to the manufacturers' manual and the recommendations of expert engineers. The HFM could not operate independently as it had to be coupled to an IXr so that the activity discharge limit (<100 Bq/kg) was met. An average of 55 Bq/kg was reached in the released water.

The concentration of boric acid was stable as there was neither increase nor decrease in the initial TT concentration of 565 ppm.

BW was an effective method of cleaning and decreasing dose rate build-up in both filters; however, the BW procedure would benefit of a higher driving pressure and a central- and/or multiple-points of entry to have a more efficient and effective washing.

Further tests with a lower MWCO (3000-1500 Da) would be of benefit to investigate if the dose rate build-up would reach even a lower level. Shielding is required as the dose rate increases further in time.

Fouling was not an important factor under this short operational time. Filtering larger volumes with higher permeate flow rates coupled with a more sensitive manometer would have revealed the fouling tendency earlier and more prominent.

The general conclusion of this study is that HFM is a promising process in decontamination facilities.

5.1 Further prospects

Using multiple HFM modules of decreasing MWCO in series should be investigated along with an automated BW bursts under optimized time intervals would produce better results and maintain the productivity of the filter modules.

It is intriguing, from the academic point if view, to investigate the possibility of extracting Co-60 from the final retentate before the cementation process; Co-60 is used in research facilities and hospitals as a gamma source.

6 References

1. Wolff, J.J. (2012). *Ion Exchange Resins For Use In Nuclear Power Plants*. PUROLITE ion Exchange Resins (20130920)

2. Bengtsson, B (2009*). Experience with Water Treatment Applications at Ringhals*. (used by kind permission of the author)

3. EPA, (2005*). Membrane Filtration Guidance Manual*.www.epa.gov. (20130225)

4. Mulder M. (1996). *Basic principles of membrane Technology*. Kluver Academic publishers.

5. Baker, R, W. (2012). *Membrane Technology and Applications, third edition.* (2012). Membrane Technology and Research, Inc. Newark, California. John Wiley and Sons, Ltd. Publication.

6. Juang, L.C et al. (2005*). Membrane processes for water reuse from the effluent of industrial park wastewater treatment plant: a study on flux and fouling of membrane*. Desalination 202 (2007) 302-309. Elsavier.

7. *Tangential membrane filtration.* (2013). www.optek.com (20130920)

8. Robles, A et al. (2012). *Factors that affect the permeability of commercial hollow-fibre membranes in a submerged anaerobic MBR (HF-SAnMBR) system*. Water Research 47 (2013) 1277 -1288. Elsavier.

9. Konieczny, K. Et al (2005), *Efficiency of the hybrid coagulation–ultrafiltration water treatment process with the use of immersed hollow-fiber membrane*. Institute of Water and Wastewater Engineering, Silesian University of Technology, Konarskiego 18, 44-100 Gliwice, Poland 2005.

10. Koch Membrane Systems www.kochmembrane.com. (20130523)

11. *Membrane Filtration: Water Filtration & Gas Transfer Contactors*. Www.membrane filtration.com (accessed 20130924)

12. Hong, S et al. (1997). *Kinetics of Permeate Flux Decline in Crossflow Membrane Filtration of Colloidal Suspensions*. JOURNAL OF COLLOID AND INTERFACE SCIENCE 196, 267–277 (1997) ARTICLE NO. CS975209.

13. Polyakov, Y. S et al. (2006) *Hollow-fiber membrane adsorber: Mathematical model*. Journal of Membrane Science 280 (2006) 610–623. Elsavier

14. Hong, S.P et al. (2002). *Fouling control in activated sludge submerged hollow fiber membrane bioreactors*. Desalination 143 (2002) 2 19-228. Elsavier

15. Guo, X et al. (2008). *Ultrafiltration of dissolved organic matter in surface water by a polyvinylchloride hollow fiber membrane*. Journal of Membrane Science 327 (2009) 254–263. Elsavier

16. Zamani, F et al. (2012). *Hydrodynamic analysis of vibrating hollow fibre membranes*. Journal of Membrane Science 429 (2013) 304–312. Elsavier

17. EPRI. (2009). *Technical Evaluation of Hollow Fiber Filtration for Liquid Radwaste Processing*.[Licensed]

18. Choppin, G. et al (2002). *Radiochemistry and Nuclear chemistry*, third edition. Butterworth Heinemann.

19. Nordlund, A (2011), *Introduction to Nuclear reactors*. Chalmers Tekniska Högskola, Göteborg.

20. Demaziere, C (2012), *Physics of Nuclear reactors lecture notes*. Chalmers Tekniska Högskola, Göteborg

21. Reinart, P. (1999). *Neutron interaction with matter*.www.fas.org. (accessed 20130906)

22. Chien C. L.(1996). *Committee on Nuclear and Radiochemistry*, National Research Council. National Academy of Science. 20130125

23. Song, M. S et al. (2003). *The evaluation of radioactive corrosion product at PWR as change of primary coolant chemistry for long-term fuel cycle*. Annals of Nuclear Energy 30 (2003) 1231–1246. Peragmon.

24. Rafique, M. Et al (2005), *Kinetic study of corrosion product activity in primary coolant pipes of a typical PWR under flow rate transients and linearly increasing corrosion rates*. Journal of Nuclear Materials 346 (2005) 282–292

25. P.M. Scott and P. Combrade (2006).*Corrosion in Pressurized Water Reactors, Corrosion: Environment and Industries.* Vol 13C. ASM Handbook. ASM International. 2006, p: 362-385.

26. Evans, J. C, et al (1984*), Long-lived Activation Products in Reactor Materials*. Division of Engineering Technology Office of Nuclear Regulatory Research US. Nuclear Regulatory Commission Washington, D.C. 20555 NRC FIN 82296.

27. JAEA NDC. (2013). *Nuclear Data Center: Japan Atomic Energy Agency*.wwndc.jaea.go.jp. (accessed 20130823)

28. *Avfall grund: Det Svenska systemet* (2010). Kärnkraftsäkerhet och Utbildning AB. [licensed]

29. The Dow Chemical Company. (2000) *DOWEX Ion Exchange Resins-Fundamentals of Ion Exchange*. www.dow.com. (20130919)

30. Seader J.D, Henley E.J., Roper D.K. (2011). *Separation process principles*. (2011). Third edition John Wiley & Sons, Inc.

31. Celeste, M et al. (2012). *The Acid−Base Titration of a Very Weak Acid: Boric Acid*. J. Chem. Educ. 2012, 89, 767−770.

32. Atkins, P. Jones, L. (2008). *Chemical Principles, The quest for insight*, Third Edition W. H. Freeman and company

33. Voeste, T et al. (2006). *Liquid-solid Extraction* (2006) Wiley-VCH Verlag GmbH & Co. KGaA

34. Emirson Process Management. (2010). *TheoryAnd Appliction Of Conductivity.Rosemount* Analytical Inc.

35. Eutech Instruments. (1997). *Introduction to Conductivity*. Eutech Instruments Pte Ltd (20130427)

36. Geochemical Instrumentation and Analysis. (2013) *Scanning Electron Microscope (SEM). http://serc.carelton.edu/research_education* (accessed 20130920)

37. Perkinelmer. (2011) *The 30-Minute Guide to ICP-MS*. www.perkinelmer.com. (accessed 20130920)

38. [Tangential flow vurses Dead-end filtration]. (2013). [image online] Available at: <www.spectrumlabs.com/filtration/Edge.html> [accessed 20130910]

39. [Membrane filtration Spectrum].(2013).[image online] Available at: <www.sswm.info/category/implementation-tools/water-purification/hardware/semi-centralised-drinking-water-treatmen-5> [accessed 20130910]

7 Appendices

Appendix A

A1 Radioactivity

A nucleus is termed radioactive if it decays spontaneously producing energy in the form of electromagnetic radiation (EMR) or energetic particles; such decay is governed by the ratio of the number of neutrons (N) to the number of protons (Z) (N/Z ratio). If the energy of decay is high enough it is termed as ionizing radiation (iR). The N/Z relationship gives rise to different modes of decay, as some nuclides decay with energetic particles such as alpha decay (helium He-4), others produce high energy electrons or positrons as the beta decay, while some produces gamma emissions as they decay which has the highest penetrative power of all the proceeding radiation. [18]

Radionuclide is the name used to designate any radioactive nuclide; radioisotope is another common term used for the same purpose; they decay in a periodic fashion, which is utilized when measuring the time required for half of the amount of atoms to decay i.e. the half-life t½. [18]

Radioactivity (also known as radioactivity) is measured by first acquiring the number of counts during a certain period of time producing the count rate per seconds termed as the observed count rate *R* which is then divided by the counting efficiency Ψ, attaining that way the absolute decay rate or radioactivity *A* in Becquerel (Bq) (eq A1). [18]

$$\boldsymbol{A_{(Bq)}} = \frac{\boldsymbol{R_{(cps)}}}{\boldsymbol{\psi_{eff}}} \qquad (eq\ \text{A1})$$

The counting efficiency depends on several factors like the type of detector used, geometry of the arrangement and the type and energy of the radioactive decay. [18]

A1.1 Modes of decay

Alpha decay

Alpha decay is generally observed in radionuclides that are heavier than lead i.e. elements with high Z-values. The element undergoing an alpha emission produces an alpha particle (helium He-4) and a daughter nuclide with a more stable N/Z ratio which could also decay by any of the different decay modes thus producing a chain of decay. [18]

$$^{A}_{Z}X \rightarrow {}^{A-4}_{Z-2}X + {}^{4}_{2}He \qquad (eq\ \text{A2})$$

Equation A2 shows a typical alpha decay where A is the atomic mass of the element in atomic mass unites (amu) and is the sum of number of neutrons (N) and the number of protons (Z).[18]

Alpha particles interacts strongly with matter due to its relatively high LET (linear energy transfer kev/µm) and it is readily absorbed by the first layer of the skin, a normal paper or 0.2mm of material, and a 1 MeV has around 0.6 cm range in air. [18]

Beta decay

Beta emission occurs when the N/Z ratio is too high (neutron rich element) or too low (proton rich element) for stability. In the first case the N/Z ratio is brought down to a more stable level by the emission of a negatron or β^- this way N is decreased while Z is increased. In the second case the opposite happens and a positron is emitted or β^+. [18]

Beta radiation has less LET than an alpha particle and as a result it penetrates matter a bit further before losing its energy to the surrounding matter. Beta radiation with energy of 1 MeV has a range of (405 cm) in air and can be absorbed by low Z material such as water (4.1 mm) and plastic from amongst others. [18] [32]

Gamma emission

Alpha or beta emission may leave the daughter nucleus in an excited state. This excess energy is removed by gamma emission or internal conversion. Measuring gamma emissions effectively is done using fluorescent crystals such as sodium iodide (NaI) or semiconductor detectors such as high purity germanium HPGe detectors; with the later having the highest precision and resolution. Gas based detectors such as ionization, proportional or Geiger counters are not so efficient in measuring gamma emissions because it produces low ionization density in gases. [18]

The gamma by far has the highest penetrative power. It could pass through any barrier such as buildings, bodies and atmosphere.

Lead and concrete (i.e in an NPP) is preferably used to attenuate the EMR as gamma ray cannot be diminished to zero as seen in the following equation:

$$\phi = k \cdot \frac{e^{-\mu \cdot x}}{r^2} \qquad (eq\ \text{A3})$$

which is the equation describing the intensity of the EMR ($\boldsymbol{\phi}$) of a point source; $\boldsymbol{\phi}$ can be decreased by either increasing the distance $\boldsymbol{r}$ or the thickness x of the barrier; a substance (absorber) with a high absorption coefficient $\boldsymbol{\mu}$ can be chosen to decrease the thickness required. [18]

A1.2 Radiation dose

The absorbed dose (D) is the amount of radiation absorbed ($\boldsymbol{dE_{abs}}$) per unit mass ($\boldsymbol{dm}$) and has the Gy=1J/kg as a unit:

$$D = \frac{dE_{abs}}{dm} \qquad (eq\ \text{A4})$$

The different modes of radiation induce different effects in the material they pass through. To measure the damage or effects of iR in the body weighting factors are used for both the type of radiation and organ in the human body. w_R is the radiation weighting factor; w_R alpha is 20 time as large as that of beta and gamma radiation. Another weighing factor is w_T the tissue weighing factor with the reproductive tissues having the highest value of 0.2 (table A1). [18]

Table A1: a table showing the different types of ionizing radiation and type of irradiated tissues with their corresponding weighting factors [18]

Type of radiation	Radiation Weighing Factor wR	Type of tissue	Tissue Weighing Factor w_T
Alpha	20	Gonads	0.2
Beta	1	Lung, bone marrow, stomach	0.12
Gamma	1	Skin, bone-surface	0.01
Neutrons	5 (*<10keV*); 10 (*2-20MeV*)	Liver, thyroid	0.05

The biologically effective dose $\boldsymbol{H_T}$ is called the equivalent dose; it is the sum of the products of the weighing factor of each radiation type $\boldsymbol{w_R}$ with the corresponding absorbed dose $\boldsymbol{D_{T,R}}$ of organ $\boldsymbol{T}$ (averaged over the organ $\boldsymbol{T}$):

$$H_T\ (Sv) = \sum w_R D_{T,R} \qquad (eq\ \text{A5})$$

The effective dose is measured in Sieverts (Sv) where 1Sv corresponds to 1 J/kg. Different tissues have different weighing factors relating their sensitivity to iR. When the tissue weighing factor ($\boldsymbol{w_T}$) is multiplied with the equivalent dose the effective dose in a specific tissue is acquired. The sum of weighted equivalent doses in all tissue is given by:

$$H_E(Sv) = \sum w_T H_T \qquad (eq\ \text{A6})$$

and it is also is measured in Sievert. The equivalent dose rate is the absorbed equivalent dose per

time unit. The equivalent dose to employees working with ionizing radiation in Sweden must not exceed 50 mSv per year or 100 mSv in a five years period. The average dose per year should therefore not exceed 20 mSv. For young people and pregnant women working with ionizing radiation there are lower limits.

Appendix B

B1 Laboratory scale

Tanktainer water

This is sample (0) that was taken directly from the TT. It was not pre-filtered with a 0.25µ m filter, even though, the water was clear and had no visible suspensions.

Radioactivity of the sample

The sample had a radioactivity concentration of $3.13 \cdot 10^5$ Bq/kg (table B1.1); this makes the total radioactivity in the $8m^3$ of TT water amount to $2.5 \cdot 10^9$ Bq (2.5GBq).

The radionuclides detected by the HPGe spectrometer in this crude sample were considered in all the samples in order to make it easy when comparing results together.

Figure B1.1 shows the different radionuclides that existed in the sample with Co-60 and Ag-110-m as the dominant nuclides making up 81% of the total radioactivity (table B1.1).

Conductivity, pH and Boron concentration

The conductivity meter showed a relatively low reading of 2.5 µS/cm indicating low concentration of electrolytes. pH was 5.7 at 23ºC (table B1.3)

The boric acid concentration (boron concentration) was about 568 ppm. That was the concentration the other samples would be compared with to decide if there were to be any decrease in the concentration of boric acid in the filtrate samples. A decrease would mean that the membrane was impermeable to the acid and would lead to a boric acid concentration build-up in the retentate of the pilot scale experiment.

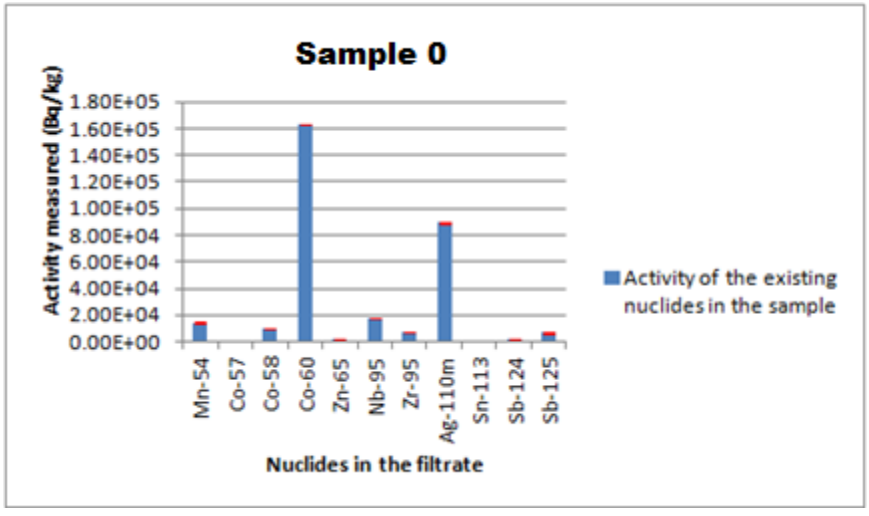

Figure B1.1: radioactivity concentration (Bq/kg) of radionuclides detected using HPGe spectrometer with a 95% confidence interval.

Filter module 1

Radioactivity of the sample

The filter module had a MWCO of $3 \cdot 10^5$ Da. It filtered a volume of 100 liters of the TT water. It had a total radioactivity of $1.2 \cdot 10^4$ Bq/kg (table B1.1).

A number of the radionuclides found in the original solution were not detected in the filtrate of this filter (figure B1.2).The conclusion was that either those radionuclides were filtered out due to their large particle size or their read-outs in the gamma spectrometer were below their MDA. The nuclide dominating over the others was Ag-110m making 84% of the total radioactivity.

Conductivity and Boron concentration

The conductivity of the filtrate was around 4 µS/cm, slightly higher than the original solution. pH was 5.5 at 23ºC (table B1.3)

The boric acid concentration was around 566 ppm hardly a remarkable change. This meant that the weak acid passed through the membrane without any problems.

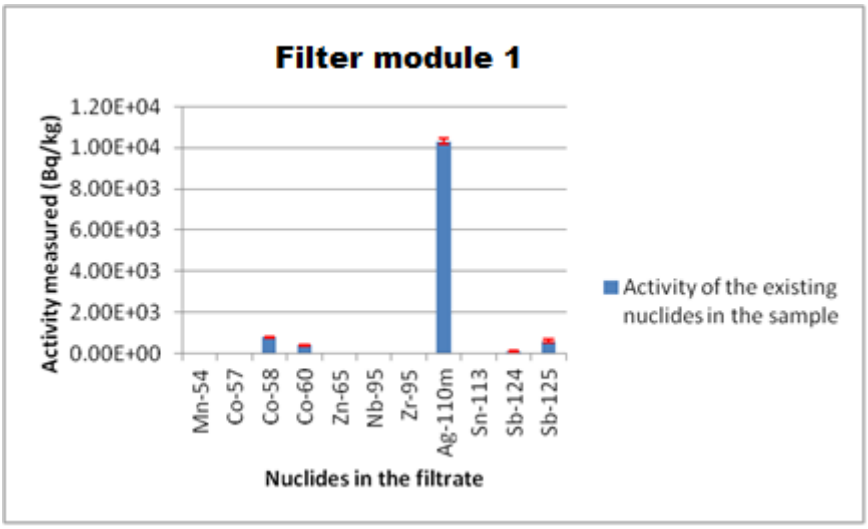

Figure B1.2: radioactivity concentration (Bq/kg) of radionuclides detected using HPGe spectrometer with a 95% confidence interval.

Filter module 2

Radioactivity of the sample

The filter module had a MWCO of 10^5 Da. It filtered a volume of 100 liters of the TT water. It had a total radioactivity concentration of $2.4 \cdot 10^3$ Bq/kg (table B1.1)

Here there was a similar result of certain nuclides not being detected by the spectrometer for similar reasons mentioned above (figure B1.3). However, the dominance of certain radionuclides has changed; Co-58 has the highest radioactivity concentration in the sample followed by Sb-125 and Co-60. The last two are quite equal in their respective radioactivity concentration.

Conductivity and Boron concentration

The conductivity of the filtrate was around 3 µS/cm; it was same low result as before though slightly lower. pH was 5.5 at 23ºC (table B1.3).

The boric acid concentration was around 565 ppm. No major changes regarding the concentration of boric acid.

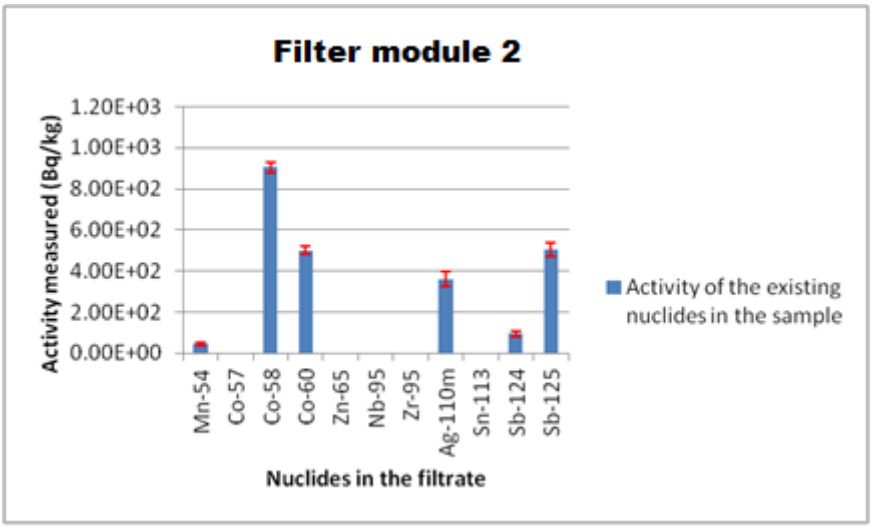

Figure B1.3: radioactivity concentration (Bq/kg) of radionuclides detected using HPGe spectrometer with a 95% confidence interval.

Filter module 3

Radioactivity of the sample

The filter module had a MWCO of $3 \cdot 10^4$ Da. It filtered a volume of 100 liters of the TT water. It had a total radioactivity concentration of $2.3 \cdot 10^4$ Bq/kg (table B1.1). It was roughly the same amount of radioactivity concentration in this sample as in filter module 2.

The same radionuclides, as in filter 2, dominated the sample however a decrease in the radioactivity concentration of Ag-110m was noticed (figure B1.4). Overall it is safe to conclude that no remarkable differences were noted between filter modules 1 and 2.

Conductivity and Boron concentration

The conductivity of the filtrate was around 3 µS/cm. The similarity here between filter modules 1 and 2 surfaces again confirms the conclusion that these two membranes would give similar results in the pilot scale experiment if the same TT water were to be used.

pH was 5.6 at 23ºC; the boric acid concentration was around 565 ppm (table B1.3).

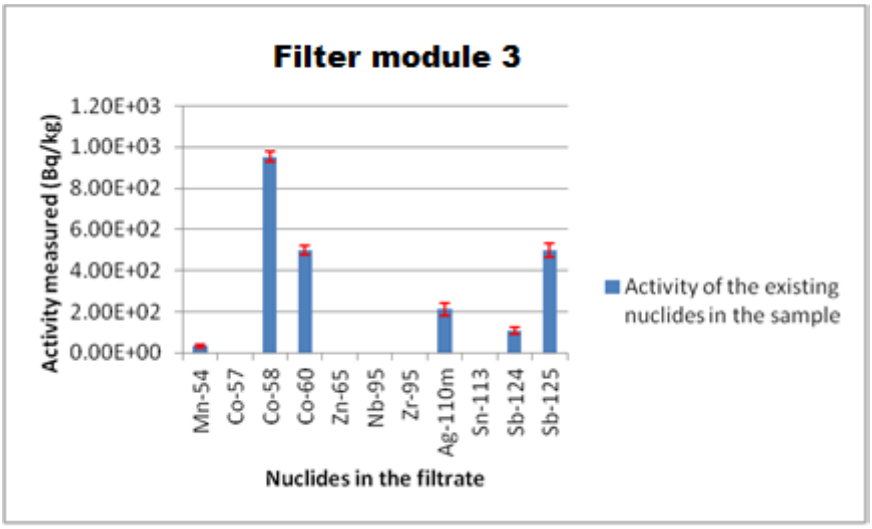

Figure B1.4: radioactivity concentration (Bq/kg) of radionuclides detected using HPGe spectrometer with a 95% confidence interval.

Filter module 4

Radioactivity of the sample

The filter module had a MWCO of 10^5 Da. It filtered a volume of 100 liters of the TT water. It had a total radioactivity concentration of $9.9 \cdot 10^2$ Bq/kg (table B1.1).

There was a decrease in the overall radioactivity concentration especially for Co-58 and Co-60. Sb-125 seemed to have the same radioactivity contribution as before and had the largest share of the radioactivity in the sample.

The nuclides dominating over the others were Sb-125 and Ag-110m making up 79% of the total radioactivity (figure B1.5).

Conductivity and Boron concentration

The conductivity of the filtrate was around 4,7 µS/cm. There was an increase in the conductivity of the solution compared with the last two filtrates. pH was 5.6 at 23ºC (table B1.3).

The boric acid concentration was around 567 ppm. There was still no change in the average the concentration of boric acid in the filtrate compared to others.

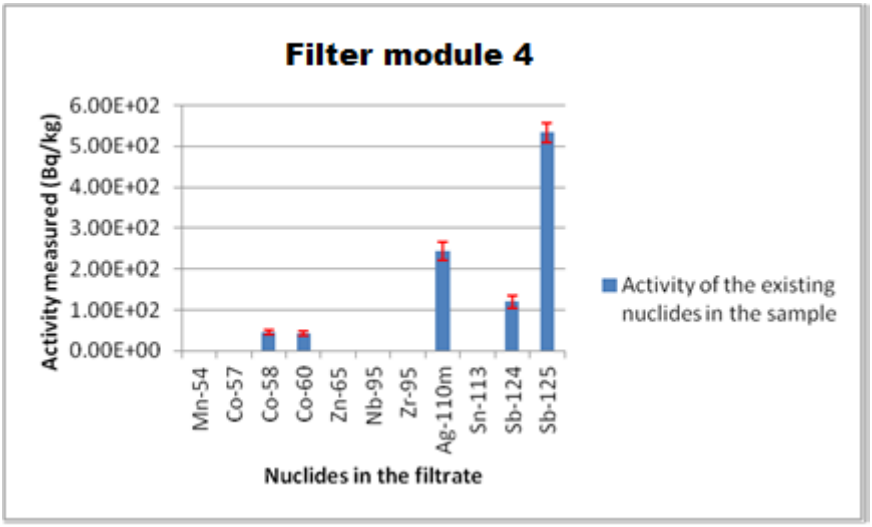

Figure B1.5: radioactivity concentration (Bq/kg) of radionuclides detected using HPGe spectrometer with a 95% confidence interval.

Filter module 5

Radioactivity of the sample

The filter module had a MWCO of $5 \cdot 10^3$ Da. It filtered a volume of 100 liters of the TT water. It had a total radioactivity concentration of 10^3 Bq/kg (table B1.1). This sample took the longest time to filter through; around 32 minutes at 4 bars.

The radionuclide dominating over the others was Sb-125 and Co-58 making up 67% of the total radioactivity concentration (figure B1.6).

Conductivity and Boron concentration

The conductivity of the filtrate was around 4.3 µS/cm. That was quite similar to other samples so no remarks were to be taken. pH was 5.7 at 23ºC (table B1.3)

The boric acid concentration was around 565. The concentration of boric acid remained roughly the same in all the tests making it possible to use in the pilot scale experiment.

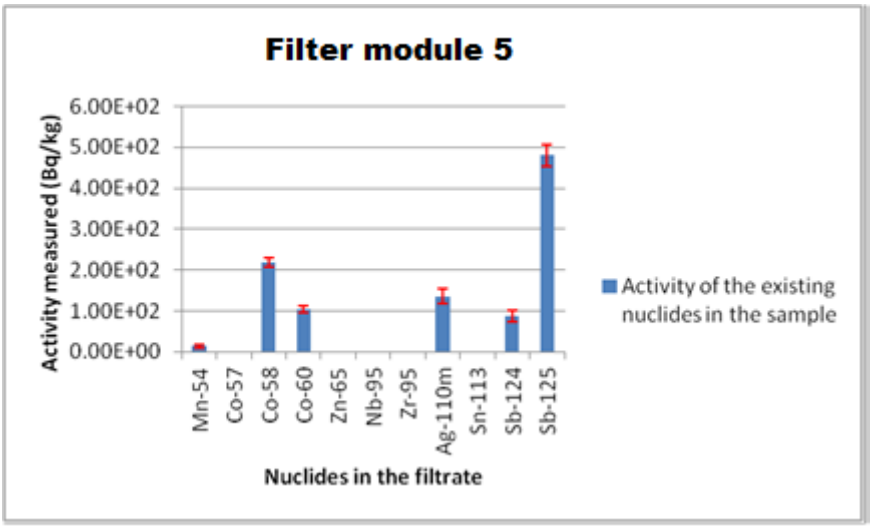

Figure B1.6: radioactivity concentration (Bq/kg) of radionuclides detected using HPGe spectrometer with a 95% confidence interval.

Table B1.1: Radioactivity concentration of radionuclides in the filtrate of TT sample 0 and in each filter module (1-5); a qualitative bar chart (the horizontal blue rectangles) shows the relationship amongst the radionuclides in each column.

Radionuclides	0	1	2	3	4	5
Mn-54	1.44E+04		4.49E+01	3.37E+01		1.41E+01
Co-57	2.73E+02					
Co-58	1.00E+04	8.00E+02	9.04E+02	9.54E+02	4.43E+01	2.18E+02
Co-60	1.63E+05	3.96E+02	5.01E+02	4.98E+02	4.24E+01	1.04E+02
Zn-65	2.17E+03					
Nb-95	1.75E+04					
Zr-95	7.30E+03					
Ag-110m	8.93E+04	1.08E+04	3.61E+02	2.12E+02	2.45E+02	1.36E+02
Sn-113	4.88E+02					
Sb-124	1.56E+03	1.02E+02	9.43E+01	1.08E+02	1.20E+02	8.83E+01
Sb-125	6.71E+03	6.00E+02	5.04E+02	5.00E+02	5.34E+02	4.80E+02
Total Activity (Bq/kg)	3.13E+05	1.22E+04	2.41E+03	2.31E+03	9.86E+02	1.04E+03
Total Uncertainty (Bq/kg)	2.08E+03	3.27E+02	1.22E+02	1.19E+02	7.42E+01	7.66E+01

Table B1.2: the decontamination factor of each filter with respect to each radionuclide detected; a qualitative bar chart (the horizontal red rectangles) shows the relationship amongst the Df of radionuclides in each column.

	Decontamination factor DF of each filter				
Df of radionuclides	1	2	3	4	5
Df Co-58	13	11	10	226	46
Df Co-60	412	325	327	3844	1567
Df Ag-110m	9	247	421	364	657
Df Sb-124	15	17	14	13	18
Df Sb-125	11	13	13	13	14

Table B1.3: the different analyses done using sample 0 and the filtrate of filter modules (1-5)

Filter index	0	1	2	3	4	5
Average time (min)	N/A	0,8	0,9	1,4	3,5	32,0
Conductivity (µS/cm) ε(0.1)	2,5	3,8	2,9	2,9	4,7	26,4
pH	5,7	5,6	5,6	5,7	5,6	5,5
Boron (ppm)	568	566	565	565	567	565
volume used (ml)	N/A	100,0	100,0	100,0	100,0	100,0
Average flow rate at 4 bars l/hr	N/A	7,7	6,8	4,2	1,7	0,2

Figure B1.7: the Vivacell70 filter modules that were used in the laboratory scale experiments

Appendix C

C1 Pilot scale

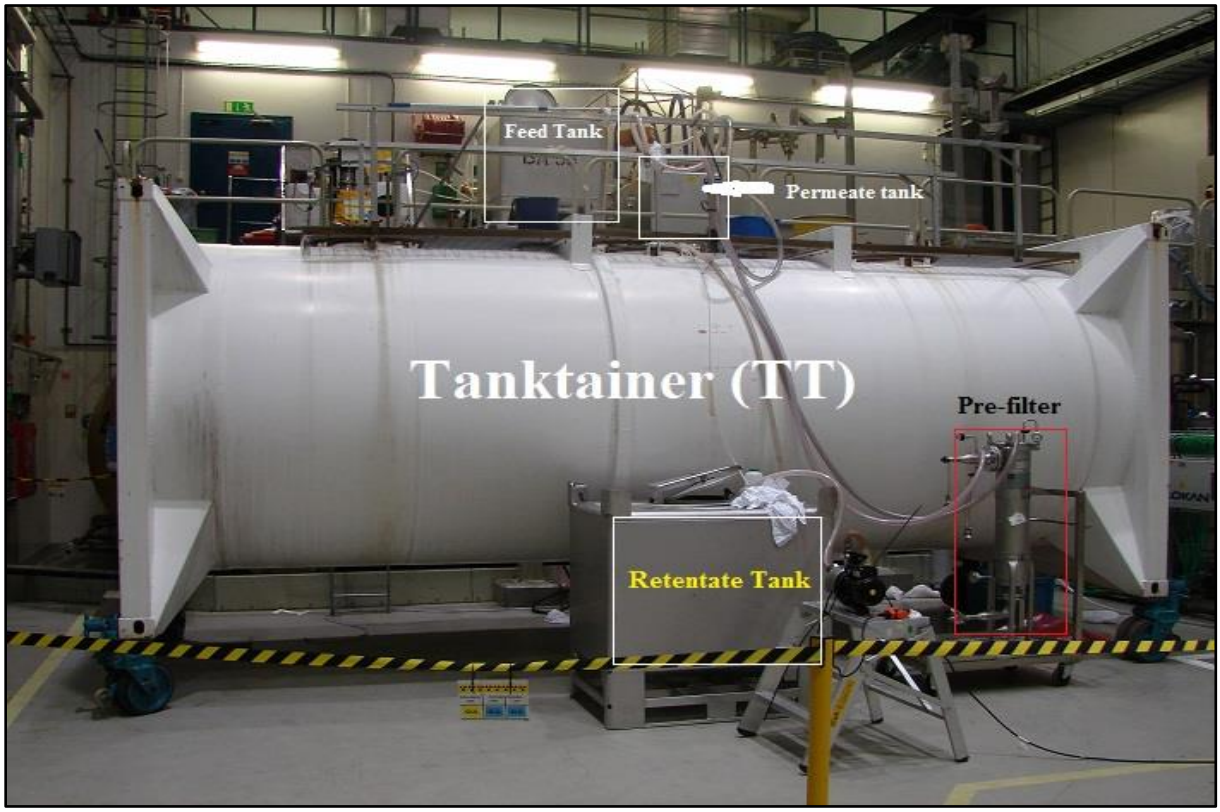

Figure C1.1: The different tanks that were used in this study and the pre-filter module which was situated between the TT and the feed tank.

Figure C1.2: a typical view of the cross-section (from one of the ends) of a HFF; here the resin potting is visible at the outer circumference of the hollow fiber bundle.

C1.1 Calculations

C1.1.1 Recovery (retention)

$$R = 1 - \frac{C_P}{C_F} \qquad (eq\ 3)$$

With $\boldsymbol{C_P}$ is the concentration of the permeate and $\boldsymbol{C_F}$ is the concentration of the feed (mole/unite volume)

$\boldsymbol{C_P}$ is used here as $\boldsymbol{A_P}$ (radioactivity concentration of the permeate Bq/kg) and $\boldsymbol{C_F}$ is changed to $\boldsymbol{A_F}$ (the radioactivity concentration of the feed Bq/kg) with 1l of water = 1kg at 25ºC which gives rise to equation C1:

$$R = 1 - \frac{A_P}{A_F} \qquad (eq\ C1)$$

C1.1.2 Radioactivity balance

$$M_B = \frac{Q_p \cdot C_p + Q_c \cdot C_c}{Q_f \cdot C_f} \qquad (eq\ 4)$$

Where $\boldsymbol{Q_P}$ is the flux of permeate, $\boldsymbol{Q_F}$ is the flux of the feed and $\boldsymbol{Q_C}$ is the flux of the retentate (m3/s or l/h); $\boldsymbol{C_P}$ is the concentration of the permeate, $\boldsymbol{C_C}$ is the concentration of the retentate, and C_F is the concentration of the feed (mole/unite volume)

$\boldsymbol{Q_P}$= 80 l/h; $\boldsymbol{Q_C}$=50 l/h and $\boldsymbol{Q_F}$= 130 l/h (were kept constant during the process).

$\boldsymbol{C_P \sim A_P}$; $\boldsymbol{C_C \sim A_C}$; $\boldsymbol{C_F \sim A_F}$ (as explained in C1) $\boldsymbol{M_B \sim A_B}$ and equation 4 becomes equation C2:

$$A_B = \frac{Q_p \cdot A_p + Q_c \cdot A_c}{Q_f \cdot A_f} \qquad (eq\ C2)$$

C1.1.3 Fouling tendency FT

$$J = \frac{\Delta P}{\mu \cdot R_T} = \frac{TMP}{FT}; here\ FT = \mu \cdot R_T = \frac{TMP}{J} \qquad (eq\ 7)$$

$$FT = \frac{TMP}{J} = \frac{PIT\text{-}01 - PI\text{-}02}{Q_P} \qquad (eq\ C3)$$

PIT-01 and PI-02 are pressure indicators that are tabulated in process parameters of each batch. $\boldsymbol{Q_P}$=80 l/h.

Decontamination Factor Df

$$Df = \frac{Feed\ \ radioactivity\ conc.\left(\frac{Bq}{kg}\right)}{Permeate\ radioactivity\ conc.\ \left(\frac{Bq}{kg}\right)} \qquad (eq\ C4)$$

Df is calculated by dividing the radioactivity concentrations of the permeate by the parent feed.

C1.2 HFPM50: Filter A

C1.2.1 Batch 0

It took around **3.5** hours; **300** liters from the TT were reduced down to ~18 liters of retentate. The latter was drained into a separate retentate tank. No samples were taken because it was a test drive for the system. No fouling was observed.

4 liters of BW water were collected with a radioactivity concentration of $8.19 \cdot 10^4$ Bq/kg and added to the feed volume of Batch 1.

C1.2.2 Batch 1

The experiment took **7** hours so that **600** liters of TT water and the 4 liters of BW water from batch 0 were reduced down to ~18 liters of retentate, which were drained into the retentate tank. Permeate tank volume was about 545 liters filtered through a 25 liters cation porous ion exchanger bed. The BW water collected at the end of the test is analyzed after washing the module to investigate any easily removed particles that built up in the membrane module and the pipes.

Batch 1 analysis

The final radioactivity concentration of the retentate was about $2.56 \cdot 10^6$ Bq/kg. Co-60 and Ag-110m were the dominant nuclides. The values of Batch 1 are found in table C1.2.1 below.

Table C1.2.1: Radioactivity concentration of radionuclides in Batch 1 of Filter A (HFPM50); a qualitative bar chart (the horizontal blue rectangles) shows the relationship amongst the radionuclides in each column.

HFPM50 Batch 1	(0 hr)	Sample 1 (0.6 hr)			Sample 2 (3.6 hr)			Sample 3 (6.8 hr)			Finish	
Radionuclides	Feed 0	Feed	Premeate	Retenate	Feed	Permeate	Retenate	Feed	Permeate	Retenate	Back Wash	IXr (cation)
Mn-54	5,86E+03	6,26E+03		1,42E+04	1,15E+04		2,69E+04	4,27E+04		9,38E+04	6,05E+03	
Co-57				2,37E+02				5,37E+02		8,82E+02		
Co-58	3,65E+03	3,66E+03	9,44E+02	7,18E+03	6,00E+03	8,82E+02	1,26E+04	1,95E+04	7,80E+02	4,19E+04	2,32E+03	
Co-60	8,31E+04	8,80E+04	6,44E+02	1,98E+05	1,62E+05	6,15E+02	3,81E+05	6,22E+05	5,12E+02	1,36E+06	9,11E+04	
Zn-65	8,15E+02	1,15E+03		2,55E+03	2,01E+03		4,42E+03	7,68E+03		1,93E+04		
Nb-95	2,44E+03	2,44E+03		6,27E+03	5,15E+03		1,20E+04	2,19E+04		4,89E+04	2,39E+03	
Zr-95	5,25E+03	5,67E+03		1,36E+04	1,12E+04		2,63E+04	4,66E+04		1,09E+05	5,40E+03	
Ag-110m	4,07E+04	4,55E+04	1,48E+02	1,03E+05	8,56E+04	1,12E+02	2,07E+05	3,73E+05	1,77E+02	8,01E+05	5,41E+04	
Sn-113		3,52E+02		6,59E+02	4,59E+02		1,19E+03	1,90E+03				
Sb-124	8,51E+02	8,41E+02	7,46E+01	2,07E+03	1,52E+03		3,89E+03	7,30E+03	1,20E+02	1,41E+04	9,70E+02	5,34E+01
Sb-125	3,83E+03	3,74E+03		8,95E+03	7,69E+03	4,07E+02	1,70E+04	2,89E+04	8,03E+02	6,25E+04	4,53E+03	4,48E+02
Total activity Conc (Bq/kg)	***1,47E+05***	***1,58E+05***	***1,81E+03***	***3,56E+05***	***2,93E+05***	***2,02E+03***	***6,93E+05***	***1,17E+06***	***2,39E+03***	***2,55E+06***	***1,69E+05***	***5,08E+03***
Tot.Act. Uncertainty (Bq/kg)	***5,76E+03***	***6,09E+03***	***1,44E+02***	***1,35E+04***	***1,12E+04***	***1,59E+02***	***2,61E+04***	***4,35E+04***	***1,83E+02***	***9,44E+04***	***6,84E+03***	***3,41E+01***

Permeate

Three permeate samples were taken having the average radioactivity concentration of $2.09 \cdot 10^3$ Bq/kg. The dominant radionuclides were found to be Co-58, Co-60 and Sb-125 as shown in table C1.2.1.

Retentate

Three retentate samples were taken; they had a radioactivity concentration that ranged between $3.56 \cdot 10^5$ Bq/kg and $2.55 \cdot 10^6$ Bq/kg (table C1.2.1). The last value is 1740% the radioactivity of the feed at t=0. The dominant radionuclides were found to be Co-60 and Ag-110m. The color of the water became more brown with respect to time, contrary to the permeate that remained clear.

Feed

Four samples were taken with the first one being the steady state sample at t=0 having a radioactivity concentration of $1.47 \cdot 10^5$ Bq/kg. The dominant radionuclides were found to be Co-60 and Ag-110m (table C1.2.1).

Backwash

One sample was taken out of the 12 liters of system 733(de-mineralized water) water were used. The BW sample had a radioactivity concentration of $1.69 \cdot 10^5$ Bq/kg with Co-60 and Ag-110m as the dominant radionuclides (table C1.2.1). The remaining BW was added to the next batch.

Ion Exchanger

One sample of the cation exchanger was analyzed and resulted in a radioactivity concentration of ~500 Bq/kg (table C1.2.1). That value was greater than the allowed value for release (100 Bq/kg) the permeate water collected after the IXr was left to circulate through the IXr until the radioactivity concentration decreased below the levels of release.

Boric acid concentration

The concentration of the boric acid did not increase in any of the samples (table C1.2.2). It remained around the same level as the level measured at the laboratory scale of 565 ppm.

Table C1.2.2: results of the chemical analysis performed using the samples obtained from Batch 1 of filter A; radioactivity concentration is denoted here as (A) and χ represents the conductivity; [B] represents the boric acid concentration.

Batch 1, sample 1	χ µS/cm	pH	[B] avg	A Bq/kg
Feed 0	3	6	566	1,47E+05
Feed	3	6	568	1,58E+05
Permeate	3	6	566	1,87E+03
Retentate	3	5	567	3,56E+05
Batch 1, sample 2	**χ µS/cm**	**pH**	**[B] avg**	**A Bq/kg**
Feed	3	6	568	2,93E+05
Permeate	3	6	571	2,02E+03
Retentate	4	6	568	6,93E+05
Batch 1, sample 3	**χ µS/cm**	**pH**	**[B] avg**	**A Bq/kg**
Feed	5	5	572	1,17E+06
Permeate	3	6	575	2,39E+03
Retentate	9	5	572	2,56E+06
Backwash	3	5	N/A	1,67E+05
IXr cation bed	4	N/A	N/A	5,02E+02

Dose build-up

The dose rate of the module was measured with respect to time during the process and after the BW. The module retained some of the radioactivity build-up from Batch 0 that explains the initial dose rate at the start of Batch 1 (t=0) (table 1.2.3).

Table C1.2.3: The dose rate build-up of the filter A during the Batch 1 process at the designated positions in µSv/h.

HFPM50 BATCH 1	Dose rate (µSv/h)			
Elapsed time (h)	Filter Top	Filter Middle	Filter Bottom	Average Dose rate (µSv/h)
0	18	31	66	38
0.6	20	40	95	52
3.6	22	50	150	74
6.8	70	106	260	145
After BW	28	40	190	86

Fouling

This batch showed no signs of fouling. The first sign of fouling is a change in the TMP or drop in the permeate flow in the Fl-03 flow meter the latter was kept constant during the entire process. In this batch the FT was constant all the time (table C1.2.4).

Table C1.2.4: the process parameters that governed Batch 1.

HFPM50 BATCH 1	Process operational parameters					
Elapsed time (h)	RPM	PIT00 (mbar)	PIT-01 (bar)	PI-02 (bar)	PDI-00 (mbar)	TI-01 (°C)
0.0	1889	102	2	1.45	1001	25.5
0.6	1899	98	2	1.25	1004	26.5
3.6	1913	73	2	1.25	1009	26.5
6.8	1914	52	2	1.25	1015	27.0

C1.2.3 Batch 2

The experiment took **6 hours** and used **600 liters** of TT water. 12 liters of BW of Batch 1 were added. Some of the feed water went through the SP-01 drainage/sampling tap into the retentate tank, therefore only 468 liters of permeate were collected which was much lower than that of Batch 1. It was found that around 95 liters of the fresh feed filled up the retentate tank.

The experiment continued as described before. Measurement and sampling procedures were carried out as usual. At the end of the test ~18 liters of retentate were drained into the CT.

Batch 2 analysis

The final radioactivity concentration of the retentate was about $1.99 \cdot 10^6$ Bq/kg. Co-60 and Ag-110m were the dominant nuclides (table C1.2.5).

Table C1.2.5: Radioactivity concentration of radionuclides in Batch 2 of filter A (HFPM50); a qualitative bar chart (the horizontal blue rectangles) shows the relationship amongst the radionuclides in each column

HFPM50 Batch 2	(0 hr)	Sample 1 (0.6 hr)			Sample 2 (4 hr)			Sample 3 (5.8 hr)			Finish	
Radionuclides	Feed	Feed	Premeate	Retentate	Feed	Permeate	Retentate	Feed	Permeate	Retentate	Back Wash	IXr (cation)
Mn-54	5,26E+03	5,99E+03	5,92E+01	1,44E+04	1,51E+04	4,35E+01	3,35E+04	4,01E+04	6,17E+01	7,17E+04	1,04E+03	
Co-57								6,30E+02				
Co-58	3,28E+03	3,58E+03	8,92E+02	7,47E+03	7,66E+03	8,16E+02	1,53E+04	1,89E+04	7,22E+02	2,81E+04	6,00E+02	
Co-60	7,81E+04	8,56E+04	6,98E+02	2,07E+05	2,15E+05	5,47E+02	4,81E+05	5,86E+05	4,79E+02	1,09E+06	1,67E+04	
Zn-65	1,23E+03	1,31E+03		2,94E+03	2,96E+03		5,73E+03	6,90E+03		1,37E+04		
Nb-95	2,28E+03	2,46E+03		5,98E+03	6,98E+03		1,52E+04	1,92E+04		3,13E+04		
Zr-95	4,74E+03	5,34E+03		1,34E+04	1,44E+04		3,29E+04	4,26E+04		7,01E+04	7,69E+02	
Ag-110m	4,14E+04	4,48E+04	1,34E+02	1,07E+05	1,10E+05		2,49E+05	3,28E+05	1,67E+02	6,28E+05	1,08E+04	
Sn-113	3,15E+02			7,73E+02	8,88E+02		1,44E+03	2,01E+03		3,22E+03		
Sb-124	8,46E+02	8,74E+02	7,07E+01	2,24E+03	1,74E+03	7,77E+01	4,54E+03	5,73E+03	1,97E+02	8,84E+03		5,07E+01
Sb-125	3,91E+03	3,81E+03	3,31E+02	8,95E+03	9,39E+03	5,58E+02	2,07E+04	2,79E+04	8,13E+02	5,22E+04	5,63E+02	4,57E+02
Total activity Conc (Bq/kg)	***1,41E+05***	***1,54E+05***	***2,19E+03***	***3,70E+05***	***3,85E+05***	***2,04E+03***	***8,60E+05***	***1,08E+06***	***2,44E+03***	***1,99E+06***	***3,20E+04***	***5,98E+03***
Tot.Act. Uncertainty (Bq/kg)	***5,51E+03***	***6,00E+03***	***1,79E+02***	***1,41E+04***	***1,46E+04***	***1,61E+02***	***3,25E+04***	***4,03E+04***	***1,99E+02***	***7,59E+04***	***1,65E+03***	***3,75E+01***

Permeate

Three permeate samples were taken having the average radioactivity concentration of $2.2 \cdot 10^3$ Bq/kg. The dominant radionuclides were found to be Sb-125, Co-58 and Co-60 as shown in table C1.2.5. There was an increase in the radioactivity concentration of permeate water with time. The same radionuclides as in Batch 1 were found in the collected permeate samples.

Retentate

Three retentate samples were taken had radioactivity concentrations that ranged between $3.7 \cdot 10^5$ Bq/kg and $1.99 \cdot 10^6$ Bq/kg as shown in table C1.2.5.The final value was 1422% the radioactivity concentration of the feed at t=0. As in Batch 1, the color of the water became more brown with respect to time, contrary to the permeate that remained clear.

Feed

Four samples were taken with the first one being the steady state sample at t=0 having a radioactivity concentration of $1.4 \cdot 10^5$ Bq/kg. The other three samples had an increasing radioactivity with the last sample having $1.1 \cdot 10^6$ Bq/kg (table C1.2.5).

Backwash

One sample was taken out of the **16** liters of BW water that were used. It had a radioactivity concentration of $3 \cdot 10^5$ Bq/kg with Co-60 $1.7 \cdot 10^4$ Bq/kg and Ag-110m $1.1 \cdot 10^4$ Bq/kg as the dominant radionuclides (table C1.2.5). The remaining BW was added to feed of Batch 3.

Ion Exchanger

One sample of the cation exchanger was analyzed and resulted in a radioactivity concentration of 570 Bq/kg (table C1.2.5). The cation bed IXr failed to bring down the radioactivity lower than 450 Bq/kg even after 2 hours of recirculation through that IXr; it had an inadequate lower capacity than what the process needed. So a new ion-exchanger with mixed bed was used to bring the radioactivity concentration down to 34 Bq/kg.

Boric acid concentration

The concentration of the boric acid did not show any significant increase in any of the samples (table C1.2.6). It remained around the same level as the level measured at the laboratory scale above of 565 ppm.

Table C1.2.6: results of the chemical analysis performed using the samples obtained from Batch 2 of filter A; radioactivity concentration is denoted here as (A) and χ represents the conductivity; [B] represents the boric acid concentration.

Batch 2, sample 1	χ μS/cm	pH	[B] avg	A Bq/kg
Feed 0	3	6	565	1,41E+05
Feed	3	6	564	1,54E+05
Permeate	2	6	564	2,18E+03
Retentate	3	5	564	3,69E+05
Batch 2, sample 2	**χ μS/cm**	**pH**	**[B] avg**	**A Bq/kg**
Feed	3	5	565	3,84E+05
Permeate	3	6	565	2,04E+03
Retentate	5	5	566	8,59E+05
Batch 2, sample 3	**χ μS/cm**	**pH**	**[B] avg**	**A Bq/kg**
Feed	5	5	568	1,08E+06
Permeate	3	6	568	2,44E+03
Retentate	9	5	568	1,99E+06
Backwash	3	5	N/A	2,99E+04
IXr cation bed	5	5	N/A	5,70E+02

Dose build-up

The dose rate of the module was measured with respect to time during the process and after the BW as shown in table C1.2.7.

Table C1.2.7: dose rate build-up of the filter A during the Batch 2 process at the designated positions in µSv/h.

HFPM50 BATCH 2	Dose rate (µSv/h)			
Elapsed time (h)	Filter Top	Filter Middle	Filter Bottom	Average Dose rate (µSv/h)
0	23	36	95	51
0.8	25	50	115	63
4.4	38	75	175	96
5.8	75	107	260	147
After BW	28	53	157	79

Fouling

No fouling tendency was observed. The TMP was constant during the entire process as a result FT was constant (table C1.2.8).

Table C1.2.8: the process parameters that governed Batch 2.

HFPM50 BATCH 2	Process operational parameters					
Elapsed time (h)	RPM	PIT00 (mbar)	PIT-01 (bar)	PI-02 (bar)	PDI-00 (mbar)	TI-01 (℃)
0.0	1890	105	2	1.45	1004	26.0
0.8	1907	91	2	1.25	1011	26.5
4.4	1926	65	2	1.25	1032	27.5
5.8	1934	52	2	1.25	1042	28.0

C1.2.4 Batch 3

The experiment took **6.5** hours so that **600** liters of TT water were concentrated down to ~18 liters, which were drained into the retentate tank. Permeate tank volume was about 545 liters filtered through a 75 liter mixed bed porous IXr (cation and anion). 15 liters of the BW from Batch 2 were added as mentioned earlier.

Batch 3 analysis

The final radioactivity concentration of the retentate was about $2.9 \cdot 10^6$ Bq/kg. Co-60 and Ag-110m were the dominant radionuclides (table 1.2.9). This value is more similar to the one in Batch 1.

Table C1.2.9: Radioactivity concentration of radionuclides in Batch 3 of filter A (HFPM50); a qualitative bar chart (the horizontal blue rectangles) shows the relationship amongst the radionuclides in each column

HFPM50 Batch 3	(0 hr)	Sample 1 (0.5 hr)			Sample 2 (3.5 hr)			Sample 3 (6.5 hr)			Finish
Radionuclides	Feed	Feed	Premeate	Retentate	Feed	Permeate	Retentate	Feed	Permeate	Retentate	Back Wash
Mn-54	5.58E+03	5.02E+03		1.15E+04	7.47E+03	5.48E+01	2.28E+04	5.16E+04		1.02E+05	2.04E+03
Co-57											
Co-58	3.29E+03	2.78E+03	8.62E+02	5.01E+03	3.93E+03	7.78E+02	1.05E+04	2.11E+04	6.65E+02	4.38E+04	1.03E+03
Co-60	7.93E+04	7.34E+04	8.37E+02	1.57E+05	1.11E+05	5.97E+02	3.44E+05	7.68E+05	6.01E+02	1.59E+06	2.93E+04
Zn-65	1.02E+03			2.65E+03	1.59E+03		4.83E+03	8.60E+03		1.63E+04	
Nb-95	2.27E+03	1.83E+03		4.15E+03	2.72E+03		8.74E+03	5.01E+04		4.46E+04	8.59E+02
Zr-95	5.06E+03	4.42E+03		9.51E+03	6.43E+03		1.77E+04	2.49E+04		9.71E+04	1.53E+03
Ag-110m	3.97E+04	3.98E+04		8.92E+04	6.77E+04		1.76E+05	4.31E+05		8.81E+05	1.95E+04
Sn-113								2.17E+03		5.09E+03	
Sb-124	6.57E+02	6.21E+02		2.04E+03	1.13E+03		3.26E+03	6.99E+03	8.98E+01	1.40E+04	
Sb-125	3.57E+03	3.27E+03		6.53E+03	4.86E+03	4.53E+02	1.55E+04	3.53E+04	8.43E+02	6.83E+04	
Total activity Conc (Bq/kg)	*1.40E+05*	*1.31E+05*	*1.70E+03*	*2.87E+05*	*2.07E+05*	*1.88E+03*	*6.03E+05*	*1.40E+06*	*2.39E+03*	*2.86E+06*	*5.43E+04*
Tot.Act. Uncertainty (Bq/kg)	*5.51E+03*	*5.66E+03*	*1.82E+02*	*1.15E+04*	*8.48E+03*	*1.74E+02*	*2.37E+04*	*5.36E+04*	*1.83E+02*	*1.10E+05*	*2.67E+03*

Permeate

Three permeate samples were taken having a radioactivity concentration range between $1.7 \cdot 10^3$ and $2.2 \cdot 10^3$ with an average of $1.9 \cdot 10^3$ Bq/kg. The dominant radionuclides were found to be Sb-125, Co-58 and Co-60 as shown in table C1.2.9. There was an increase in the radioactivity of permeate water with time.

Retentate

Three retentate samples were taken had radioactivity concentrations that ranged between $2.9 \cdot 10^5$ Bq/kg and $2.9 \cdot 10^6$ Bq/kg as shown in table C1.2.9. The last value is 2036% the radioactivity of the feed at t=0. The retentate of Batch 3 seems to follow the same color trend as the previous batches.

Feed

Four samples were taken; the first sample at (t=0) has a radioactivity concentration of $1.4 \cdot 10^5$ Bq/kg, while the last sample amounted to $1.4 \cdot 10^6$ Bq/kg. Co-60 and Ag-110m were the dominant radionuclides (table C1.2.9).

Backwash

The backwash sample had a radioactivity concentration of $5.4 \cdot 10^4$ Bq/kg with Co-60 $2.9 \cdot 10^4$ Bq/kg and Ag-110m $2.0 \cdot 10^4$ Bq/kg as the dominant radionuclides (table C1.2.9). The remaining BW was added to the next batch.

Ion Exchanger

The radioactivity of the sample was 55 Bq/kg (table C1.2.10), which was an acceptable value. No recirculation through the exchanger of the permeate water was needed.

Boric acid concentration

The concentration of the boric acid did not increase in any of the samples. The average boric acid concentration was about 560 ppm (table C1.2.10).

Table C1.2.10: results of the chemical analysis performed using the samples obtained from Batch 3 of filter A; radioactivity concentration is denoted here as (A) and χ represents the conductivity; [B] represents the boric acid concentration.

Batch 3, sample 1	χ µS/cm	pH	[B] avg	A Bq/kg
Feed 0	3	5	555	1,40E+05
Feed	3	6	555	1,31E+05
Permeate	2	6	563	1,70E+03
Retentate	3	5	555	2,87E+05
Batch 3, sample 2	**χ µS/cm**	**pH**	**[B] avg**	**A Bq/kg**
Feed	3	6	555	2,07E+05
Permeate	2	6	562	1,88E+03
Retentate	4	5	555	6,03E+05
Batch 3, sample 3	**χ µS/cm**	**pH**	**[B] avg**	**A Bq/kg**
Feed	6	5	562	1,41E+06
Permeate	3	5	570	2,20E+03
Retentate	9	5	565	2,86E+06
Backwash	2	5	N/A	5,43E+04
IXr mixed bed	1	5	N/A	5,48E+01

Dose build-up

The dose rate of the module was measured with respect to time during the process and after the BW as shown in table C1.2.11.

Table C1.2.11: dose rate build-up of the filter A during the Batch 3 process at the designated positions in µSv/h.

HFPM50 BATCH 3	Dose rate (µSv/h)			
Elapsed time (h)	Filter Top	Filter Middle	Filter Bottom	Average Dose rate (µSv/h)
0	28	53	157	79
0.5	40	95	160	98
3.5	40	95	200	112
6.5	88	130	340	186
After BW	35	80	220	112

Fouling

Batch 3 has exhibited no fouling tendency. There was no change in the TMP value; FT was constant all the time (table C1.2.12).

Table C1.2.12: the process parameters that governed Batch 3.

HFPM50 BATCH 3	Process operational parameters					
Elapsed time (h)	RPM	PIT00 (mbar)	PIT-01 (bar)	PI-02 (bar)	PDI-00 (mbar)	TI-01 (°C)
0.0	1895	105	2	1.45	1001	26.5
0.5	1901	101	2	1.25	1006	26.5
3.5	1912	78	2	1.25	1018	27
6.5	1924	52	2	1.25	1032	27.5

C1.2.5 Batch 4

The experiment took little bit more than **6** hours so that **600** liters of TT water were concentrated down to ~18 liters. 11 liters of BW from Batch 3 were added to the feed tank. Permeate tank volume was about 565 liters filtered through a 75 liter a porous mixed bed IXr.

Batch 4 analysis

The final radioactivity concentration of the retentate was about $2.1 \cdot 10^6$ Bq/kg. Co-60 and Ag-110m were the dominant radionuclides (table C1.2.13).

Table C1.2.13: Radioactivity concentration of radionuclides in Batch 4 of filter A (HFPM50); a qualitative bar chart (the horizontal blue rectangles) shows the relationship amongst the radionuclides in each column

HFPM50 Batch 4	(0 hr)	Sample 1 (1 hr)			Sample 2 (4 hr)			Sample 3 (6.5 hr)			Finish
Radionuclides	Feed	Feed	Premeate	Retentate	Feed	Permeate	Retentate	Feed	Permeate	Retentate	Back Wash
Mn-54	2.84E+03	3.75E+03	5.08E+01	8.50E+03	7.20E+03	4.88E+01	1.93E+04	3.41E+04		6.57E+04	7.31E+02
Co-57								7.25E+02			
Co-58	2.23E+03	2.19E+03	7.79E+02	4.37E+03	4.14E+03	7.64E+02	9.38E+03	1.47E+04	6.86E+02	2.74E+04	5.04E+02
Co-60	4.78E+04	5.64E+04	6.57E+02	1.37E+05	1.15E+05	5.80E+02	2.96E+05	5.25E+05	5.50E+02	1.04E+06	1.16E+04
Zn-65	8.97E+02				1.49E+03		3.47E+03	8.25E+03		1.27E+04	
Nb-95	2.14E+03	2.42E+03		6.08E+03	5.77E+03		1.44E+04	2.78E+04		5.72E+04	4.29E+02
Zr-95	1.15E+03	1.23E+03		2.75E+03	2.96E+03		6.77E+03	1.31E+04		2.63E+04	
Ag-110m	3.72E+04	4.24E+04	2.54E+02	1.03E+05	9.05E+04		2.22E+05	4.15E+05	2.34E+02	8.40E+05	8.05E+03
Sn-113								2.32E+03		4.33E+03	
Sb-124	6.72E+02	6.96E+02	9.17E+01	1.85E+03	1.23E+03	1.01E+02	2.49E+03	5.88E+03	1.93E+02	1.10E+04	
Sb-125	2.55E+03		4.05E+02		5.32E+03	5.30E+02	1.19E+04	2.40E+04	8.37E+02	4.47E+04	
Total activity Conc (Bq/kg)	***9.74E+04***	***1.09E+05***	***2.24E+03***	***2.63E+05***	***2.33E+05***	***2.23E+03***	***5.86E+05***	***1.07E+06***	***2.50E+03***	***2.12E+06***	***2.13E+04***
Tot.Act. Uncertainty (Bq/kg)	***4.32E+03***	***4.79E+03***	***1.45E+02***	***1.09E+04***	***9.49E+03***	***1.78E+02***	***2.29E+04***	***4.09E+04***	***2.29E+02***	***8.05E+04***	***1.31E+03***

Permeate

Three permeate samples were taken having an average radioactivity concentration of $2.2 \cdot 10^3$ Bq/kg. The dominant radionuclides were found to be Sb-125, Co-58 and Co-60 as shown in table C1.2.13. The trend where the radioactivity concentration of Sb-125 increased to a level higher than Co-58 and Co-60 was seen here too.

Retentate

Three retentate samples were taken had radioactivity concentrations that ranged between $2.6 \cdot 10^5$ Bq/kg and $2.1 \cdot 10^6$ Bq/kg (table C1.2.13). The last value was 2183% the radioactivity of the feed at t=0.

Feed

Four samples were taken where the radioactivity concentration at t=0 was $9.7 \cdot 10^4$ Bq/kg (table C1.2.13). The three samples that followed showed an increasing radioactivity as the concentration process proceeded.

Backwash

One sample was taken for analysis of the BW water and had a radioactivity concentration of $2.1 \cdot 10^5$ Bq/kg with Co-60 having $4.8 \cdot 10^4$ Bq/kg and Ag-110m having $3.7 \cdot 10^4$ as the dominant radionuclides (table C1.2.13). The remaining BW water was added to the Batch 5.

Ion Exchanger

One sample was acquired after the IXr and was about 49 Bq/kg (table C1.2.14); this value was lower than the radioactivity concentration limit of 100 Bq/kg and thus no recirculation was applied.

Boric acid concentration

The concentration of the boric acid did not increase in any of the samples. It remained around the same level of 565 ppm (table C1.2.14).

Table C1.2.14: results of the chemical analysis performed using the samples obtained from Batch 4 of filter A; radioactivity concentration is denoted here as (A) and χ represents the conductivity; [B] represents the boric acid concentration.

Batch 4, sample 1	χ µS/cm	pH	[B] avg	A Bq/kg
Feed 0	3	6	559	9,74E+04
Feed	3	6	560	1,09E+05
Permeate	3	6	560	2,24E+03
Retentate	3	6	560	2,64E+05
Batch 4, sample 2	**χ µS/cm**	**pH**	**[B] avg**	**A Bq/kg**
Feed	3	6	561	2,33E+05
Permeate	3	6	560	2,23E+03
Retentate	4	5	562	5,86E+05
Batch 4, sample 3	**χ µS/cm**	**pH**	**[B] avg**	**A Bq/kg**
Feed	5	5	565	1,07E+06
Permeate	3	5	563	2,50E+03
Retentate	8	6	565	2,13E+06
Backwash	2	5	N/A	2,14E+04
IXr mixed bed	1	6	N/A	3,60E+01

Dose build-up

The dose rate of the module was measured with respect to time during the process and after the BW as shown in table C1.2.15.

Table C1.2.15: dose rate build-up of the filter A during the Batch 4 process at the designated positions in µSv/h.

HFPM50 BATCH 4	Dose rate (µSv/h)			
Elapsed time (h)	Filter Top	Filter Middle	Filter Bottom	Average Dose rate (µSv/h)
0	33	80	200	104
1	32	75	210	106
4	40	96	260	132
6.2	80	140	340	187
After BW	40	95	250	128

Fouling

Again no fouling was observed during this batch. TMP showed no change during the test; FT was constant (table C1.2.16).

Table C1.2.16: the process parameters that governed Batch 4

HFPM50 BATCH 4	Process operational parameters					
Elapsed time (h)	RPM	PIT00 (mbar)	PIT-01 (bar)	PI-02 (bar)	PDI-00 (mbar)	TI-01 (°C)
0.0	1878	105	2	1.45	1005	24.5
1.0	1902	97	2	1.25	1014	27
4.0	1912	72	2	1.25	1025	27.5
6.2	1921	52	2	1.25	1036	28

C1.2.6 Batch 5

The experiment took **2.5** hours so that **100** liters, the result of concentrating a volume of 2.7m^3 of TT; there was also the **98** liter added unintentionally, as described earlier. That makes it roughly 200 liters that were concentrated down to ~10 liters.

Permeate tank volume was about 182 liters filtered through a 75 liters porous mixed bed IXr. The BW water was analyzed after washing the module to investigate any easily removed particles that have built up in the membrane module and the pipes.

The system was then washed with a solution of sodium hydroxide (NaOH, pH 12,5), left for a period of time to run through the system then followed by an acid wash using phosphoric acid (H_3P0_4, pH 2) then left to soak in the solution overnight (table C1.2.21).

Batch 5 analysis

Five samples were taken; the final radioactivity concentration of the retentate was about $4.5 \cdot 10^6$ Bq/kg. Co-60 and Ag-110m were the dominant radionuclides with the latter having the highest radioactivity concentration of $2.8 \cdot 10^6$ Bq/kg (table C1.2.17).

All retentate samples were diluted 1:50 before being measured using the HPGe detector to avoid paralyzing the detector (dead time was greater than 60%). Then the true results were calculated back by multiplying the acquired radioactivity with 50.

Table C1.2.17: Radioactivity concentration of radionuclides in Batch 5 of filter A (HFPM50); a qualitative bar chart (the horizontal blue rectangles) shows the relationship amongst the radionuclides in each column

HFPM50 Batch 5	(0hr)	sample 1 (0.5 hr)			sample 2 (1 hr)			sample 3 (1.5 hr)			sample 4 (2 hr)			sample 5 (2.5 hr)		Finish	
Radionuclides	Feed	Feed	Premeate	Retentate	Feed	Permeate	Retentate	Feed	Permeate	Retentate	Feed	Permeate	Retentate	Permeate	Retentate	Back Wash	IXr (mixed)
Mn-54	5,45E+03	7,35E+03	3,42E+01	1,54E+04	8,83E+03		2,70E+04	1,31E+04		2,60E+04	2,51E+04	6,24E+01	4,72E+04	6,76E+01	8,53E+04	6,11E+03	
Co-57																	
Co-58	4,81E+03		5,05E+02	8,91E+03	6,12E+03	5,10E+02	1,45E+04	6,58E+03	5,64E+02	1,09E+04	1,31E+04	6,15E+02	1,94E+04	7,51E+02	3,23E+04	3,21E+03	
Co-60	1,27E+05	1,38E+05	4,69E+02	2,93E+05	1,63E+05	4,73E+02	4,77E+05	2,41E+05	5,24E+02	5,11E+05	4,15E+05	5,59E+02	8,65E+05	7,14E+02	1,40E+06	1,07E+05	2,70E+01
Zn-65																1,23E+03	
Nb-95				1,59E+04			2,25E+04	1,14E+04		2,29E+04	2,49E+04		5,13E+04		8,27E+04	5,73E+03	
Zr-95													2,63E+04		4,89E+04	2,50E+03	
Ag-110m	2,03E+05	2,51E+05		5,30E+05	3,02E+05		7,89E+05	4,52E+05		9,63E+05	8,94E+05		1,66E+06		2,77E+06	1,64E+05	2,89E+01
Sn-113																	
Sb-124		4,21E+03	8,89E+01	9,02E+03	7,97E+03	4,88E+01	9,82E+03		1,19E+02	1,04E+04	1,43E+04	1,48E+02	1,89E+04	1,87E+02	2,73E+04	1,40E+03	
Sb-125			7,68E+02			8,06E+02			9,03E+02			1,01E+03		1,34E+03		7,21E+03	
Total activity Conc (Bq/kg)	*4,01E+05*	*4,01E+05*	*1,87E+03*	*8,72E+05*	*4,88E+05*	*1,84E+03*	*1,34E+06*	*7,23E+05*	*2,11E+03*	*1,54E+06*	*1,39E+06*	*2,39E+03*	*2,69E+06*	*3,06E+03*	*4,45E+06*	*2,99E+05*	*5,59E+01*
Tot.Act. Uncertainty (Bq/kg)	*2,73E+04*	*2,73E+04*	*1,20E+02*	*4,74E+04*	*3,05E+04*	*1,48E+02*	*6,74E+04*	*4,19E+04*	*1,89E+02*	*7,76E+04*	*6,90E+04*	*2,06E+02*	*1,23E+05*	*2,28E+02*	*1,99E+05*	*1,21E+04*	*1,49E+01*

Permeate

Five permeate samples were taken having a radioactivity concentration that ranged between $1.9 \cdot 10^3$ Bq/kg and $3.1 \cdot 10^3$ Bq/kg with an average of $2.3 \cdot 10^3$ Bq/kg. The dominant nuclides were found to be Sb-125, Co-58 and Co-60 as shown in table C1.2.17.

Retentate

Five retentate samples were taken that had radioactivity concentration that ranged between $8.7 \cdot 10^5$ Bq/kg and $4.5 \cdot 10^6$ Bq/kg table (C1.2.17). The last value was 1309% the radioactivity of the feed at t=0.

The color of the water became more brown with respect to time, contrary to the permeate that remained clear. The brown particulate material started building up slag on the metallic pre-filter mesh as well as on the transparent corner-pipe at the output of the filter module.

A certain volume of the sample was filtered using a Millipore filter paper of pore size 0,45μm to collect the sedimentations in OT filtration procedure. The filtrate was measured then with the HPGe detector that measured a radioactivity concentration of $3.4 \cdot 10^5$ Bq/kg. The sedimentation contained around 90% of the radioactivity after filtration (table C1.2.18).

Feed

Five samples were taken with the first having a radioactivity concentration of $1.5 \cdot 10^5$ Bq/kg (table C1.2.17). The water from the retentate tank was full of slag and precipitants. One concern was if such slag would plug the valves resulting in a decrease in the flow of the feed water.

Another concern was also if those large flocks of slag would settle in the metallic mesh protection grid at the base of the membrane module. Those concerns disappeared after the pump broke the slag flocks into very small particulates, so no flow was largely obstructed. It took a while before the system settled into the steady state process.

Backwash

The backwash sample had a radioactivity concentration of $3 \cdot 10^5$ Bq/kg with Ag-110m $1.6 \cdot 10^5$ Bq/kg and Co-60 $1.1 \cdot 10^5$ as the dominant radionuclides (table C1.2.17). The remaining BW was added to Batch 1 of Filter B. The BW water contained dark flakes (scaling) of compressed precipitate.

Ion Exchanger

A previous study using SWM produced a radioactivity concentration of 250 Bq/kg in the permeate water; it was filtered through a mixed bed IXr producing a permeate radioactivity concentration of only 3Bq/kg, which was about **1% retention**. While in this study a $2.3 \cdot 10^3$ Bq/kg was filtered using the same type of IXr into 56 Bq/kg which is **2% retention** (table C1.2.17).

Boric acid concentration

The concentration of the boric acid did not increase in any of the samples. It remained around the same level of 565 ppm (table C1.2.18).

Table C1.2.18: results of the chemical analysis performed using the samples obtained from Batch 5 of filter A; radioactivity concentration is denoted here as (A) and χ represents the conductivity; [B] represents the boric acid concentration.

Batch 5, sample 1	χ µS/cm	pH	[B] avg	A Bq/kg
Feed 0	10	5,9	559	6,79E+03
Feed	10	5,9	561	8,03E+03
Permeate	8	5,8	561	1,87E+03
Retentate	14	6	562	1,74E+04
Batch 5, sample 2	**χ µS/cm**	**pH**	**[B] avg**	**A Bq/kg**
Feed	11	6	562	9,76E+03
Permeate	8	5,8	562	1,84E+03
Retentate	16	6	562	2,68E+04
Batch 5, sample 3	**χ µS/cm**	**pH**	**[B] avg**	**A Bq/kg**
Feed	13	6	562	1,45E+04
Permeate	9	6	561	2,11E+03
Retentate	18	6	563	3,09E+04
Batch 5, sample 4	**χ µS/cm**	**pH**	**[B] avg**	**A Bq/kg**
Feed	17	6	564	2,77E+04
Permeate	10	6	562	2,39E+03
Retentate	23	6	564	5,37E+04
Batch 5, sample 5	**χ µS/cm**	**pH**	**[B] avg**	**A Bq/kg**
Feed	N/A	6	N/A	N/A
Permeate	13	6	562	8,90E+04
Retentate	28	6	558	8,90E+04
Retentate (0.45µm)	N/A	N/A	N/A	3,39E+05
Backwash	9	6	N/A	2,99E+05
IXr mixed bed	1	6	N/A	5,59E+01

Dose build-up

The dose rate of the module was measured with respect to time during the process and after the BW as shown in table C1.2.19. **Table C1.2.19: dose rate build-up of the filter A during the Batch 5 process at the designated positions in µSv/h.**

HFPM50 BATCH 5	Dose rate (µSv/h)			
Elapsed time (h)	Filter Top	Filter Middle	Filter Bottom	Average Dose rate (µSv/h)
0	40	85	250	125
0.5	58	130	300	163
1	70	133	330	178
1.5	92	157	360	203
2	120	215	460	265
2.5	130	260	485	292
Empty	134	350	615	366
After BW	62	125	280	156

Fouling

Batch 5 showed a clear evidence of fouling. 30 minutes after start up the PI-02 started decreasing, while the PID regulator maintained a constant input pressure at 2 bar as indicated by input pressure indicator PIT-01. The flow of the permeate and retentate were maintained constant at 80 and 50 l/h respectively, leaving the change in TMP as the only variable, thus giving rise to an increase in the term $\mu \cdot R_{tot}$ (FT).

The last batch contained a lot of the brown sediment that settled down in the retentate tank since the start of the pilot experiment. These precipitations had a direct impact on the TMP very shortly after the start as seen in figure C1.2.1

The filter and the system were checked later on for any sedimentation or slag build-up on the protective metallic mesh at the input side to the filter. The slag covered a great portion of the metallic mesh which probably contributed to the pressure drop along the filter as was displayed by the pressure gauge PDI-00 (table C1.2.20).

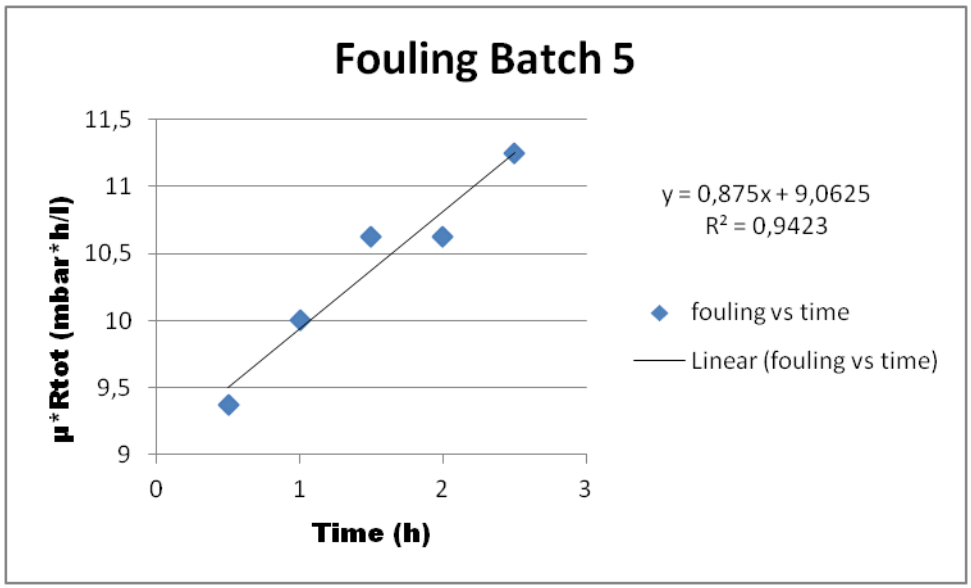

Figure C1.2.1: The fouling tendency in the final batch, a clear indication of the effects of cake and slag build up.

Table C1.2.20: the process parameters that governed Batch 5

HFPM50 BATCH 5	Process operational parameters					
Elapsed time (h)	RPM	PIT00 (mbar)	PIT-01 (bar)	PI-02 (bar)	PDI-00 (mbar)	TI-01 (°C)
0.0	1868	70	2	1.45	1010	25
0.5	1880	65	2	1.25	1016	27
1.0	1885	61	2	1.2	1029	27
1.5	1888	56	2	1.15	1035	27
2.0	1894	51	2	1.15	1046	27.5
2.5	1904	24	2	1.1	1060	31

Chemical cleaning

The CC process used a base (NaOH) followed by an acid (H_3PO_4); the dose rate was measured during the CC process (table C 1.2.21).

Table C 1.2.21: The dose rate measurements as a result of the multistage chemical wash method using solutions of NaOH and H3PO4 at pH 12,5 and 2 respectively.

HFPM50 Chemical Cleaning	Dose rate (µSv/h)			
Elapsed time (h)	Filter Top	Filter Middle	Filter Bottom	Average Dose rate (µSv/h)
NaOH pH 12,5				
0.0	45	100	260	135
0.3	81	185	350	205
1.5	80	200	355	212
After BW	67	180	340	196
Acid (H3PO4) pH 2				
0	67	180	350	199
18	67	180	350	199
After BW	62	175	350	196

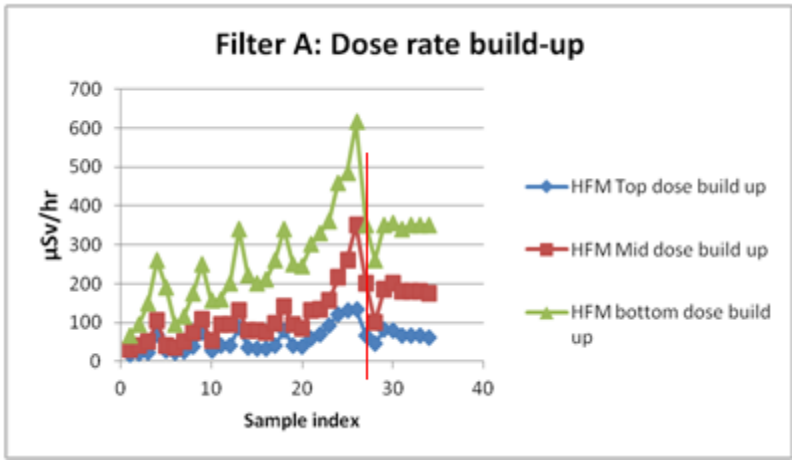

Figure C1.2.2: plot of all the dose rate build-up data at the three different measurement locations (top, middle and bottom sections of filter module A); tops are the maximum dose rate accumulated at the end of each batch, while troughs are the remained dose rate build-up after a BW procedure. The portion lying after the red line concerns the CC procedure.

C1.3 HFPM5: Filter B

C1.3.1 Batch 1

The experiment took around **4** hours so that **400** liters of TT water and the **6** liters of BW water from Batch 5 of filter A to be concentrated down to ~18 liters, which were then drained into the retentate tank. Permeate tank volume was about 362 liters filtered through the same 75 liter mixed bed IXr used in the experiment of filter A.

Batch 1 analysis

The final radioactivity concentration of the retentate was about $6.3 \cdot 10^5$ Bq/kg. Co-60 and Ag-110m were the dominant radionuclides (table C1.3.1).

Table C1.3.1: Radioactivity concentration of radionuclides in Batch 1 of Filter B (HFPM5); a qualitative bar chart (the horizontal red rectangles) shows the relationship amongst the radionuclides in each column.

HFPM5 Batch 1	(0 h)		Sample 1 (1.5 hr)			Sample 2 (4 hr)			Finish
Radionuclides	TankTainer	Feed	Feed	Premeate	Retentate	Feed	Permeate	Retentate	Back Wash
Mn-54	1.43E+03	1.48E+03	1.70E+03	3.59E+01	4.15E+03	6.88E+03	5.02E+01	1.35E+04	5.31E+02
Co-57									
Co-58	1.38E+03	1.30E+03	1.39E+03	7.28E+02	2.81E+03	3.97E+03	7.38E+02	6.19E+03	3.29E+02
Co-60	2.52E+04	2.40E+04	2.98E+04	5.68E+02	7.37E+04	1.20E+05	6.08E+02	2.34E+05	9.91E+03
Zn-65	5.47E+02					1.50E+03		3.85E+03	
Nb-95	7.97E+02	1.02E+03	1.14E+03		3.15E+03	5.23E+03		1.07E+04	4.82E+02
Zr-95	4.71E+02	4.51E+02	6.78E+02		1.73E+03	2.59E+03		5.02E+03	
Ag-110m	2.81E+04	2.84E+04	3.73E+04	1.14E+02	8.96E+04	1.73E+05		3.44E+05	1.43E+04
Sn-113									
Sb-124	3.69E+02	3.80E+02	3.72E+02	1.07E+02		1.14E+03	6.69E+01	3.32E+03	2.31E+02
Sb-125	4.57E+02			4.61E+02		6.58E+03	5.79E+02	1.26E+04	
Total activity Conc (Bq/kg)	**5.83E+04**	**5.70E+04**	**7.23E+04**	**2.02E+03**	**1.75E+05**	**3.21E+05**	**2.04E+03**	**6.32E+05**	**2.58E+04**
Tot.Act. Uncertainty (Bq/kg)	**2.53E+03**	**2.52E+03**	**3.07E+03**	**1.55E+02**	**7.53E+03**	**1.29E+04**	**1.40E+02**	**2.56E+04**	**1.27E+03**

Tanktainer

One sample of the tanktainer water was taken prior mixing in the feed tank. The TT sample had a radioactivity concentration of $5.8 \cdot 10^4$ Bq/kg (table C1.3.1).

Permeate

Two permeate samples were taken having an average radioactivity concentration of $2 \cdot 10^3$ Bq/kg. The dominant radionuclides were found to be Sb-125, Co-58 and Co-60 as shown in table C1.3.1. These were the first permeate samples of filter B.

The same radionuclides of the previous membrane showed up in the HPGe spectrometer that also confirmed the results of the laboratory scale experiment (table B.1).

Retentate

Two retentate samples were taken; they had a radioactivity concentration that ranged between $1.8 \cdot 10^5$ Bq/kg and $6.3 \cdot 10^5$ Bq/kg (table C1.3.1). The last value is 1110% the radioactivity of the feed at t=0. There was a shift to brown color in the concentration side which was absent in the permeate side.

Feed

Three samples were taken one being the steady state sample at t=0 having a radioactivity concentration of $5.7 \cdot 10^4$ Bq/kg, while the other two samples were taken under the course of the filtration process had $7.3 \cdot 10^4$ then $3.2 \cdot 10^5$ Bq/kg. Ag-110m and Co-60 were the dominant nuclides (table C1.3.1).

Backwash

One sample was taken out of the 8 liters of the used BW water. It had a radioactivity concentration of $2.6 \cdot 10^4$ Bq/kg with Co-60 $9.9 \cdot 10^3$ Bq/kg and Ag-110m $1.4 \cdot 10^4$ as the dominant radionuclides (table C1.3.1). The remaining BW was added to Batch 2.

Ion Exchanger

The mixed bed IXr diminished the radioactivity of the permeate water down to 49 Bq/kg (table C1.3.2).

Boric acid concentration

The results of the laboratory scale experiment showed no sign of increased concentration of boric acid in the filter module 5 (table B2). These results were confirmed in the first batch of filter B. The result was 554 ppm a bit lower than that of the TT's boric acid concentration that was 570 ppm (table C1.3.2).

Table C1.3.2: results of the chemical analysis performed using the samples obtained from Batch 1 of filter A; radioactivity concentration is denoted here as (A) and χ represents the conductivity; [B1], [B2] and [B] represent the boric acid concentration.

Batch 1, sample 1	χ µS/cm	pH	[B1] ppm	[B2] ppm	[B] avg	A Bq/kg
Tanktainer	2,8	5,6	569,8	570,4	570,1	5,83E+04
Feed 0	3,18	5,7	550	550,3	550,15	5,69E+04
Feed	3,3	5,7	551	553,4	552,2	7,23E+04
Permeate	3,1	5,7	551,3	551,3	551,3	2,02E+03
Retentate	3,4	5,7	551,2	551,2	551,2	1,75E+05
Batch 1, sample 2	**χ µS/cm**	**pH**	**[B1] ppm**	**[B2] ppm**	**[B] avg**	**A Bq/kg**
Feed	3,5	5,7	554,9	555,2	555,05	3,21E+05
Permeate	3,2	5,7	554,5	554,4	554,45	2,04E+03
Retentate	3,9	5,7	554,8	554,9	554,85	6,33E+05
Backwash	1,2	6,1	NaN	NaN	NaN	2,58E+04
IXr mixed bed	0,85	6,3	NaN	NaN	NaN	4,90E+01

Dose build-up

The dose rate of the module was measured with respect to time during the process and after the BW as shown in table C1.3.3. The module exhibited asymmetry with respect to dose-build up. The filter was divided into frontal and dorsal part to monitor the asymmetry in dose rate build-up.

Table C1.3.3: The dose rate build-up of the filter B during the Batch 1 process at the designated positions in µSv/h.

HFPM5 Batch 1			Dose rate (µSv/h)				
Filter Front			Elapsed time (h)	Filter back			Average dose rate
Top	Mid	Bottom		Top	Mid	Bottom	
30	32	35	**0.0**	35	65	37	39
27	45	38	**1.5**	50	80	55	49
46	67	70	**4.0**	70	115	110	80
37	67	70	**After BW**	57	105	80	69

Fouling

No fouling was observed as there were no changes in the TMP values (table C1.3.4).

Table C1.3.4: the process parameters that governed Batch 1

HFPM5 BATCH 1	Process operational parameters					
Elapsed time (h)	RPM	PIT00 (mbar)	PIT-01 (bar)	PI-02 (bar)	PDI-00 (mbar)	TI-01 (°C)
0.0	1847	87	2	1.2	1031	26.5
1.5	1836	75	2	1.2	1015	27.5
4.0	1851	53	2	1.2	1040	28

C1.3.2 Batch 2

It took around **4.5** hours to concentrate **410** liters of TT water down to 18 liters of retentate.

Batch 2 analysis

The final radioactivity concentration of the retentate was about $8.1 \cdot 10^5$ Bq/kg. Co-60 and Ag-110m were the dominant radionuclides (table C1.3.5).

Table C1.3.5: Radioactivity concentration of radionuclides in Batch 2 of Filter B (HFPM5); a qualitative bar chart (the horizontal red rectangles) shows the relationship amongst the radionuclides in each column.

HFPM5 Batch 2	(0 h)		Sample 1 (1.5 hr)			Sample 2 (4 hr)			Finish
Radionuclides	TankTainer	Feed	Feed	Premeate	Retentate	Feed	Permeate	Retentate	Back Wash
Mn-54	1.26E+03	1.46E+03	1.85E+03	5.44E+01	4.93E+03	8.53E+03	3.27E+01	1.74E+04	8.69E+02
Co-57									
Co-58	1.20E+03	1.39E+03	1.51E+03	6.71E+02	2.76E+03	4.34E+03	6.78E+02	8.87E+03	7.78E+02
Co-60	2.32E+04	2.48E+04	3.30E+04	6.12E+02	8.73E+04	1.58E+05	6.25E+02	3.18E+05	1.49E+04
Zn-65		5.78E+02	7.00E+02			2.35E+03		3.99E+03	
Nb-95	9.74E+02	1.02E+03	1.25E+03		3.32E+03	6.59E+03		1.37E+04	5.36E+02
Zr-95	4.94E+02	4.01E+02	8.04E+02		1.51E+03	3.12E+03		6.17E+03	
Ag-110m	2.73E+04	2.87E+04	3.87E+04		9.70E+04	2.04E+05	9.44E+01	4.23E+05	1.96E+04
Sn-113	2.40E+02					7.30E+02			
Sb-124		3.15E+02	5.50E+02	7.04E+01	1.44E+03	1.73E+03	6.99E+01	3.15E+03	
Sb-125	1.33E+03		1.92E+03	5.25E+02		7.43E+03	5.81E+02	1.41E+04	
Total activity Conc (Bq/kg)	**5.61E+04**	**5.87E+04**	**8.04E+04**	**1.93E+03**	**1.98E+05**	**3.97E+05**	**2.08E+03**	**8.09E+05**	**3.66E+04**
Tot.Act. Uncertainty (Bq/kg)	**2.45E+03**	**2.57E+03**	**3.36E+03**	**1.34E+02**	**8.36E+03**	**1.57E+04**	**1.34E+02**	**3.24E+04**	**1.96E+03**

Tanktainer

A radioactivity concentration of $5.6 \cdot 10^4$ Bq/kg was measured using HPGe spectrometer (table C1.3.5). That was lower than Batch 1.

Permeate

Two permeate samples were taken having the average radioactivity of $2 \cdot 10^3$ Bq/kg. The dominant radionuclides were found to be Sb-125, Co-58 and Co-60 as shown in table C1.3.5.

Retentate

Two retentate samples were taken having the activities $2 \cdot 10^5$ Bq/kg and $8.1 \cdot 10^5$ Bq/kg as shown in table C1.3.5. The last value is 1379% the radioactivity of the feed at t=0. Ag-110m and Co-60 were the dominant radionuclides.

Feed

Three samples were taken with the first one being the steady state sample at t=0 having a radioactivity concentration of $5.9 \cdot 10^4$ Bq/kg (table C1.3.5). Ag-110m and Co-60 dominated over the other radionuclides.

Backwash

One sample was taken out of the 7 liters of BW water which had a radioactivity concentration of $3.7 \cdot 10^4$ Bq/kg with Co-60 $1.5 \cdot 10^4$ Bq/kg and Ag-110m $2 \cdot 10^4$ Bq/kg as the dominant radionuclides (table C1.3.5). The remaining BW was added to Batch 3.

Ion Exchanger

A radioactivity concentration of 39 Bq/kg remained after the mixed bed IXr (table C1.3.6).

Boric acid concentration

The concentration of the boric acid did not increase in any of the samples. The measured concentrations had an average of 563 ppm (table C1.3.6).

Table C1.3.6: results of the chemical analysis performed using the samples obtained from Batch 2 of filter A; radioactivity concentration is denoted here as (A) and χ represents the conductivity; [B1], [B2] and [B] represent the boric acid concentration.

Batch 2, sample 1	χ µS/cm	pH	[B1] ppm	[B2] ppm	[B] avg	A Bq/kg
Tanktainer	2,8	5,6	570,7	571	570,85	5,61E+04
Feed 0	2,9	5,6	559,3	559,4	559,35	5,87E+04
Feed	2,9	5,6	560	560,2	560,1	8,04E+04
Permeate	2,8	5,7	561,8	559,8	560,8	1,93E+03
Retentate	3,2	5,6	560,1	560	560,05	1,98E+05
Batch 2, sample 2	**χ µS/cm**	**pH**	**[B1] ppm**	**[B2] ppm**	**[B] avg**	**A Bq/kg**
Feed	3,8	5,7	563,9	564,7	564,3	3,97E+05
Permeate	3	5,6	563,8	563,5	563,65	2,10E+03
Retentate	4	5,7	564	563,9	563,95	8,10E+05
Backwash	1,9	5,7	NaN	NaN	NaN	3,66E+04
IXr mixed bed	1	6	NaN	NaN	NaN	3,90E+01

Dose build-up

The dose rate of the Filter B was measured with respect to time during the process and after the BW as shown in table C1.3.7.

Table C1.3.7: The dose rate build-up of the filter B during the Batch 2 process at the designated positions in µSv/h.

HFPM5 Batch 2			Dose rate (µSv/h)				
Filter Front			Elapsed time (h)	Filter back			Average dose rate
Top	Mid	Bottom		Top	Mid	Bottom	
33	60	45	**0.0**	52	95	72	60
34	57	47	**1.5**	53	103	75	62
31	80	80	**4.3**	86	135	125	90
33	58	55	**After BW**	65	120	85	69

Fouling

No fouling was observed as there were no changes in the TMP values (table C1.3.8).

Table C1.3.8: the process parameters that governed Batch 2

HFPM5 BATCH 2	Process operational parameters					
Elapsed time (h)	RPM	PIT00 (mbar)	PIT-01 (bar)	PI-02 (bar)	PDI-00 (mbar)	TI-01 (°C)
0.0	1857	88	2	1.2	1006	23.5
1.5	1849	76	2	1.15	1032	25.5
4.3	1860	53	2	1.15	1050	26.5

C1.3.3 Batch 3

The experiment took **7** hours so that **626** liters of TT water were concentrated down to ~12 liters, which were then drained into the retentate tank. Permeate tank volume was about 617 liters filtered through a 75 liter mixed bed IXr. 7 liters of the BW from Batch 2 were added to the feed tank.

Batch 3 analysis

This batch produced around 18 liters of retentate having the radioactivity concentration of $9.3 \cdot 10^5$ Bq/kg. The dominant radionuclides were found to be Ag-110m and Co-60 as shown in table C1.3.9.

Table C1.3.9: Radioactivity concentration of radionuclides in Batch 3 of Filter B (HFPM5); a qualitative bar chart (the horizontal red rectangles) shows the relationship amongst the radionuclides in each column.

HFPM5 Batch 3	(0 h)		Sample 1 (4 hr)			Sample 2 (7 hr)			Finish	
Radionuclides	TankTainer	Feed	Feed	Premeate	Retentate	Feed	Permeate	Retentate	Back Wash	IXr (mixed)
Mn-54	1,09E+03	1,19E+03	2,57E+03	4,20E+01	6,44E+03	1,36E+04		1,80E+04	3,20E+02	
Co-57										
Co-58	1,03E+03	1,09E+03	1,93E+03	6,11E+02	3,23E+03	6,70E+03	6,33E+02	8,05E+03	2,63E+02	
Co-60	1,90E+04	2,14E+04	4,64E+04	6,06E+02	1,13E+05	2,54E+05	5,44E+02	3,40E+05	5,04E+03	
Zn-65					1,49E+03	2,41E+03				
Nb-95	6,19E+02	6,55E+02	1,70E+03		3,86E+03	1,01E+04		1,43E+04		
Zr-95		3,88E+02	1,12E+03		2,41E+03	4,33E+03		7,40E+03		
Ag-110m	2,39E+04	2,58E+04	5,81E+04	1,61E+02	1,44E+05	3,96E+05	1,25E+02	5,19E+05	7,32E+03	
Sn-113						1,59E+03				
Sb-124	2,86E+02	5,09E+02	7,42E+02	6,34E+01	1,30E+03	3,20E+03	6,86E+01	3,73E+03		3,57E+01
Sb-125	1,36E+03			5,16E+02	6,00E+03	1,35E+04	6,08E+02	1,48E+04		
Total activity Conc (Bq/kg)	**4,73E+04**	**5,11E+04**	**1,13E+05**	**2,00E+03**	**2,82E+05**	**7,06E+05**	**1,98E+03**	**9,25E+05**	**1,29E+04**	**3,57E+01**
Tot.Act. Uncertainty (Bq/kg)	**2,14E+03**	**2,27E+03**	**4,74E+03**	**1,51E+02**	**1,16E+04**	**2,83E+04**	**1,48E+02**	**3,78E+04**	**7,63E+02**	**1,74E+01**

Tanktainer

One sample of the incoming 625 liters of TT water was taken; it had a radioactivity concentration of $4.7 \cdot 10^4$ Bq/kg; it was lower than the previous two TT samples taken before. Ag-110m and CO-60 were the dominant radionuclides (table C1.3.9).

Permeate

Two permeate samples were taken during the filtration process having an average radioactivity concentration of $2 \cdot 10^3$ Bq/kg. Co-58, Co-60 and Sb-125 were the dominant radionuclides (table C1.3.9).

Retentate

Two retentate samples were that had an increasing radioactivity concentration from $2.8 \cdot 10^5$ Bq/kg to $9.3 \cdot 10^5$ Bq/kg (table C1.3.9). The last value is 1812% the radioactivity of the feed at t=0. The retentate of Batch 3 seems to follow the same trend as the previous batches. The dominant radionuclides were Ag-110m and Co-60.

Feed

Three samples were taken. The first sample at (t=0) had a radioactivity concentration of $5.1 \cdot 10^4$ Bq/kg, while the last sample had $7.1 \cdot 10^5$ Bq/kg. Co-60 and Ag-110m were the dominant radionuclides (table C1.3.9).

Backwash

The BW sample had a radioactivity concentration of $1.3 \cdot 10^4$ Bq/kg with Co-60 and Ag-110m as the dominant radionuclides (table C1.3.9). The remaining BW water was added to Batch 4.

Ion Exchanger

It produced a sample with the radioactivity concentration of 36 Bq/kg (table C1.3.10), the only contribution to this radioactivity was from Sb-125.

Boric acid concentration

The concentration of the boric acid did not increase in any of the samples. The average boric acid concentration was about 569 ppm (table C1.3.9).

Table C1.3.10: results of the chemical analysis performed using the samples obtained from Batch 3 of filter A; radioactivity concentration is denoted here as (A) and χ represents the conductivity; [B1], [B2] and [B] represent the boric acid concentration.

Batch 3, sample 1	χ µS/cm	pH	[B1] ppm	[B2] ppm	[B] avg	A Bq/kg
Tanktainer	2,85	5,7	570,9	571,1	571	4,73E+04
Feed 0	3	5,7	568,5	565,7	567,1	5,11E+04
Feed	3,2	5,7	567,2	567,5	567,35	1,13E+05
Permeate	3	5,7	566,9	567,1	567	2,00E+03
Retentate	3,6	5,7	567,5	567,5	567,5	2,80E+05
Batch 3, sample 2	**χ µS/cm**	**pH**	**[B1] ppm**	**[B2] ppm**	**[B] avg**	**A Bq/kg**
Feed	4,3	5,6	571,7	571,8	571,75	7,01E+05
Permeate	3,2	5,7	570,3	570,1	570,2	1,98E+03
Retentate	4,6	5,5	571,2	572,7	571,95	9,25E+05
Backwash	1,4	5,9	NaN	NaN	NaN	1,30E+04
IXr mixed bed	1,6	5,8	NaN	NaN	NaN	3,60E+01

Dose build-up

The dose rate in filter B was measured during the filtration process and after the BW. The results are in the table C1.3.11 below.

Table C1.3.11: The dose rate build-up of the filter B during the Batch 3 process at the designated positions in µSv/h.

HFPM5 Batch 3			Dose rate (µSv/h)				
Filter Front			Elapsed time (h)	Filter back			Average dose rate
Top	Mid	Bottom		Top	Mid	Bottom	
30	50	52	**0.0**	78	92	82	64
40	60	66	**4.3**	81	130	107	81
65	94	97	**6.9**	111	180	175	120
42	68	70	**After BW**	86	143	129	90

Fouling

No fouling was observed as there were no changes in the TMP values (table C1.3.12).

Table C1.3.12: the process parameters that governed Batch 3

HFPM5 BATCH 3	Process operational parameters					
Elapsed time (h)	RPM	PIT00 (mbar)	PIT-01 (bar)	PI-02 (bar)	PDI-00 (mbar)	TI-01 (°C)
0.0	1860	106	2	1.2	1008	24
4.3	1850	72	2	1.15	1045	26
6.9	1850	50	2	1.15	1060	26.5

C1.3.4 Batch 4

That run took around **7.5** hours so that **630** liters of (TT) water were concentrated down to ~10 liters. 11 liters of BW water from Batch 3 were added to the feed tank. Permeate water had a volume of 620 liters that were filtered through the IXr.

Batch 4 analysis

This batch produced around 18 liters of retentate having the radioactivity concentration of $1.6 \cdot 10^6$ Bq/kg. The dominant radionuclides were found to be Ag-110m and Co-60 as shown in table C1.3.13.

Table C1.3.13: Radioactivity concentration of radionuclides in Batch 4 of Filter B (HFPM5); a qualitative bar chart (the horizontal red rectangles) shows the relationship amongst the radionuclides in each column.

HFPM5 Batch 4	(0 h)		Sample 1 (4 hr)			Sample 2 (7.5 hr)			Finish
Radionuclides	TankTainer	Feed	Feed	Premeate	Retentate	Feed	Permeate	Retentate	Back Wash
Mn-54	8.97E+02	1.07E+03	2.09E+03	4.06E+01	5.16E+03	2.63E+04		3.22E+04	4.20E+02
Co-57									
Co-58	9.97E+02	9.86E+02	1.78E+03	6.53E+02	2.98E+03	1.18E+04	5.82E+02	1.47E+04	3.94E+02
Co-60	1.77E+04	1.84E+04	4.12E+04	5.36E+02	9.50E+04	5.07E+05	5.88E+02	6.17E+05	6.46E+03
Zn-65					1.58E+03	5.44E+03			
Nb-95	5.58E+02	5.61E+02	1.32E+03		3.05E+03	2.11E+04		2.54E+04	
Zr-95		3.43E+02	8.52E+02		2.26E+03	8.40E+03		1.33E+04	
Ag-110m	2.49E+04	2.45E+04	5.35E+04	1.70E+02	1.26E+05	7.20E+05	1.03E+02	8.62E+05	8.63E+03
Sn-113						1.79E+03			
Sb-124	3.40E+02	2.39E+02	7.93E+02	8.17E+01	1.16E+03	5.38E+03	8.29E+01	6.69E+03	
Sb-125	6.02E+02			4.98E+02	4.47E+03	2.49E+04	7.12E+02	2.95E+04	
Total activity Conc (Bq/kg)	***4.54E+04***	***4.57E+04***	***1.04E+05***	***1.98E+03***	***2.40E+05***	***1.33E+06***	***2.00E+03***	***1.61E+06***	***1.63E+04***
Tot.Act. Uncertainty (Bq/kg)	**2.03E+03**	**2.10E+03**	**4.38E+03**	**1.55E+02**	**1.01E+04**	**5.29E+04**	**1.37E+02**	**6.44E+04**	**8.67E+02**

Tanktainer

The sample had a radioactivity concentration of $4.5 \cdot 10^4$ Bq/kg. It had the lowest radioactivity concentration as compared with other samples of the same source. Ag-110m and CO-60 were the dominant radionuclides (table C1.3.13).

Permeate

The two permeate samples had a radioactivity concentration of $2 \cdot 10^3$ Bq/kg. The dominant radionuclides were found to be Sb-125, Co-58and Co-60 as shown in (table C1.3.13).

Retentate

Two retentate samples were taken that ranged between $2.4 \cdot 10^5$ Bq/kg and $1.6 \cdot 10^6$ Bq/kg; the last value is 3521% the radioactivity of the feed at t=0. Ag-110m and Co-60 were the dominant radionuclides (table C1.3.13).

Feed

Three samples were taken where the radioactivity at t=0 was $4.6 \cdot 10^4$ Bq/kg. Ag-110m and Co-60 were the dominant radionuclides (table C1.3.13).

Backwash

9 liters of 733 water were used to wash the filter. The sample taken for analysis had a radioactivity concentration of $1.6 \cdot 10^4$ Bq/kg. The rest of the volume was added to the next and final batch. Ag-110m and Co-60 were the dominant radionuclides (table C1.3.13)

Ion Exchanger

One sample was acquired; it had a radioactivity concentration of 42 Bq/kg (C1.3.14).

Boric acid concentration

The concentration of the boric acid did not increase. The concentration of boric acid remained around the average of 564 ppm. The concentration of boric acid in the TT sample was 570 ppm (table C1.3.14).

Table C1.3.14: results of the chemical analysis performed using the samples obtained from Batch 4 of filter A; radioactivity concentration is denoted here as (A) and χ represents the conductivity; [B1], [B2] and [B] represent the boric acid concentration.

Batch 4, sample 1	χ µS/cm	pH	[B1] ppm	[B2] ppm	[B] avg	A Bq/kg
Tanktainer	2,85	5,6	570,6	570,7	570,65	4,54E+04
Feed 0	2,85	5,6	561,1	561,1	561,1	4,57E+04
Feed	3	5,6	562	561,7	561,85	1,04E+05
Permeate	2,7	5,6	560,8	560,8	560,8	1,98E+03
Retentate	3,4	5,5	561,8	561,8	561,8	2,40E+05
Batch 4, sample 2	**χ µS/cm**	**pH**	**[B1] ppm**	**[B2] ppm**	**[B] avg**	**A Bq/kg**
Feed	5,3	5,3	566,2	566,2	566,2	1,33E+06
Permeate	3,2	5,6	565,2	565,1	565,15	2,00E+03
Retentate	5,6	5,3	565,8	566,2	566	1,61E+06
Backwash	1,75	5,4	NaN	NaN	NaN	1,63E+04
IXr mixed bed	2,3	5,7	NaN	NaN	NaN	4,20E+01

Dose build-up

The dose rate build-up in filter B was measured with respect to time during the process and after the BW as shown in table C1.3.15.

Table C1.3.15: The dose rate build-up of the filter B during the Batch 4 process at the designated positions in µSv/h.

HFPM5 Batch 4			Dose rate (µSv/h)				
Filter Front			Elapsed time (h)	Filter back			Average dose rate
Top	Mid	Bottom		Top	Mid	Bottom	
37	60	62	**0.0**	82	134	107	80
40	71	71	**4.0**	90	155	135	94
80	117	134	**7.5**	153	225	230	157
46	80	80	**After BW**	110	170	165	109

Fouling

There was no fouling occurrence as there was no change in the TMP (table C1.3.16).

Table C1.3.16: the process parameters that governed Batch 4

HFPM5 BATCH 4	Process operational parameters					
Elapsed time (h)	RPM	PIT00 (mbar)	PIT-01 (bar)	PI-02 (bar)	PDI-00 (mbar)	TI-01 (°C)
0.0	1830	108	2	1.2	1002	23
4.0	1850	74	2	1.15	1050	25.5
7.5	1863	46	2	1.15	1073	27

C1.3.5 Batch 5

The experiment took **1.4** hours so that 120 liters, which were taken from the retentate tank, were concentrated down to ~10 liters, which were then collected in a plastic portable container.

Permeate tank volume was about 109 liters filtered through the IXr. The BW water was analyzed, after washing the module after emptying the TT, to investigate any easily removed particles that had built up on the membrane module and the pipes. No CC procedure was used.

Batch 5 analysis

The final radioactivity of the retentate was about $5.1 \cdot 10^6$ Bq/kg. Co-60 and Ag-110m were the dominant radionuclides (table C1.3.17). All retentate samples were diluted 1:50 before being measured using the HPGe detector to avoid paralyzing the detector. Then the true results were calculated back by multiplying the acquired radioactivity with 50.

Table C1.3.17: Radioactivity concentration of radionuclides in Batch 5 of Filter B (HFPM5); a qualitative bar chart (the horizontal red rectangles) shows the relationship amongst the radionuclides in each column.

HFPM5 Batch 5	(0 hr)		Sample 1 (1 hr)			Sample 2 (1.3 hr)		Sample 3 (1.5 hr)		Finish	
Radionuclides	Reten. Tank	Feed	Feed	Premeate	Retenate	Permeate	Retenate	Permeate	Retentate	Back Wash	IXr (mixed)
Mn-54	8,21E+03	8,48E+03	2,19E+04	5,17E+01	4,03E+04		7,56E+04	7,45E+01	8,26E+04	3,70E+03	
Co-57											
Co-58	4,51E+03	4,13E+03	9,69E+03	8,09E+02	1,83E+04	7,73E+02	3,53E+04	7,65E+02	3,81E+04	1,29E+03	
Co-60	1,66E+05	1,74E+05	4,35E+05	7,96E+02	7,95E+05	7,96E+02	1,39E+06	8,24E+02	1,50E+06	6,75E+04	1,71E+01
Zn-65					1,48E+04				2,10E+04		
Nb-95	6,09E+03	6,70E+03	1,88E+04		3,12E+04		5,93E+04		6,21E+04		
Zr-95	3,49E+03	3,35E+03	8,90E+03		1,83E+04		3,26E+04		3,06E+04		
Ag-110m	2,87E+05	3,01E+05	7,93E+05	1,05E+02	1,53E+06	8,10E+01	2,74E+06		3,22E+06	1,19E+05	3,85E+01
Sn-113											
Sb-124	1,63E+03	2,04E+03	4,21E+03	9,04E+01	9,44E+03	1,10E+02	1,67E+04	1,28E+02	2,54E+04		
Sb-125	1,02E+04			5,99E+02	4,21E+04	6,61E+02	8,02E+04	6,51E+02	1,09E+05		
Total activity Conc (Bq/kg)	***4,89E+05***	***5,12E+05***	***1,32E+06***	***2,35E+03***	***2,49E+06***	***2,41E+03***	***4,45E+06***	***2,44E+03***	***5,07E+06***	***2,01E+05***	***5,57E+01***
Tot.Act. Uncertainty (Bq/kg)	***2,01E+04***	***2,11E+04***	***5,42E+04***	***1,48E+02***	***1,06E+05***	***1,47E+02***	***1,91E+05***	***1,53E+02***	***2,18E+05***	***8,50E+03***	***1,67E+01***

Retentate tank (Reten. Tank)

A sample was taken for analysis out of the incoming retentate water from retentate tank. It had a radioactivity concentration of $4.9 \cdot 10^5$ Bq/kg (table C1.3.17). That water had very fine particulate matter, however a lot of that remained sediment in the tank. A loss of measured radioactivity was anticipated.

Permeate

Three permeate samples were taken that had a radioactivity concentration range between $2.35 \cdot 10^3$ Bq/kg and $2.4 \cdot 10^3$ Bq/kg; the latter was acquired by draining the mantel side into a collecting flask. The dominant radionuclides were found to be Co-58, Co-60 and Sb-125as shown in table C1.3.17.

Retentate

Three retentate samples were taken that ranged between $2.5 \cdot 10^6$ Bq/kg and $5.1 \cdot 10^6$ Bq/kg. The last value is 990% the radioactivity of the feed at t=0. Ag-110m and Co-60 were the dominant radionuclides (table C1.3.17).

The last retentate sample was taken by draining the filter module into a collecting flask. No samples were taken for analysis with the SEM as there was not much time left for extra experiments.

Feed

Only two samples were taken, the first one when the system reached a steady state at the start (t=0) and another after one hour. The reason for the absence of a third sample is that there was so little feed left that it was considered the same radioactivity as the retentate. The first sample had a radioactivity concentration of $5.1 \cdot 10^5$ Bq/kg while the last had $1.3 \cdot 10^6$ Bq/kg (table C1.3.17).

Backwash

One sample was taken out of the 11 liters of 733 water were used. It had a radioactivity concentration of $2 \cdot 10^5$ Bq/kg with Ag-110m and Co-60 as the dominant radionuclides (table C1.3.17). The remaining BW was added to the feed tank later on for the final task of emptying the remaining water in the TT.

Ion Exchanger

The sample yielded a left over radioactivity concentration of 56 Bq/kg, with Ag-110m (dominant) and Co-60 the only radionuclides after 9 hours of measurement in HPGe spectrometer (table C1.3.17), which is 2.33% of the average radioactivity concentration of the permeate samples.

Boric acid concentration

There was a very slight increase in the concentration of boric acid, but it is so little that it was negligible when considering that the retentate tank sample had 516 ppm when the average was 522 ppm (table C1.3.18). This is a mere 1% increase after concentrating around 2070 liters of radioactive water that had a boric acid concentration of around 565 ppm..

Table C1.3.18: results of the chemical analysis performed using the samples obtained from Batch 5 of filter A; radioactivity concentration is denoted here as (A) and χ represents the conductivity; [B1], [B2] and [B] represent the boric acid concentration.

Batch 5, sample 1	χ µS/cm	pH	[B1] ppm	[B2] ppm	[B] avg	A Bq/kg
Tanktainer CT	85,6	7,41	516	515,9	515,95	4,89E+05
Feed 0	89	7,42	519,2	519,9	519,55	5,12E+05
Feed	121,6	7,54	523,6	523,9	523,75	1,33E+06
Permeate	96,5	7,5	519,9	520	519,95	2,35E+03
Retentate	109,4	7,4	523,6	523,6	523,6	2,49E+06
Batch 5, sample 2	**χ µS/cm**	**pH**	**[B1] ppm**	**[B2] ppm**	**[B] avg**	**A Bq/kg**
Feed	NaN	NaN	NaN	NaN	NaN	NaN
Permeate	103	7,51	521	520,7	520,85	2,41E+03
Retentate	121,6	7,4	526,3	526,5	526,4	4,45E+06
Batch 5, sample 3	**χ µS/cm**	**pH**	**[B1] ppm**	**[B2] ppm**	**[B] avg**	**A Bq/kg**
Feed	NaN	NaN	NaN	NaN	NaN	NaN
Permeate	107	7,51	522,2	521,5	521,85	2,44E+03
Retentate	126,4	7,43	525,2	525	525,1	5,07E+06
Backwash	46	7,56	NaN	NaN	NaN	2,01E+05
IXr mixed bed	2,21	5,56	NaN	NaN	NaN	5,57E+01

Dose build-up

The dose rate in filter B was measured with respect to time during the process and after the BW as shown in table C1.3.19.

Table C1.3.19: The dose rate build-up of the filter B during the Batch 5 process at the designated positions in µSv/h.

HFPM5 Batch 5			Dose rate (µSv/h)				
Filter Front			Elapsed time (h)	Filter back			Average dose rate
Top	Mid	Bottom		Top	Mid	Bottom	
58	85	97	0.0	102	170	170	114
108	150	225	1.0	180	225	320	201
145	205	290	1.3	210	350	400	267
155	215	305	1.5	225	370	358	271
61	100	150	After BW	130	210	230	147

Fouling

There was a change in the TMP values as the process proceeded with time (table C1.3.20). The large concentration of particles in the retentate water was the reason behind this fouling occurrence (figure C1.3.1)

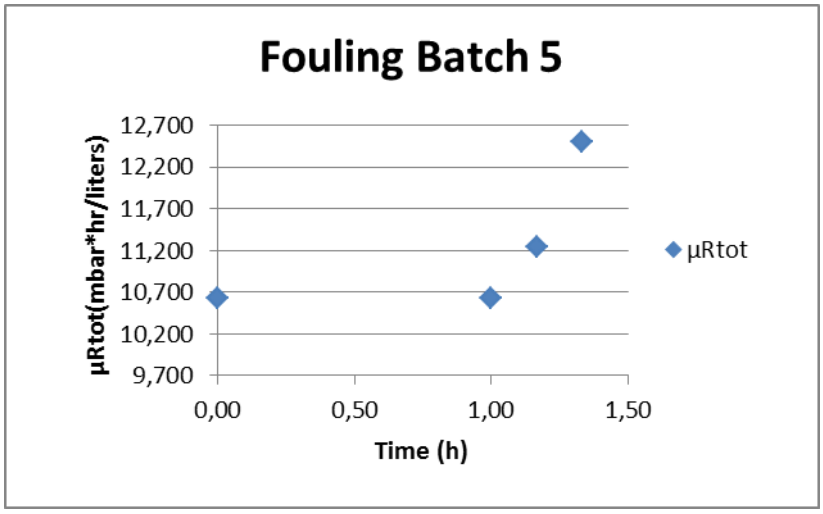

Figure C1.3.1: The fouling tendency in the final batch; seems to follow a linear increasing trend if the value at t=0 is neglected.

Table C1.3.20: the process parameters that governed Batch 5

HFPM5 BATCH 5	Process operational parameters					
Elapsed time (h)	RPM	PIT00 (mbar)	PIT-01 (bar)	PI-02 (bar)	PDI-00 (mbar)	TI-01 (℃)
0.0	1855	61	2	1.15	1010	22.5
1.0	1850	51	2	1.15	1075	26
1.3	1854	30	2	1.1	1083	27.5
1.5	1855	28	2	1	1085	28

Table C1.3.21: The dose rate build-up of the filter B during emptying of TT at the designated positions in µSv/h.

HFPM5 Tanktainer			Dose rate (µSv/h)				
Filter Front			Elapsed time (h)	Filter back			Average dose rate
Top	Mid	Bottom		Top	Mid	Bottom	
95	140	200	9	180	300	330	208
100	350	415	17	200	380	640	348
200	360	420	25	350	560	650	423
250	540	620	32	400	860	1300	662
680	900	900	39	1020	1400	1600	1083
135	245	250	After BW	350	660	370	335

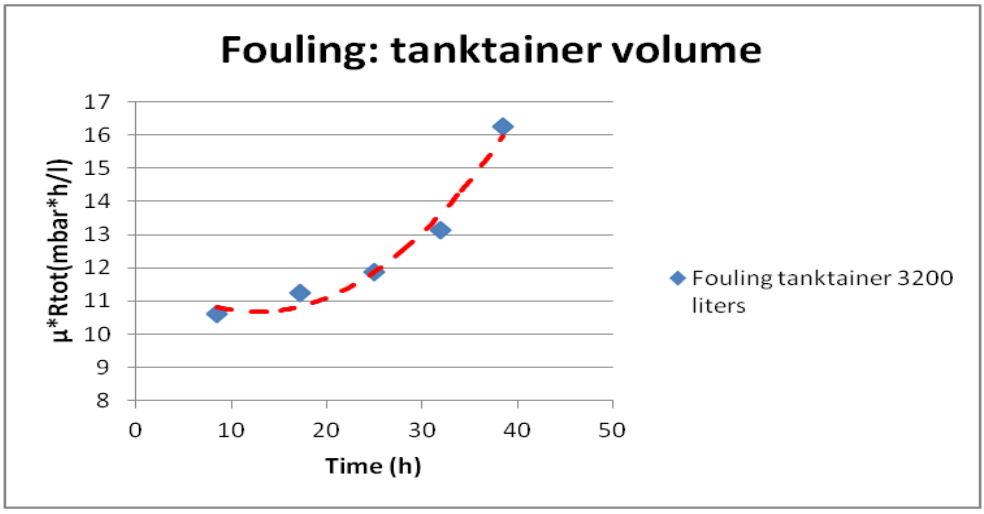

Figure C1.3.2: fouling trend as the remaining TT water was filtered through filter B. Values were acquired to calculate the TMP and FT using the data in table C1.3.22.

Table C1.3.22: the process parameters that governed the process of emptying the TT.

Elapsed time (h) for each batch	Processed volumes (liters)	PIT-01 (bar)	PI-02 (bar)
9	700	2	1.15
9	700	2	1.1
8	600	2	1.05
8	600	2	0.95
7	520	2	0.7

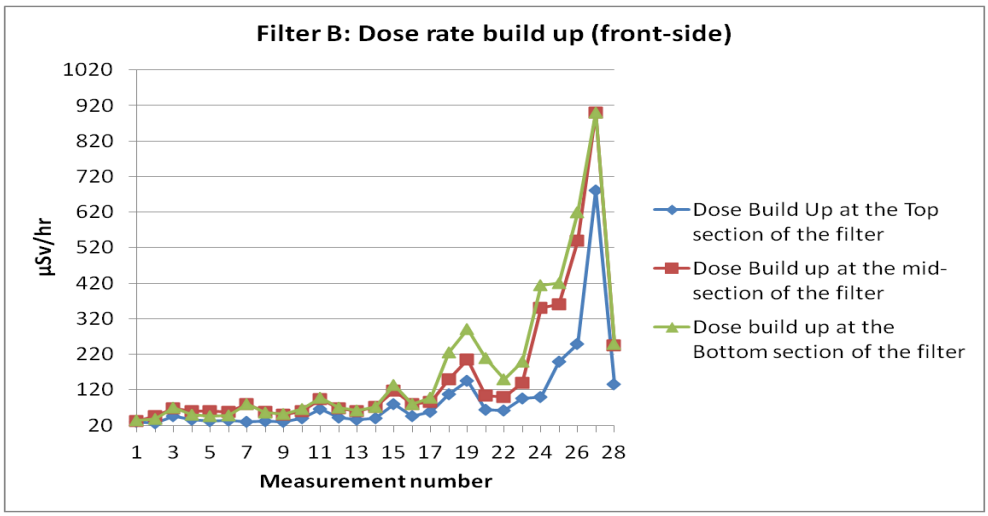

Figure C1.3.3: dose rate build-up in filter B (front-side) from batch 1-5 (first five tops) and the remaining TT water; the troughs are measurements done after a BW procedure

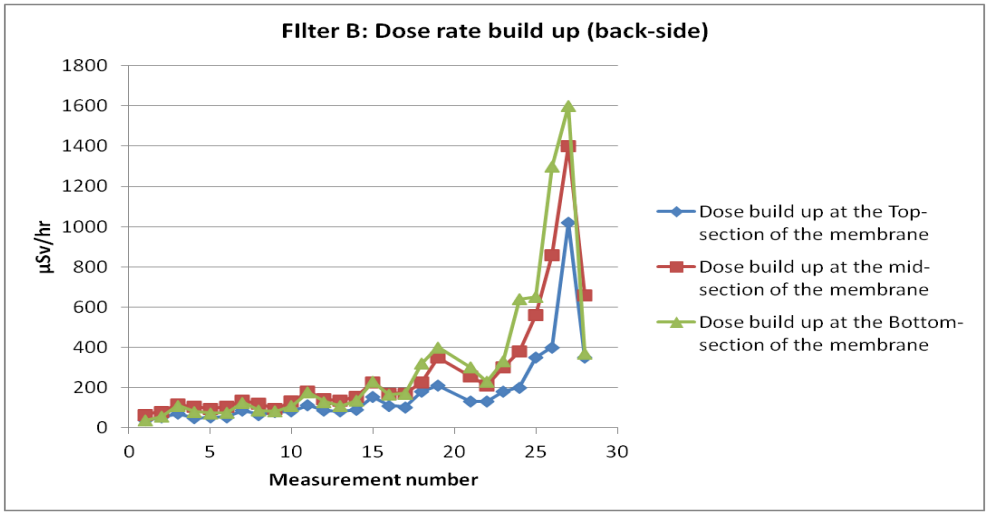

Figure C1.3.4: dose rate build-up in filter B (back-side) from batch 1-5 (first five tops) and the remaining TT water; the troughs are measurements done after a BW procedure

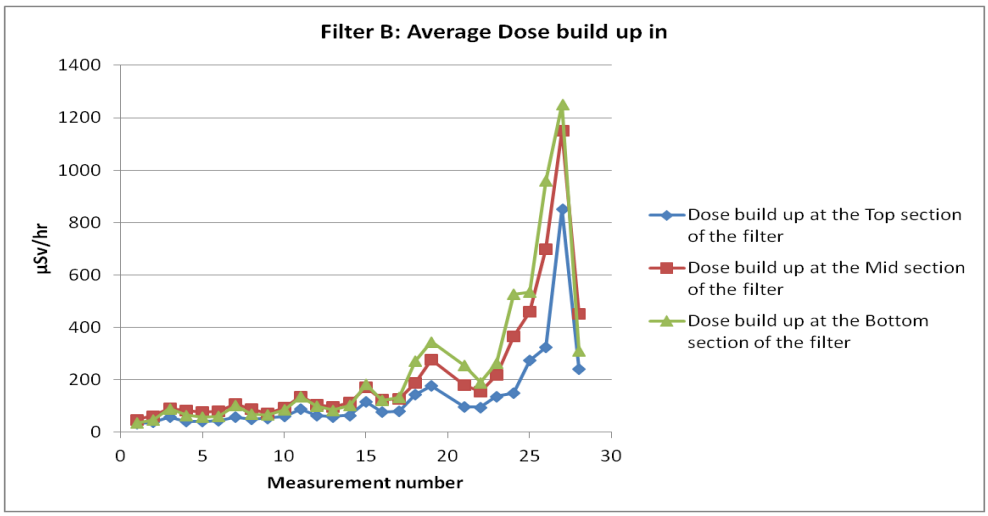

Figure C1.3.5: dose rate build-up in filter B (averaged over front- and back-side) from batch 1-5 (first five tops) and the remaining TT water.

Appendix D

D1 SEM images over fibers from Filter A

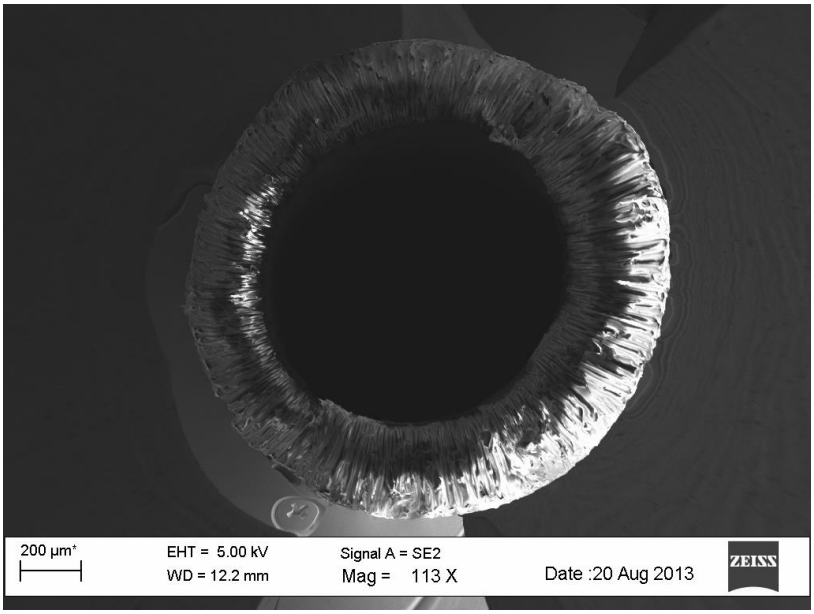

Figure D1.1: Cross-sectional view (SEM) of a bottom hollow fiber (filter A)

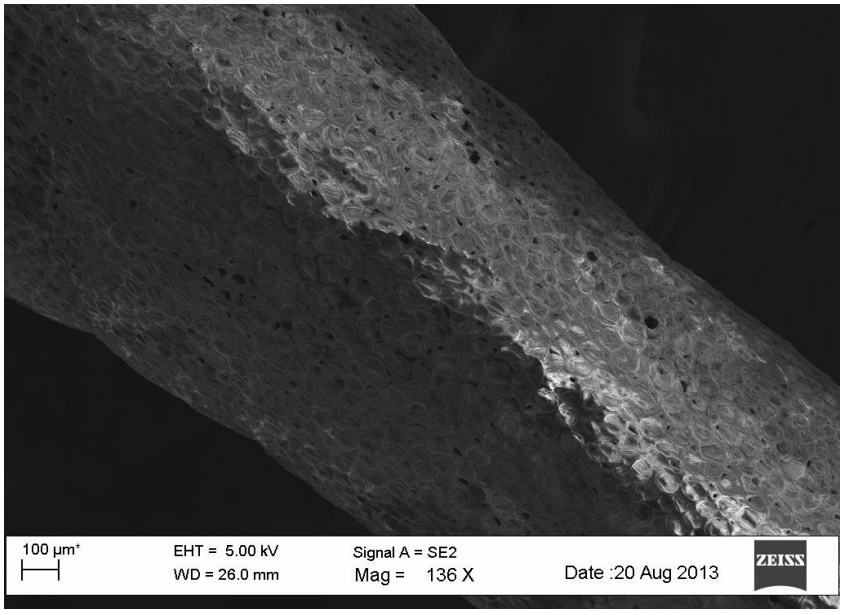

Figure D1.2: surface view (SEM) of a bottom hollow fiber (filter A)

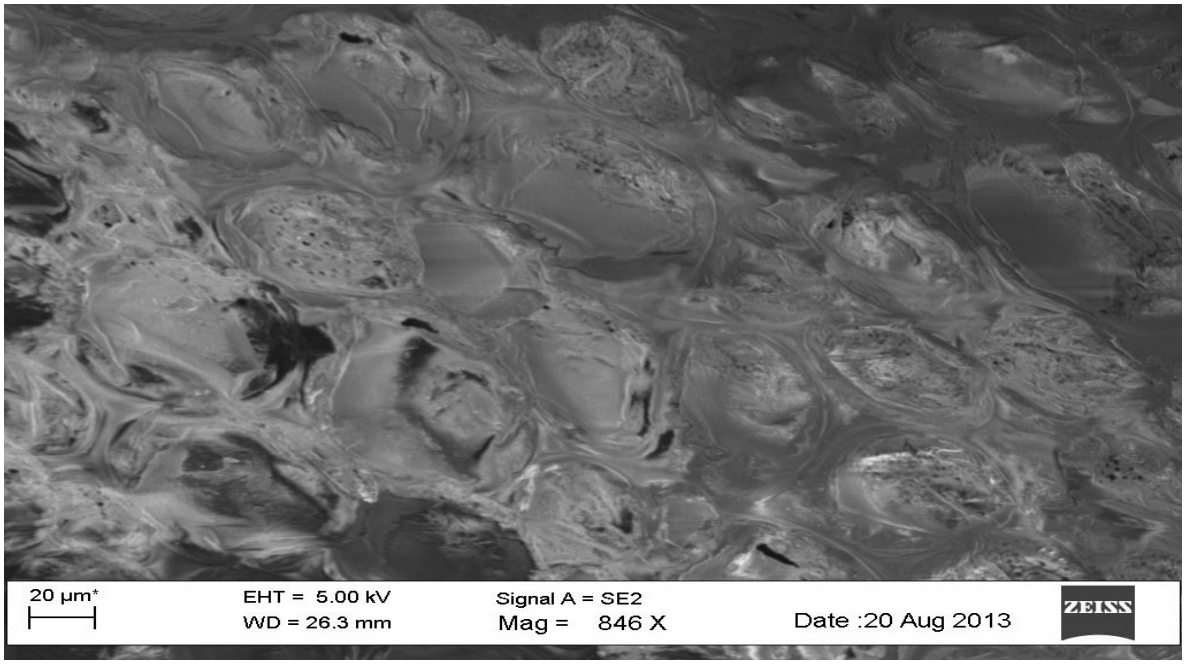

Figure D1.3: a closer surface view of figure D1.2 (SEM) of a bottom hollow fiber (filter A).

D2 SEM images from retentate of Batch 5 Filter A

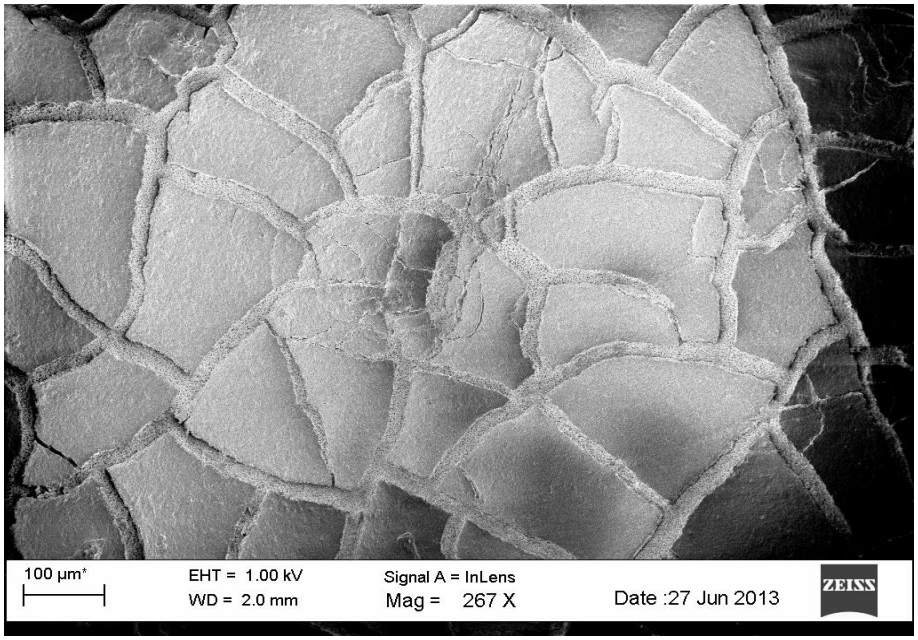

Figure D1.4: SEM image (top view) of the cake formed after an OT filtration of the final retentate of Batch 5; the filter paper is visible from within the cracks in the cake.

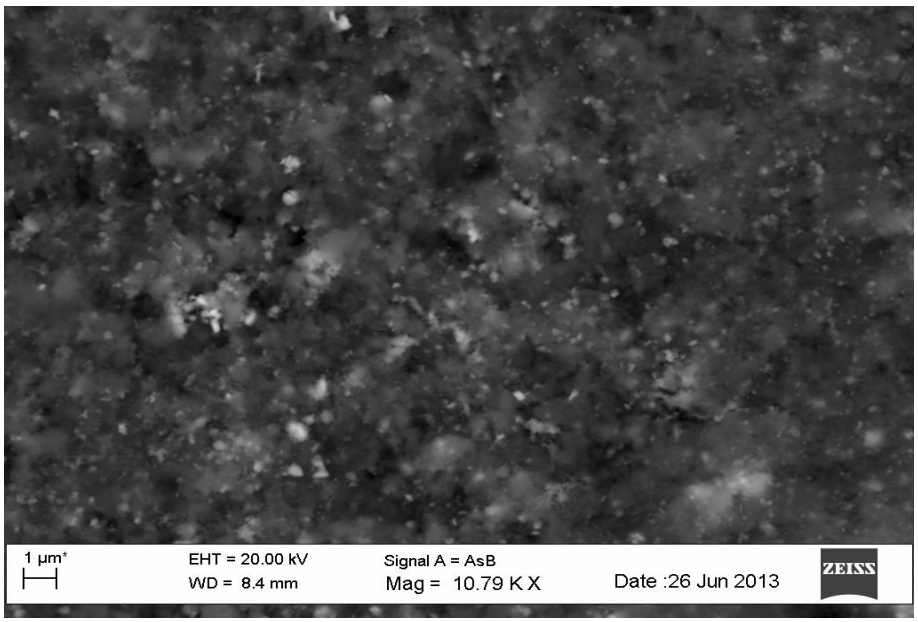

Figure D1.5: SEM image (from the bottom of the cake) of the cake formed after an OT filtration of the final retentate of Batch 5; the cake was carefully peeled off the Millipore filter before scanning. Notice the different types of particle sizes especially those containing metals (the more whitish shades of grey)

Appendix E

E1 Effect of boric acid on settling time of cement

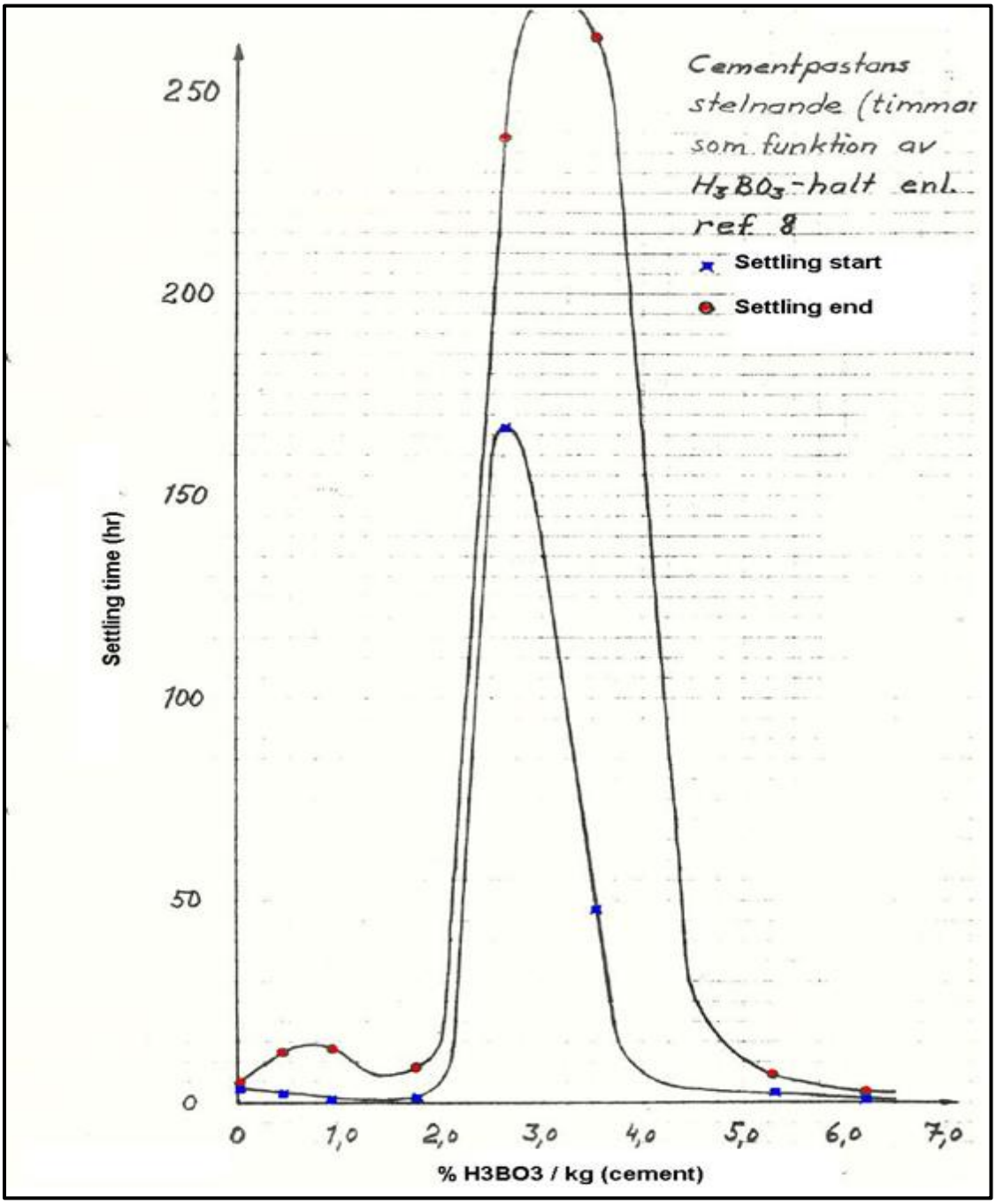

Figure E1.1: the curve that describes the settling (hardening) behavior of cement in relation to the concentration of boric acid in the cement mix; the blue values represent the initiation time of hardening, while the red ones are the time when cement hardening is finished. [This curve is the courtesy of Ringhals AB, used by permission of Anders Höglund]

Appendix F

F1 Process and Instrument Diagram (PID)

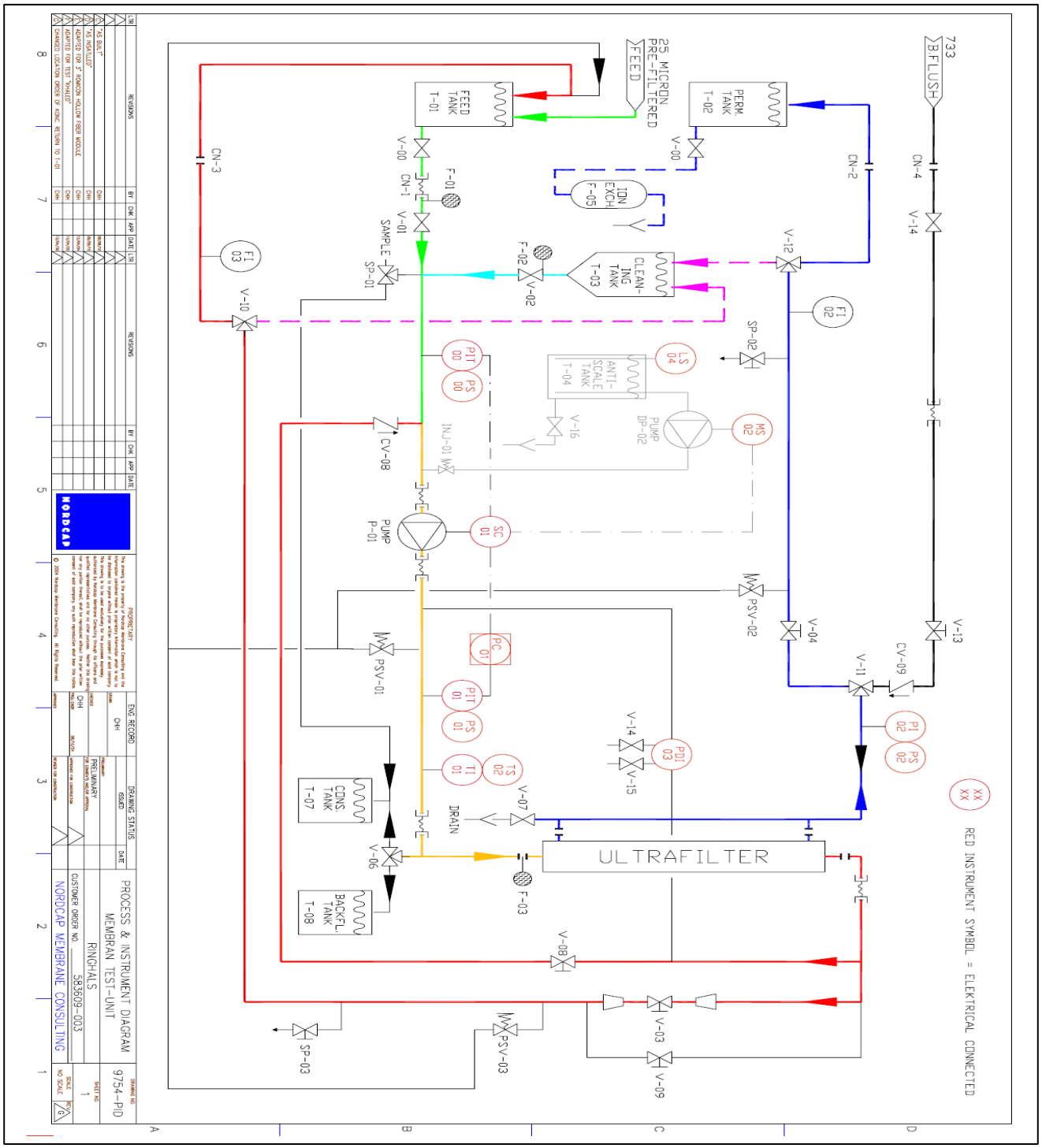

Figure F1.1: The detailed PID diagram of the filtration process that was done using a HFF. [Courtesy of NORDCAP MEMBRANE CONSULTING, used with permission of Carl-Henrik Hansson]

F2 Filter specifications

KOCH MEMBRANE SYSTEMS

ROMICON® 3" HOLLOW FIBER CARTRIDGES

3" Diameter Hollow Fiber Ultrafiltration Cartridges

PRODUCT DESCRIPTION

Membrane Polymer: Polysulfone
Housing Construction: Polysulfone
Seal/Potting Material: Proprietary Epoxy Compound
Storage Solution: Glycerin
Options:
Lumen size: 20 mil (0.5 mm), 43 mil (1.1 mm), 60 mil (1.5 mm), 75 mil (1.9 mm), 106 mil (2.7 mm)
Membrane Type: PM5, PM10, PM30, PM50, PM100, or PM500
Special Construction for Specific Applications:
Vinegar Filtration: Selected PM50 and PM500 cartridges are available for vinegar filtration.
Citrus Filtration: Selected PM10, PM50 and PM500 cartridges are available for citrus filtration.
ROMIPRO™ Cartridges: Selected cartridges of all membrane types are available with components that have passed USP Class VI test guidelines.

CARTRIDGE AVAILABILITY AND MEMBRANE AREA

Membrane Type	MWCO (Dalton) or Pore size (µm)	Fiber Diameter [mil (mm)]				
		20 (0.5)	43 (1.1)	60 (1.5)	75 (1.9)	106 (2.7)
PM5	5,000		•			
PM10	10,000	•	•	•		
PM30	30,000		•			
PM50	50,000		•	•	•	
PM100	100,000	•	•			
PM500	500,000		•		•	•
Membrane Area [ft^2 (m^2)]		53 (4.9)	25 (2.3)	25 (2.3)	21 (1.9)	16 (1.5)

OPERATING AND DESIGN INFORMATION*

Maximum Inlet Pressure: 40 psi (2.8 bar)
Maximum Transmembrane Pressure: 35 psi (2.4 bar)
Maximum Operating Temperature (at pH 6.0): 140°F (60°C)
Maximum Permeate Side Back Pressure: 20 psi (1.4 bar)
Maximum Differential Pressure Feed Side: 30 psi (2.1 bar)
Allowable pH: 1.5 – 13.0 @ 130°F (54°C)
Maximum Total Chlorine (During Cleaning): 200 ppm @ pH 10-10.5, 130°F (54°C), 0 ppm @ pH < 9.5

* Consult KMS Process Technology Group for specific applications.

NOMINAL DIMENSIONS

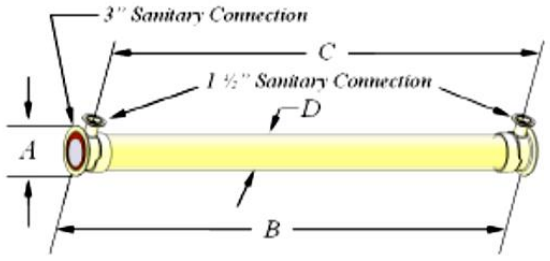

Model	A inches (mm)	B inches (mm)	C inches (mm)	D inches (mm)	Permeate Connection	Process Connection
3043	4.0 (102)	43 (1092)	40 15/16 (1040)	3 (76)	1½" T/C	3" T/C

ROMICON® 3" HOLLOW FIBER CARTRIDGES

Membrane Characteristics

- Koch Membrane Systems (KMS) ROMICON® cartridges should be selected for filtration of process streams when the separation range is in the range of 5000 to 500,000 dalton. They provide stable productivity, ease of cleaning and reliable operation.
- ROMICON cartridges should be selected for filtration of liquids based on the separation range needed. They provide stable productivity, ease of cleaning and reliable operation. KMS ROMICON cartridges are crossflow-type filters, in which the feed solution is pumped across the cartridge to minimize solids cake buildup on the membrane. Crossflow filters provide efficient filtration at low operating pressure, allowing long process runs while reducing cleaning time, cleaning frequency, and labor costs.

Product Nomenclature

	HF	,	Vinegar	50	43	-	40	-	106	-	PM	500
Field:	1		2	3	4		5		6			7

Field 1: HF – Hollow fiber cartridge

Field 2 (optional field): Market or application designation

Field 3: Cartridge diameter times 10 in inches

Field 4: Cartridge length in inches

Field 5: Active membrane area in ft^2

Field 6: Fiber diameter in mils (1000 mil = 1 inch)

Field 7: Molecular Weight Cutoff divided by 1000 in Daltons

The example shown above describes a 5-inch diameter by 43-inch long hollow fiber cartridge for vinegar filtration, utilizing fibers with diameter of 106 mil and 500,000 Dalton. The active membrane area of this cartridge is 40 ft^2.

Operating Limits

- **Operating Pressure:** Maximum operating pressure for a ROMICON® cartridge is 40 psi (2.8 bar) or 100 psi (if permeate side is pressurized). Actual operating pressure is dependent upon type of feed stream, recovery and temperature conditions.
- **Permeate Pressure:** Permeate pressure should not exceed 20 psi (1.4 bar) pressure at any time, including backflush.
- **Differential Pressure:** Maximum differential pressure limit is 30 psi (2.1 bar) per cartridge.
- **Temperature:** Maximum operating temperature is 140°F (60°C) and maximum cleaning temperature is 130°F (54°C).

Water Quality for Cleaning

- **pH:** Allowable range for cleaning is 1.5 to 13.0.
- **Guidelines:** Please refer to the "KMS Water Quality Guidelines" for more detailed information

Exposure to Chemical Oxidants

While not recommended for use on a daily basis, exposure to chemical oxidants for thorough cleaning and sanitization may prove necessary and useful.

Potassium metabisulfite (without catalyst such as cobalt) is the preferred chemical to eliminate residual chlorine or similar oxidizers prior to processing process liquid.

Lubricants

For cartridge installation, use only water or glycerin to lubricate seals. The use of petroleum or vegetable-based oils or solvents may damage the cartridge and will void the warranty

Service and Ongoing Technical Support

Koch Membrane Systems, Inc. has an experienced staff of professionals available to assist end-users and OEMs for optimization of existing systems and support the development of new applications. Along with the availability of supplemental technical bulletins, Koch Membrane Systems, Inc. also offers a complete line of KOCHKLEEN® cleaning chemicals.

KMS Capability

KMS is the leader in crossflow membrane technology, manufacturing reverse osmosis, nanofiltration, microfiltration, and ultrafiltration membranes and membrane systems. The industries served include food, dairy and beverage, pharmaceutical, biotechnology, water and wastewater, semiconductors, automotive, chemical and general manufacturing. KMS adds value by providing top quality membrane products and by sharing its experience in the design and supply of thousands of crossflow membrane systems worldwide.

Koch Membrane Systems, Inc., www.kochmembrane.com

Corporate Headquarters: 850 Main Street, Wilmington, Massachusetts 01887-3388, US, Tel. Toll Free: 1-888-677-5624, Telephone: 1-978-694-7000, Fax: 1-978-657-5208
European Headquarters: Koch Chemical Technology Group Ltd., Units 3-6, Frank Foley Way, Stafford ST16 2ST, GB, Telephone: +44-178-527-2500, Fax: +44-178-522-3149

• San Diego US • Aachen DE • Lyon FR • Madrid ES • Milan IT • Wijnegem BE • Beijing & Shanghai CN • Mumbai & Chennai IN • Melbourne & Sydney AU • SG • Sao Paulo BR • Manama BH •

07/11 Rev 11-3